

ANRCP-1998-7  
July 1998

# Amarillo National Resource Center for Plutonium

A Higher Education Consortium of The Texas A&M University System,  
Texas Tech University, and The University of Texas System

**RECEIVED**

JUL 28 1998

**OSTI**

## Investigation of Groundwater Recirculation for the Removal of RDX from the Pantex Plant Perched Aquifer

Karen Marie Boles and Randall J. Charbeneau  
The University of Texas at Austin

Sara Black and Ken Rainwater  
Water Resources Center  
Texas Tech University

David L. Barnes  
Amarillo National Resource Center for Plutonium

**MASTER**

**DISTRIBUTION OF THIS DOCUMENT IS UNLIMITED**  
Edited by

Angela L. Woods  
Technical Editor

600 South Tyler • Suite 800 • Amarillo, TX 79101  
(806) 376-5533 • Fax: (806) 376-5561  
<http://www.pu.org>

This report was prepared with the support of the U.S. Department of Energy (DOE), Cooperative Agreement No. DE-FC02-93JA83852. However, any opinions, findings, conclusions, or recommendations expressed herein are those of the author(s) and do not necessarily reflect the views of DOE. This work was conducted through the Amarillo National Resource Center for Plutonium.

### **DISCLAIMER**

This report was prepared as an account of work sponsored by an agency of the United States Government. Neither the United States Government nor any agency thereof, nor any of their employees, makes any warranty, express or implied, or assumes any legal liability or responsibility for the accuracy, completeness, or usefulness of any information, apparatus, product, or process disclosed, or represents that its use would not infringe privately owned rights. Reference herein to any specific commercial product, process, or service by trade name, trademark, manufacturer, or otherwise does not necessarily constitute or imply its endorsement, recommendation, or favoring by the United States Government or any agency thereof. The views and opinions of authors expressed herein do not necessarily state or reflect those of the United States Government or any agency thereof.

## **DISCLAIMER**

**Portions of this document may be illegible electronic image products. Images are produced from the best available original document.**

AMARILLO NATIONAL RESOURCE CENTER FOR PLUTONIUM/  
A HIGHER EDUCATION CONSORTIUM

A Report on

**Investigation of Groundwater Recirculation for the Removal of RDX from the  
Pantex Plant Perched Aquifer**

Karen Marie Boles and Randall J. Charbeneau  
The University of Texas at Austin, Austin, Texas 78712

Sara Black and Ken Rainwater  
Water Resources Center  
Texas Tech University, Lubbock, Texas

David L. Barnes  
Amarillo National Resource Center for Plutonium  
Amarillo, Texas 79101

Submitted for publication to

**Amarillo National Resource Center for Plutonium**

July 1998

# Investigation of Groundwater Recirculation for the Removal of RDX from the Pantex Plant Perched Aquifer

Karen Marie Boles and Randall J. Charbeneau  
The University of Texas at Austin, Austin, Texas 78712

Sara Black and Ken Rainwater  
Water Resources Center  
Texas Tech University, Lubbock, Texas

David L. Barnes  
Amarillo National Resource Center for Plutonium  
Amarillo, Texas 79101

## *Abstract*

The Pantex Plant near Amarillo, Texas, is a U.S. Department of Energy (DOE) facility that has been in operation since 1942. Past and present operations at Pantex include the creation of chemical high explosives components for nuclear weapons and assembly and disassembly of nuclear weapons.

The Pantex Plant is underlain by the Ogallala aquifer, which in this area, consists of the main water-bearing unit and a perched water zone. These are separated by a fine-grained zone of low permeability. Multiple contaminant plumes containing high explosive (HE) compounds have been detected in the perched aquifer beneath the plant. The occurrence of these contaminants is the result of past waste disposal practices at the facility. RDX is an HE compound, which has been detected in the groundwater of the perched aquifer at significant concentrations. A pilot-scale, dual-phase extraction treatment system has been installed at one location at the plant, east of Zone 12, to test the effectiveness of such a system on the removal of these contaminants from the subsurface.

A tracer test using a conservative tracer, bromide (Br), was conducted at the treatment site in 1996. In addition to the bromide, RDX and water elevations in the aquifer were monitored. Using data from the tracer test and other relevant data from the investigations at Pantex, flow and contaminant transport in the perched aquifer were simulated with groundwater models. The flow was modeled using MODFLOW and the transport of contaminants in the aqueous phase was modeled using MT3D. Modeling the perched aquifer had been conducted to characterize the flow in the perched aquifer; estimate RDX retardation in the perched aquifer; and evaluate the use of groundwater re-circulation to enhance the extraction of RDX from the perched aquifer.

## TABLE OF CONTENTS

List of Tables .....	vi
List of Figures .....	vii
<b>CHAPTER 1: INTRODUCTION.....</b>	<b>3</b>
1.1 Objectives .....	3
1.2 Pantex History.....	4
1.3 Site Description.....	4
1.3.1 Zone 12 Hydrogeology .....	4
1.3.2 Zone 12 Contaminants .....	8
1.3.3 Zone 12 Treatment System .....	10
<b>CHAPTER 2: ZONE 12 PERCHED AQUIFER TRACER TEST .....</b>	<b>13</b>
2.1 Equipment Installation .....	13
2.2 The Tracer Test .....	13
2.3 Tracer Test Monitoring .....	16
<b>CHAPTER 3: THE GROUNDWATER MODELS .....</b>	<b>25</b>
3.1 MODFLOW .....	25
3.2 MT3D.....	28
3.2.1 Eulerian-Lagrangian Solution.....	29
3.2.2 Hybrid Method of Characteristics Solution .....	30
3.3. Linking MODFLOW and MT3D.....	31
<b>CHAPTER 4: GROUNDWATER MODELING OF THE PERCHED AQUIFER.....</b>	<b>33</b>
4.1 Grid Representation of the Perched Aquifer.....	33
4.1.1 Spatial Discretization .....	33
4.1.2 Boundary Conditions .....	34
4.1.3 Sources and Sinks .....	34

4.2 Initial Injection at PV-4 During Tracer Test.....	35
4.2.1 MODFLOW Model of Initial Injection at PV-4.....	36
4.2.2 This Analysis.....	39
4.3 Model Calibration.....	41
4.3.1 Temporal Discretization.....	42
4.3.2 Grid Zones.....	43
4.3.3 Use of a Two-Layer Model.....	43
4.3.4 Fitting the Breakthrough Curves.....	46
4.3.5 Hydraulic Conductivity.....	49
4.3.6 Porosity.....	51
4.3.7 Specific Yield.....	52
4.3.8 Dispersivity.....	54
4.3.9 Vertical Hydraulic Conductivity.....	56
4.3.10 Storage Coefficient.....	56
4.4 Sensitivity Analysis.....	56
4.4.1 Sensitivity to Hydraulic Conductivity.....	56
4.4.2 Sensitivity to Porosity.....	58
4.4.3 Sensitivity to Specific Yield.....	59
4.4.4 Sensitivity to Dispersivity.....	59
4.4.5 Sensitivity to Vertical Hydraulic Conductivity.....	60
4.4.6 Sensitivity to Storage Coefficient.....	60
4.4.7 Additional Model Parameters.....	61
4.5 RDX Retardation.....	61
4.5.1 Procedure for Estimation of RDX Retardation.....	62
4.5.2 Removal of RDX from Perched Aquifer During the Tracer Test.....	64
4.6 Evaluation of Re-Circulation.....	67

**CHAPTER 5: SUMMARY, CONCLUSIONS, AND RECOMMENDATIONS**

5.1 Summary .....68  
5.2 Conclusions .....69  
5.3 Recommendations .....71

**REFERENCES .....73**

**APPENDIX A ..... A-1**

**APPENDIX B .....B-1**

## LIST OF TABLES

Table 4-1	Temporal Discretization for Modeling of Initial Injection at PV-4.....	37
Table 4-2	Temporal Discretization of the Perched Aquifer Model.....	42
Table 4-3	EPACML Method of Estimating Longitudinal Dispersivity.....	55
Table 4-4	Calculated Dispersivity with Analytical Models.....	55
Table 4-5	Figures Corresponding to Zone, Layer, and Well for Hydraulic Conductivity Sensitivity Analysis.....	57
Table 4-6	Figures Corresponding to Zone, Layer, and Well for Porosity Sensitivity Analysis.....	58
Table A-1	MT3D Internal Parameters Related to Advective Transport.....	B-2

## LIST OF FIGURES

Figure 1-1	Pantex Plant Site Layout.....	2
Figure 1-2	Generalized Cross-Section of the Stratigraphy in the Zone 12 Area.....	5
Figure 1-3	FGZ Contours .....	6
Figure 1-4	Groundwater Contours.....	7
Figure 1-5	Cross-Section Location.....	7
Figure 1-6	Cross-Section of the Perched Aquifer.....	8
Figure 1-7	RDX Contours at the Start of the Tracer Test.....	9
Figure 1-8	Layout of Zone 12 Treatment System .....	11
Figure 2-1	Schematic Drawing of the Site Arrangement .....	14
Figure 2-2	Daily Injection Volumes.....	15
Figure 2-3	Daily Bromide Concentrations .....	16
Figure 2-4	Weekly Bromide Concentrations.....	17
Figure 2-5	Weekly Bromide Concentrations.....	17
Figure 2-6	Weekly/Daily Bromide Concentrations.....	18
Figure 2-7	RDX Concentrations.....	19
Figure 2-8	RDX Concentrations.....	19
Figure 2-9	RDX Concentrations.....	19
Figure 2-10	Teaney and Hudak Comparison of DTECH RDX Test Results vs. EPA SW-846 8330 Results .....	20
Figure 2-11	Comparison of DTECH RDX Results to Method 8330.....	21
Figure 2-12	PV-1, PV-2, and PV-3 Water Elevations During the Tracer Test .....	21
Figure 2-13	One-Hour Moving Average of PV-4 Water Elevation .....	22
Figure 2-14	Pumping Rates and Monitoring During Tracer Test.....	23
Figure 3-1	Row, Column, and Layer Configuration in a Finite-Difference Grid.....	27
Figure 3-2	Block-Centered Cell Formation.....	27
Figure 3-3	Flow Through Cells in a Finite-Difference Grid .....	28
Figure 4-1	Grid Representation of the Perched Aquifer.....	35
Figure 4-2	Water Elevation in PV-4 During Start of Tracer Test .....	36
Figure 4-3	Water Elevations During Initial Injection Period at PV-4 .....	37

Figure 4-4	Sensitivity to Hydraulic Conductivity in Initial Injection Model at PV-4.....	38
Figure 4-5	Sensitivity to Specific Yield in Initial Injection Model at PV-4.....	38
Figure 4-6	Corrected Drawdown in PV-4 During Initial Injection Period.....	40
Figure 4-7	Model Predicted Breakthrough Curve at EW-3 from One-Layer Model ..	44
Figure 4-8	Lithology of Perched Aquifer Cross-Section.....	45
Figure 4-9	Comparison of Model Breakthrough to Field Breakthrough for EW-1.....	45
Figure 4-10	Comparison of Model Breakthrough to Field Breakthrough for EW-2.....	46
Figure 4-11	Comparison of Model Breakthrough to Field Breakthrough for EW-3.....	46
Figure 4-12	Bromide Contours for 15 and 30 Days of the Tracer Test.....	48
Figure 4-13	Bromide Contours for 15 and 30 Days of the Tracer Test.....	48
Figure 4-14	Bromide Contours for 45 and 66 Days of the Tracer Test.....	49
Figure 4-15	Bromide Contours for 45 and 66 Days of the Tracer Test.....	49
Figure 4-16	Hydraulic Conductivity Zones for Layer 1 .....	50
Figure 4-17	Hydraulic Conductivity Zones for Layer 2.....	51
Figure 4-18	Porosity Zones for Layers 1 and 2 .....	52
Figure 4-19	PV-1 Field and Model Groundwater Elevations.....	52
Figure 4-20	PV-2 Field and Model Groundwater Elevations.....	53
Figure 4-21	PV-3 Field and Model Groundwater Elevations.....	53
Figure 4-22	Comparison of Model Output to RDX Analytical Data for EW-1 .....	63
Figure 4-23	Comparison of Model Output to RDX Analytical Data for EW-2 .....	63
Figure 4-24	Comparison of Model Output to RDX Analytical Data for EW-3 .....	63
Figure 4-25	RDX Contours at 15 and 30 Days in the Tracer Test .....	65
Figure 4-26	RDX Contours at 15 and 30 Days in the Tracer Test .....	65
Figure 4-27	RDX Contours at 45 and 66 Days in the Tracer Test .....	66
Figure 4-28	RDX Contours at 45 and 66 Days in the Tracer Test .....	66
Figure A-1	Sensitivity at EW-1 to Changes in Zone 1 Hydraulic Conductivity .....	A-2
Figure A-2	Sensitivity at EW-2 to Changes in Zone 1 Hydraulic Conductivity .....	A-2
Figure A-3	Sensitivity at EW-3 to Changes in Zone 1 Hydraulic Conductivity .....	A-2
Figure A-4	Sensitivity at EW-1 to Changes in Zone 2 Hydraulic Conductivity .....	A-3
Figure A-5	Sensitivity at EW-2 to Changes in Zone 2 Hydraulic Conductivity .....	A-3

Figure A-6	Sensitivity at EW-3 to Changes in Zone 2 Hydraulic Conductivity .....	A-3
Figure A-7	Sensitivity at EW-1 to Changes in Zone 3, Layer 1 Hydraulic Conductivity .....	A-4
Figure A-8	Sensitivity at EW-2 to Changes in Zone 2, Layer 1 Hydraulic Conductivity .....	A-4
Figure A-9	Sensitivity at EW-3 to Changes in Zone 3, Layer 1 Hydraulic Conductivity .....	A-4
Figure A-10	Sensitivity at EW-1 to Changes in Zone 3, Layer 2 Hydraulic Conductivity .....	A-5
Figure A-11	Sensitivity at EW-2 to Changes in Zone 3, Layer 2 Hydraulic Conductivity .....	A-5
Figure A-12	Sensitivity at EW-3 to Changes in Zone 3, Layer 2 Hydraulic Conductivity .....	A-5
Figure A-13	Sensitivity at EW-1 to Changes in Zone 1 Porosity .....	A-6
Figure A-14	Sensitivity at EW-2 to Changes in Zone 1 Porosity .....	A-6
Figure A-15	Sensitivity at EW-3 to Changes in Zone 1 Porosity .....	A-6
Figure A-16	Sensitivity at EW-1 to Changes in Zone 2 Porosity .....	A-7
Figure A-17	Sensitivity at EW-2 to Changes in Zone 2 Porosity .....	A-7
Figure A-18	Sensitivity at EW-3 to Changes in Zone 2 Porosity .....	A-7
Figure A-19	Sensitivity at EW-1 to Changes in Zone 3 Porosity .....	A-8
Figure A-20	Sensitivity at EW-2 to Changes in Zone 3 Porosity .....	A-8
Figure A-21	Sensitivity at EW-3 to Changes in Zone 3 Porosity .....	A-8
Figure A-22	Sensitivity at EW-1 to Changes in Specific Yield .....	A-9
Figure A-23	Sensitivity at EW-2 to Changes in Specific Yield .....	A-9
Figure A-24	Sensitivity at EW-3 to Changes in Specific Yield .....	A-9
Figure A-25	Sensitivity at EW-1 to Changes in Dispersivity .....	A-10
Figure A-26	Sensitivity at EW-2 to Changes in Dispersivity .....	A-10
Figure A-27	Sensitivity at EW-3 to Changes in Dispersivity .....	A-10
Figure A-28	Sensitivity at EW-1 to Changes in Vertical Hydraulic Conductivity ...	A-11
Figure A-29	Sensitivity at EW-2 to Changes in Vertical Hydraulic Conductivity ...	A-11
Figure A-30	Sensitivity at EW-3 to Changes in Vertical Hydraulic Conductivity ...	A-11

Figure A-31	Sensitivity at EW-1 to Changes in Storage Parameter.....	A-12
Figure A-32	Sensitivity at EW-2 to Changes in Storage Parameter.....	A-12
Figure A-33	Sensitivity at EW-3 to Changes in Storage Parameter.....	A-12

## 1. INTRODUCTION

The Pantex Plant is a U. S. Department of Energy (DOE) facility located approximately 17 miles northeast of Amarillo in the Texas Panhandle. After being built in the early 1940s, the plant's original mission was to process explosive ordinances and nuclear weapons.

The facility is located over the Ogallala Aquifer, which serves as the primary water source for a variety of purposes. These include its use as drinking water, agricultural irrigation water, and water for industry. In the subsurface beneath the Pantex Plant, a discontinuous perched aquifer overlies the main unit of the Ogallala Aquifer. These two water-bearing units are separated by a formation termed the fine-grained zone (FGZ), which has very low permeability. A number of contaminants have been detected in subsurface soils beneath the facility and in the groundwater of the perched aquifer. These include high-explosive (HE) compounds, volatile organic compounds (VOCs), and metals (chromium). The occurrence of these chemicals in the soil and groundwater is a result of past waste disposal practices at the Pantex facility. To date, none of these compounds associated with the Pantex Plant have been detected in the groundwater of the main unit Ogallala Aquifer. Acknowledging that protection of the Ogallala Aquifer is of primary importance, it is necessary to obtain an understanding of the groundwater transport in the perched aquifer.

Figure 1-1 is a map of the Pantex Plant showing the major areas of the facility, which are designated by zone numbers. Zone 11 is the experimental explosive development area. Zone 12 is the location at the plant where weapons are assembled and disassembled. Activities in these two areas are the focus of this report.

A pilot-scale, dual-phase extraction treatment system has been installed east of Zone 12 (refer to Figure 1-1). Multiple contaminant plumes have been detected in the soil and groundwater in this particular area including RDX (hexahydro-1,3,5-trinitro-1,3,5-triazine). RDX has been detected in significant concentrations in the perched aquifer beneath the Zone 12 area. The extraction system consists of seven wells and a treatment system for gaseous and dissolved phase contaminants. The purpose of the system is to test the effectiveness of the extraction of gaseous phase constituents from the vadose zone and dissolved phase constituents in the groundwater from the perched aquifer. The relevance of the Zone 12 treatment system to this study is limited to the extraction of groundwater from the perched aquifer.

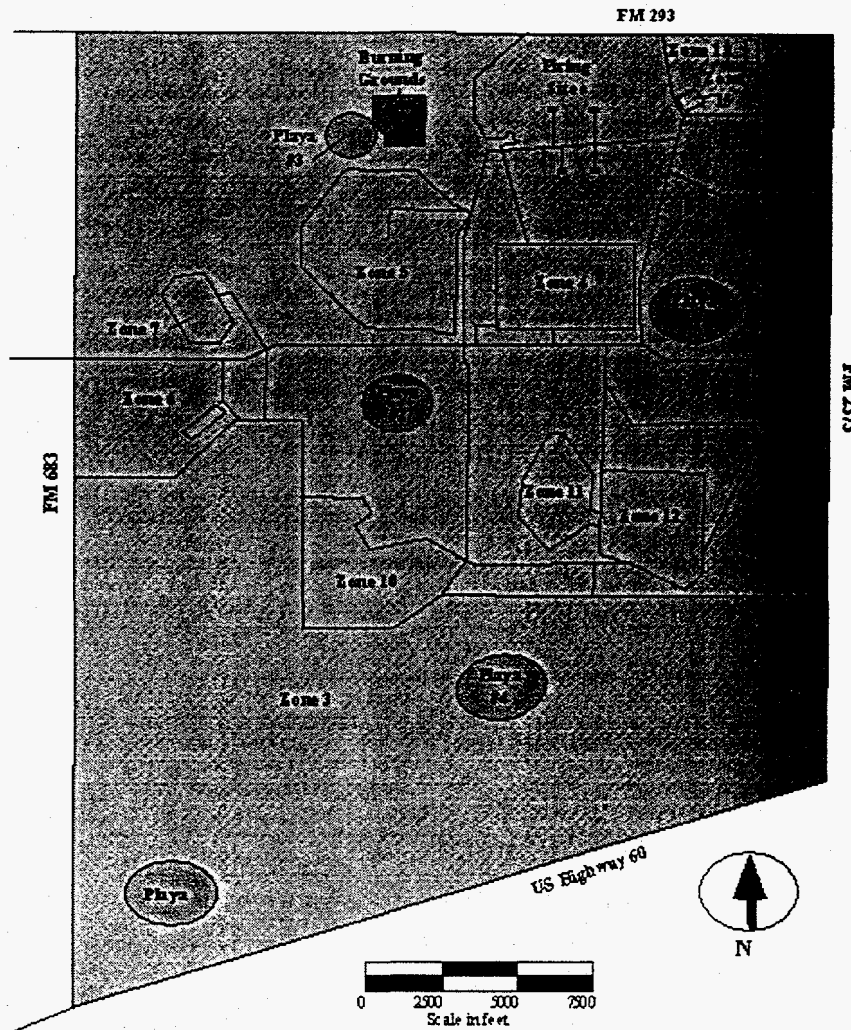


Figure 1-1: Pantex Plant Site Layout (Adapted from "Pantex Facility, Amarillo, Texas")

A tracer test using a conservative bromide tracer was conducted at the treatment site in 1996. In addition to the bromide tracer, RDX, which was one of the HE compounds detected in the groundwater, was monitored during the test. Using data gathered during the tracer test and other relevant data from other investigations at the Pantex Plant, flow and RDX transport in the perched aquifer were simulated with groundwater models. The groundwater flow was modeled using MODFLOW (McDonald and Harbaugh, 1988) and the transport of bromide and RDX in the dissolved phase were modeled using MT3D (Zheng, 1990). The tracer test and modeling of the test results was conducted as a part of the research at the Pantex Plant performed by the Amarillo National Resource Center for Plutonium, which consists of researchers from the University of Texas System, Texas Tech University System, and Texas A&M University System.

## 1.1 OBJECTIVES

The work described in this report includes both the field tracer test and the modeling of the resulting field data. The specific objectives of the field tracer test include the following:

- Design of the hydraulic and chemical aspects of the tracer test for implementation within the existing Zone 12 Treatability system.
- Installation of the necessary plumbing and equipment for the tracer test at the Pantex Plant.
- Performance of the tracer test.

Researchers affiliated with the Texas Tech University Water Resources Center accomplished these objectives. The tracer test benefited from the cooperation of the Environmental Restoration division of Battelle Pantex and the operating contractor for the treatability system, engineering-environmental Management. The specific objectives of the modeling phase of the project include the following:

- Determine the flow characterization of the perched aquifer.
- Estimate the retardation of RDX.
- Evaluate the removal of RDX from the perched aquifer with the dual-phase extraction system.
- Evaluate the use of groundwater re-circulation to enhance the extraction of RDX from the perched aquifer.

Researchers from the University of Texas at Austin performed the modeling work.

## 1.2 PANTEX HISTORY

The Pantex Plant is located approximately 17 miles northeast of Amarillo in Carson County, Texas. Farm-to-Market roads border Pantex to the north, east, and west. U.S. Highway 60 borders the site to the south.

The original Pantex Plant was constructed in 1942. It served as a conventional explosive ordnance factory for the U. S. Army during World War II. Once the war ended, the plant ceased operations. In 1949, Texas Technological College, now Texas Tech University (TTU), purchased

the site for \$1 and used the land to conduct cattle feeding experiments. Pantex occupies approximately 16,000 acres.

In 1951, the U. S. Army exercised an option contained in the purchase contract of the Pantex site in which it reclaimed approximately 10,000 acres including the main plant. This was done at the request of the Atomic Energy Commission, which later became the DOE. In the following years, Pantex operations included the assembly and disassembly of nuclear weapons.

In 1989, the DOE leased the remaining 6,000 acres of the original Pantex site from TTU. This land serves as a security buffer zone to part of the plant. In 1989, an event at another DOE site impacted operations at Pantex. Due to public and environmental concerns, the DOE Rocky Flats Plant in Colorado ceased serving as a plutonium processing facility. As a result of this action and because of its available facilities, Pantex was assigned to serve as a storage site for the plutonium pits from nuclear weapons.

Today, DOE owns approximately 9,100 acres of the Pantex site. TTU leases approximately 6,000 additional acres to DOE. These 6,000 acres along with 5,900 acres of the land owned by DOE are used by TTU for agricultural purposes and serve as a buffer zone to the main operational facilities at the plant. Pantex currently has five main operations: weapons assembly, weapons disassembly, weapons evaluation, research and development of high explosives, and interim storage of plutonium pits.

### **1.3 SITE DESCRIPTION**

The scope of this investigation of the perched aquifer is limited to the Zone 12 proximity. This section discusses the conditions in the Zone 12 area, which are relevant to the groundwater flow and transport modeling. Also included is a discussion of the site hydrogeology, descriptions of the contaminants present, and a description of the pilot-scale treatment system, which was installed for the investigation of the perched aquifer.

#### ***1.3.1 Zone 12 Hydrogeology***

The vadose zone beneath Zone 12 at the Pantex Plant consists partially of soils of the Blackwater Draw Formation. These soils include a mixture of sands, silts, clays, and caliche. In the Zone 12 area, the typical depth to the bottom of the Blackwater Draw Formation is 50 feet. Beneath the Blackwater Draw Formation is the Ogallala Formation. The uppermost portion of the

Ogallala Formation in the Zone 12 area consists primarily of well-sorted, poorly cemented, quartz sand. This part of the formation forms the remainder of the vadose zone.

Below the uppermost formation at a depth of approximately 220 ft. below ground surface (bgs), the formation material consists of primarily sand and gravel which is present in one or more layers that formed as a result of fluvial deposition. This part of the Ogallala Formation extends downward to the top relief of the FGZ. The FGZ is described as pink, clayey, fine-grained sandstone and has very low permeability. Because of its low permeability, the FGZ is considered a confining layer to the main unit of the Ogallala Aquifer, which is located beneath the FGZ in this area. The top of the main unit of the aquifer is at an approximate depth of 400 feet bgs. Figure 1-2 shows a generalized cross-section of the stratigraphy beneath the Zone 12 area and includes all of the features described (Argonne, 1995).

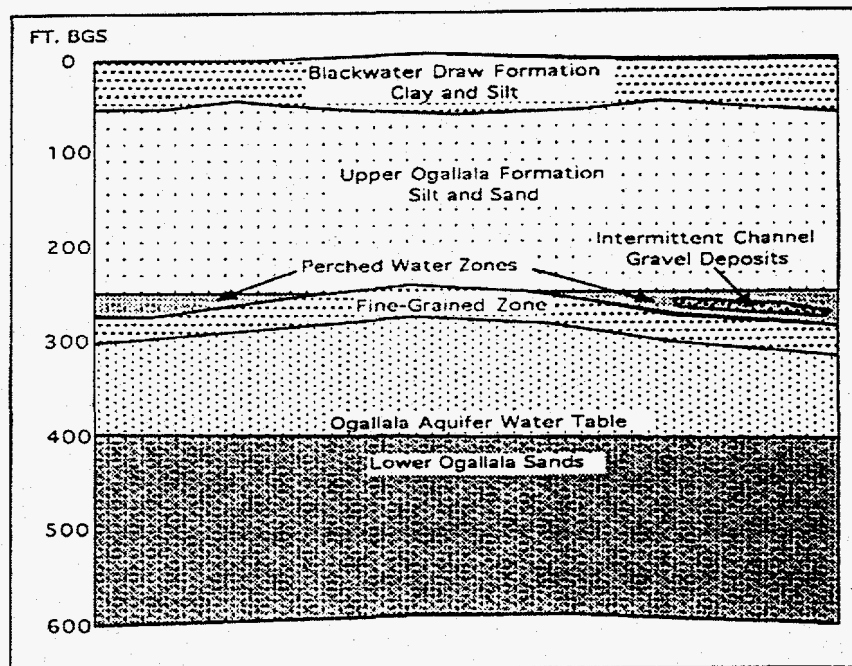


Figure 1-2: Generalized Cross-Section of the Stratigraphy in the Zone 12 Area (Kendrick, 1996)

The flow of the groundwater in the perched aquifer is influenced by the subsurface stratigraphy. In the Zone 12 area of the Pantex facility, the FGZ separates the main aquifer of the Ogallala Formation from the perched aquifer. The direction of groundwater flow within the perched aquifer is largely determined by a paleochannel formed as a result of deposition, which occurred along the relief of the top of the FGZ. Figure 1-3 shows the relief of the top of the FGZ. In this figure, the estimated elevation of the top of the FGZ decreases from the northwestern corner

to the southeastern corner. The paleochannel follows this approximate pathway and is marked by intermittent gravel deposits indicating deposition due to fluvial processes (Argonne, 1995).

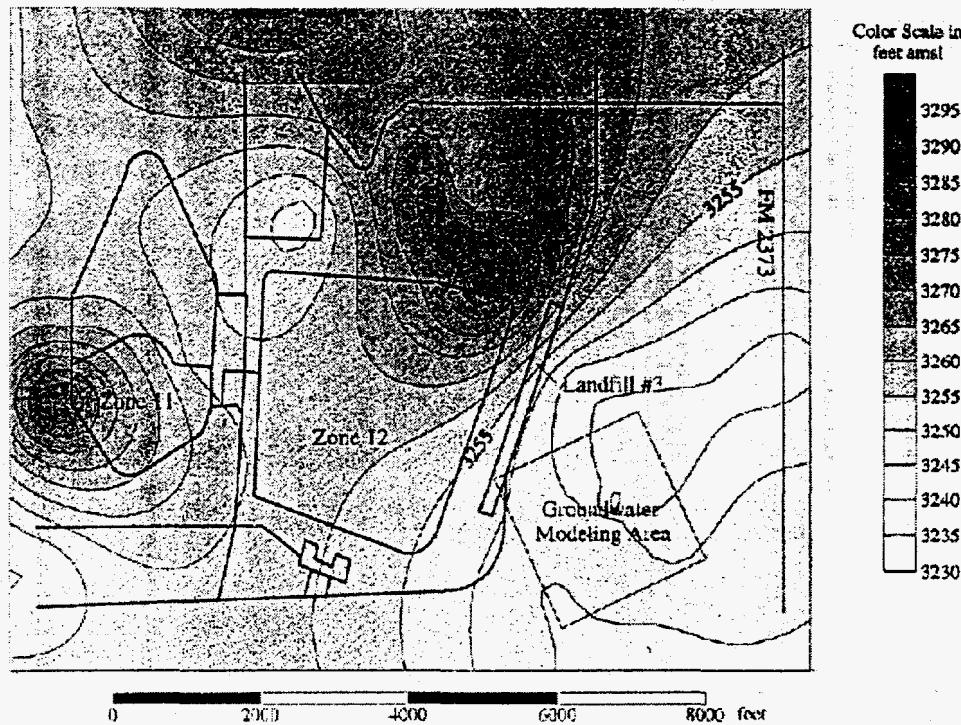


Figure 1-3: FGZ Contours (surfer file)

The groundwater in the perched aquifer flows primarily in a southeastern and southwestern direction beneath the Zone 12 area. Figure 1-4 shows contours of the water table elevation of the perched aquifer. The area, which was used in the modeling of the groundwater tracer test in the perched aquifer, is shown in both Figures 1-3 and 1-4. In the modeling area, the groundwater flow was in the southeast direction. This area was selected for the tracer test because the Zone 12 treatment system is located in the center of this area and its wells were readily available. The saturated thickness of the perched aquifer in the Zone 12 area ranges from approximately 0 to 35 feet. An aquifer cross-section was developed using boring logs and water level measurements from wells located in the Zone 12 area (Argonne, 1995). Figure 1-5 shows the locations of the wells used to develop this vertical cross-section of the perched aquifer. The cross-section runs through the modeling area. Figure 1-6 is the cross-section of the perched aquifer beneath the Zone 12 area. This figure shows the saturated thickness of the aquifer and the cross-section of the channel in which the water flows.

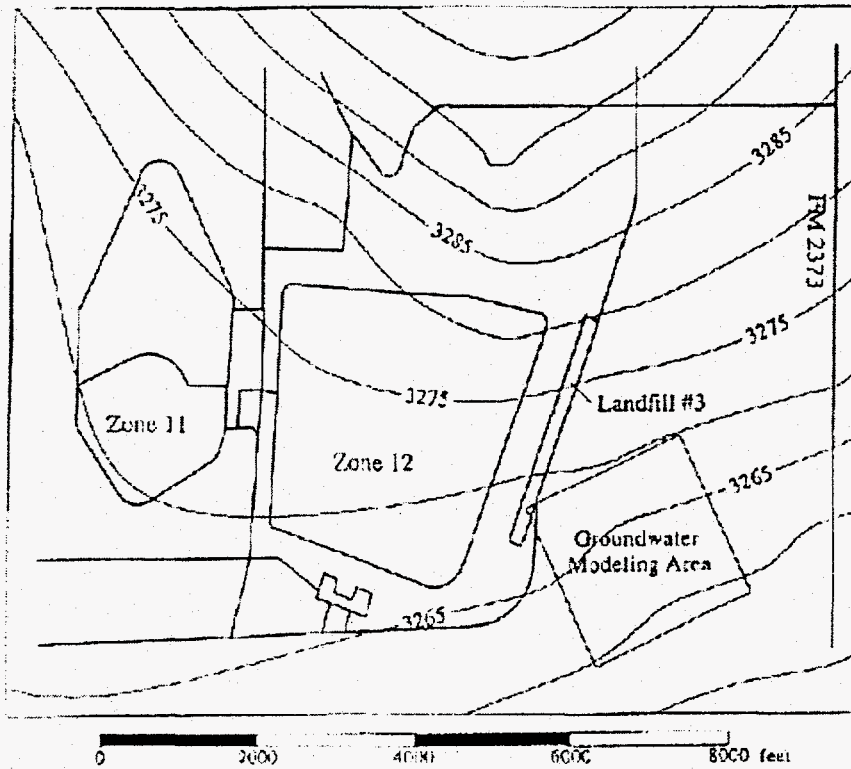


Figure 1-4: Groundwater Contours (surfer file)

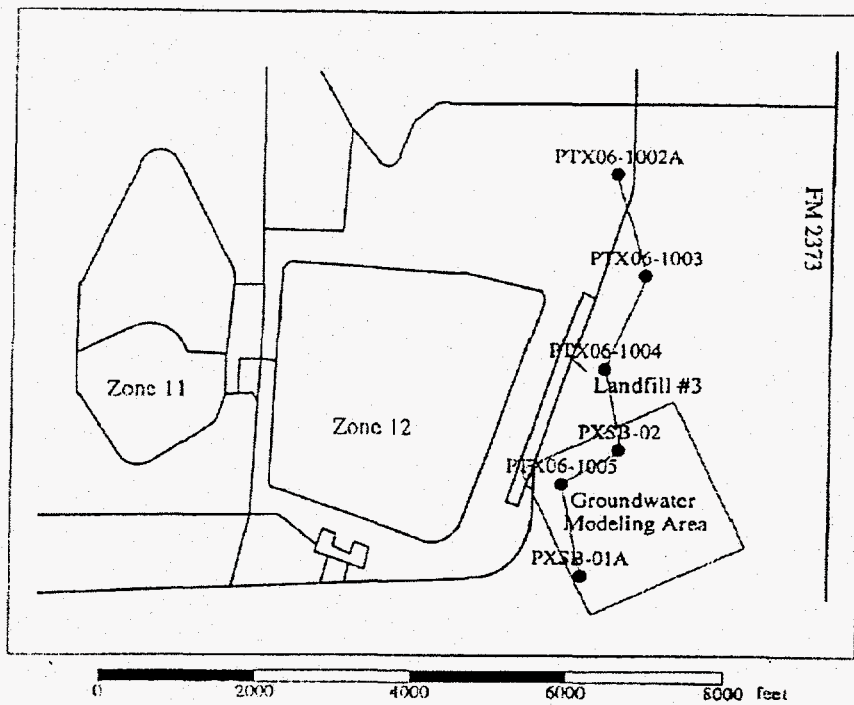


Figure 1-5: Cross-Section Location (surfer file)

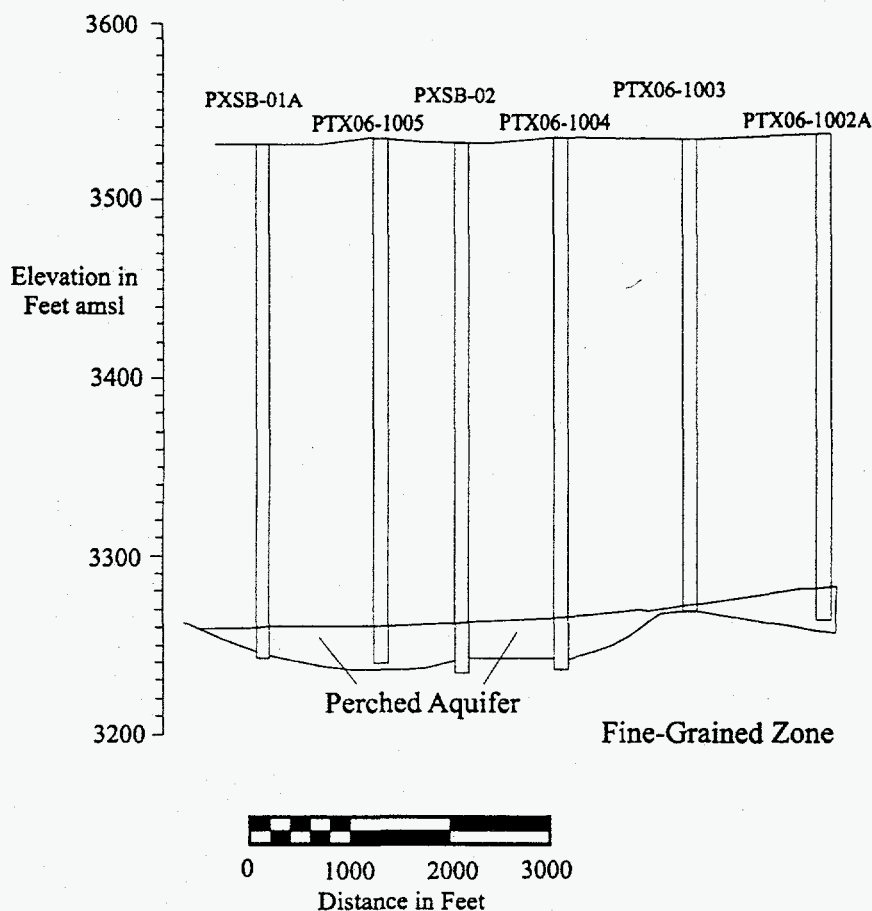


Figure 1-6: Cross-Section of the Perched Aquifer (Adapted from Argonne, 1995)

### 1.3.2 Zone 12 Contaminants

Several chemical compounds have been detected in both soil and groundwater samples from the perched aquifer in the Zone 12 area of the Pantex Plant. These chemicals include the HE compounds RDX, HMX (octahydro-1,3,5,7-tetranitro-1,3,5,7-tetraazocine), and TNT (2,4,6-trinitrotoluene). VOCs and metals (chromium) have been detected at elevated levels in the soil and groundwater as well.

Both RDX and HMX have been detected at significant concentrations in the groundwater of the perched aquifer. Analytical results from groundwater samples have indicated concentrations of RDX as high as 4.92 milligrams per liter (mg/L). HMX concentrations have been measured as high as 11.0 mg/L (Brownlow, 1995). However, RDX has a significantly lower health-based limit than HMX. The U.S. Environmental Protection Agency's (EPA) recommended drinking water limit for RDX is 2 micrograms per liter (mg/L) (U.S. Dept. of Health and Human Services, 1995); the limit for HMX is 400 mg/L (U.S. Dept. of Health and Human Services, 1994). For this reason, estimated

RDX was selected as the focus compound of this investigation. Figure 1-7 shows the RDX concentration contours prior to the 1996 tracer test for the 2000 feet by 2000 feet square area from where the flow and transport of the groundwater in the perched aquifer is simulated.

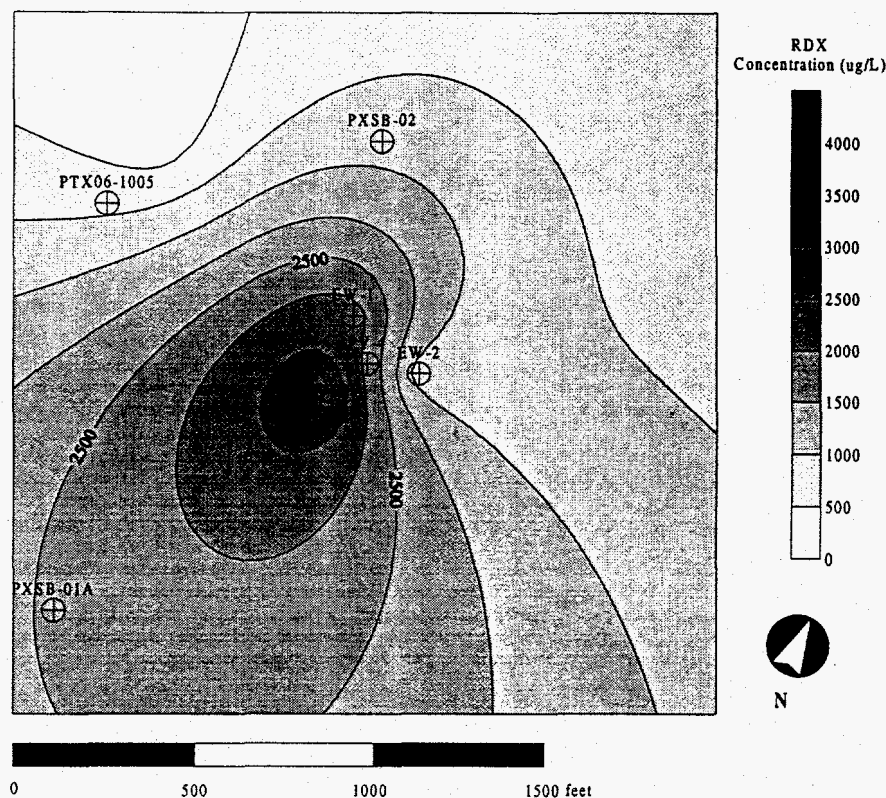


Figure 1-7: RDX Contours at the Start of the Tracer Test

The contours of the RDX concentrations in Figure 1-7 were developed using analytical data from two sources. RDX analytical data was available from groundwater samples collected from the perched aquifer at wells EW-1, EW-2, and EW-3 at the start of the tracer test. Also, RDX analytical data was available from other wells at the facility from quarterly sampling events. The closest quarterly sampling event prior to the start of the tracer test occurred in April 1996. RDX analytical results from the seven wells in the closest proximity to the treatment site were obtained from the April 1996 sampling event. These data were used along with that from EW-1, EW-2, and EW-3 to develop the initial RDX concentration contours for the tracer test.

The RDX concentrations in the groundwater from this part of the plant range from values less than 500 ug/L to almost 4000 ug/L. As shown in Figure 1-7, some of the highest RDX concentrations have been detected close to the center of this area.

### ***1.3.3 Zone 12 Treatment System***

A pilot-scale, dual-phase extraction system was installed to the southeast of Zone 12 at the Pantex Plant in the fall of 1995 as a part of the Zone 12 Treatability Study. The purpose of the system is to aid in the investigation of the perched aquifer. The system consists of seven wells and the treatment system for contaminated liquids and vapors.

Three of the wells, EW-1, EW-2, and EW-3, are extraction wells. Each extraction well has a two-horsepower pump and 2 separate sections of screen. Also, each of the extraction wells has two sections of piping. The first section, which consists of approximately 200 feet of screen in the vadose zone, is used for the extraction of VOCs. The second section of piping in each extraction well is screened from a depth of approximately 10 feet above the water table through the perched aquifer; groundwater from the perched aquifer is pumped from this section and then piped to the treatment system.

The other four wells, PV-1, PV-2, PV-3, and PV-4, are passive vent wells. Each passive vent well has one screened section, which extends from approximately twenty feet bgs down through the vadose zone and the perched aquifer. Figure 1-8 shows the layout of these seven wells of the Zone 12-treatment system. Passive vent Well PV-4 is located in the center of the other six wells.

The treatment system is a carbon adsorption system. Vapors from the vadose zone and groundwater from the perched aquifer can be extracted from the subsurface. Each phase can then be routed to a separate carbon adsorption reactor where contaminants are removed. The groundwater can be re-injected into the subsurface once it has been treated.

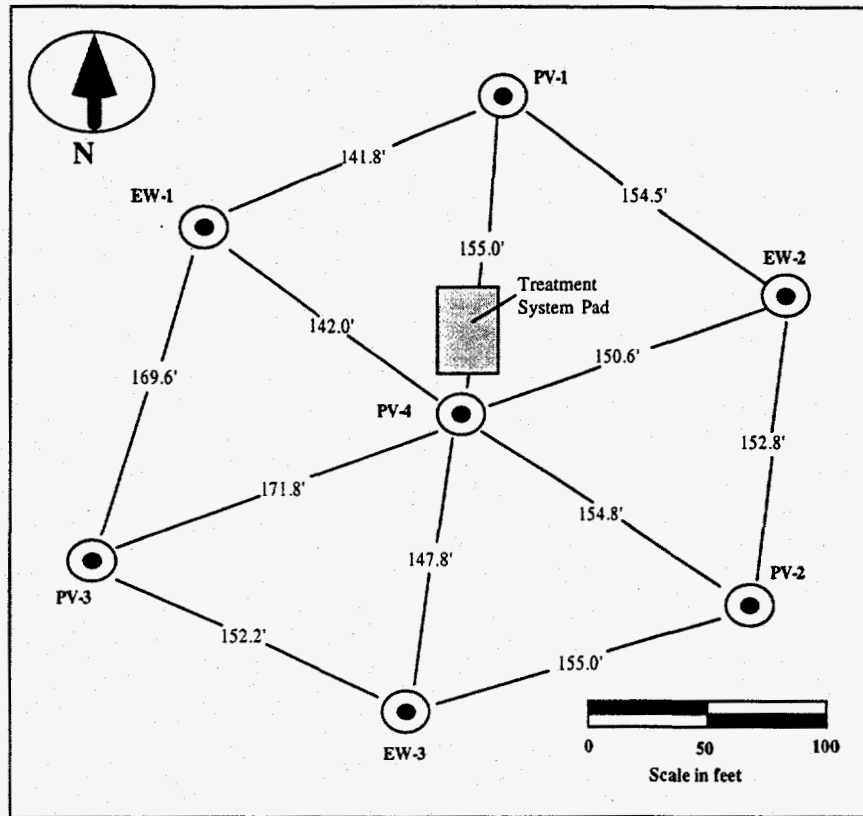
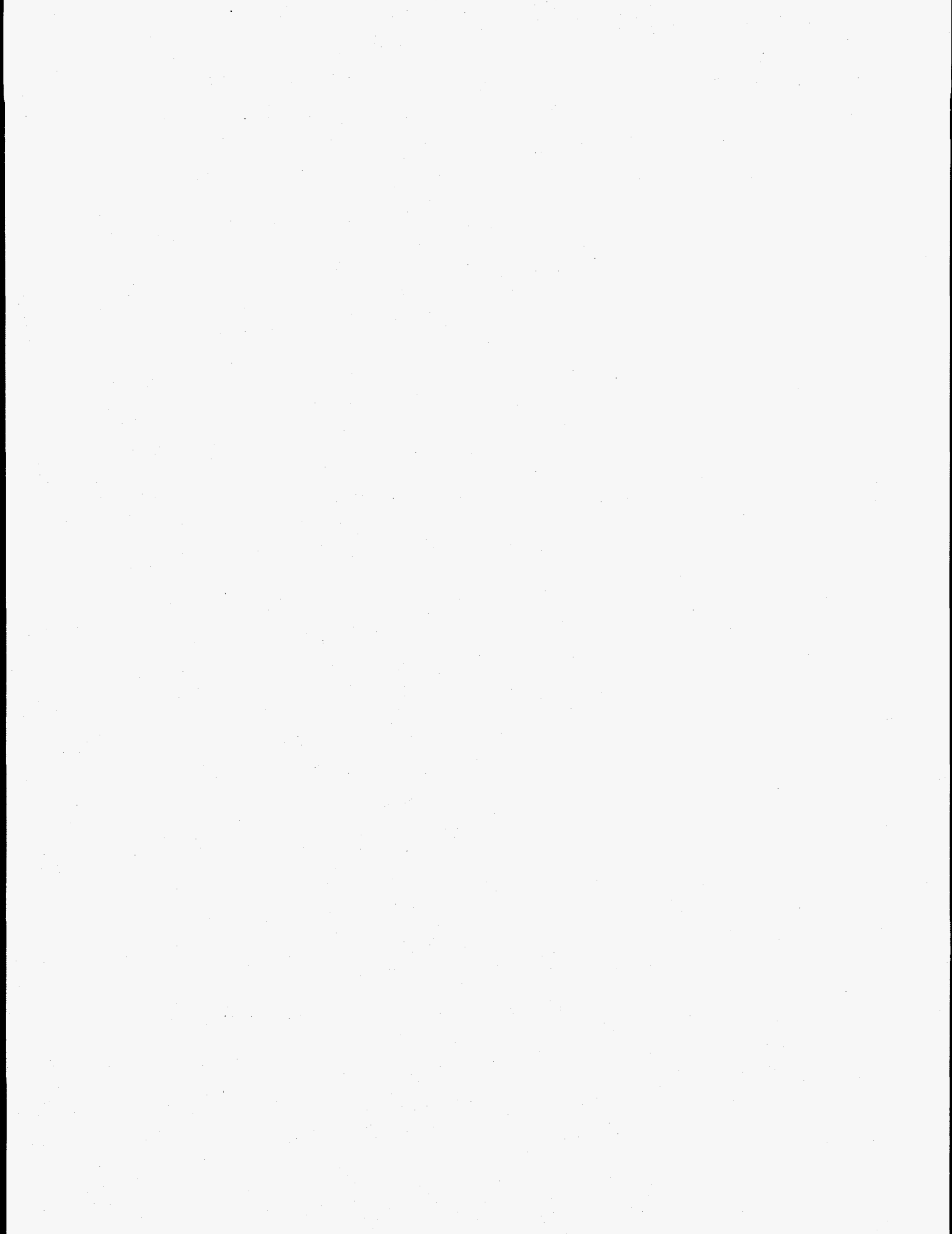


Figure 1-8: Layout of Zone 12 Treatment System (Adapted from Mason & Hanger, 1995)



## **2. ZONE 12 PERCHED AQUIFIER TRACER TEST**

A tracer test was conducted in the perched aquifer beginning at 3:00 p.m. on July 15, 1996, and ending at 1:00 p.m. on September 19, 1996, at the Zone 12 treatment system. The total time of the test was approximately 65.9 days. The purpose of conducting the tracer test was to evaluate the effectiveness of the contaminated groundwater extraction system at the treatability study site. This chapter outlines the important factors of the tracer tests, which were used in the modeling of the perched aquifer. Included is a brief description of the events of the tracer test and a description of the data collected during the test which was used in the flow and RDX transport modeling.

### **2.1 EQUIPMENT INSTALLATION**

A schematic drawing of the site arrangement can be found in Figure 2-1. A 500-gallon plastic tank was brought to the site to use as a holding tank for the tracer solution. Plastic tubing, 0.5-inches in diameter, carried the solution to a regulating pump and flow meter, then to PV-4 to combine with the treated effluent. The injected water was carried from the effluent line of the treatment system by a two-inch PVC pipe encased in 4-inch PVC for secondary containment. The tracer injection pump was synchronized with the treatment system transfer pump by using solenoid valves at the tracer tank and at PV-4. Flexible 1-1/2-in PVC hose, 270 foot long, carried the treatment system treated water down PV-4. A two-inch diameter, 10-foot long, well screen allowed the mixed tracer solution and treated water to enter the perched aquifer within the lower portion of the screened interval of the well. In Situ, Inc., model number PXD-260, pressure transducers, were installed in PV-1, 2, 3, and 4 to detect changes in water surface elevation. Well Sentinel data loggers (In Situ, Inc.) were connected to the transducers in PV-1, 2, and 3, while a Hermit SE 1000C was connected to the transducer in PV-4.

### **2.2 THE TRACER TEST**

The tracer test was divided into two injection phases. During the first phase, which lasted 24.1 days, a potassium bromide (KBr) solution was injected into the perched aquifer. Bromide, being a conservative species (a conservative tracer is assumed not to adsorb to soil), will transport at the same rate that the groundwater travels.

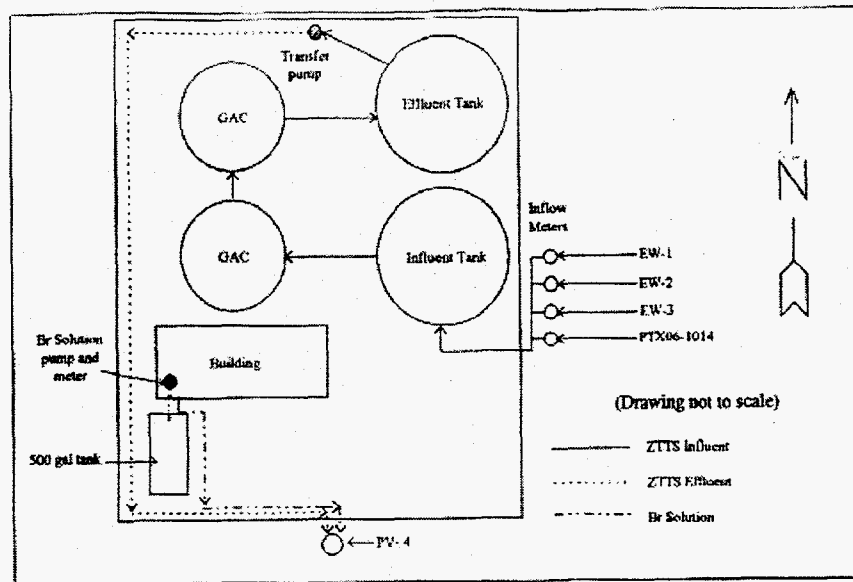


Figure 2-1: Schematic Drawing of the Site Arrangement

The KBr solution was prepared in batches using 32 lbs. of photo-grade KBr (Moore-Tech Industries) mixed with 50 gallons of reverse osmosis purified water. This mixture reflects an average concentration of 50 g/L of bromide. The mixture was hauled in 55-gallon drums to the site and transferred into the 500-gallon holding tank. The ability of bromide to remain in solution at such a high concentration was verified at the TTU Environmental Sciences Laboratory (ESL) by allowing a similar solution to stand for two weeks. When the KBr concentration was tested over time, repeatable results were obtained; therefore, a stirring device was not required in the holding tank.

The KBr solution was mixed with the treatment system effluent in PV-4 to cause a diluted target bromide concentration of 100 mg/L. This dilution was achieved by regulating the flow rate of the KBr solution pump to 0.2 percent of the treatment system effluent flow rate. The average background Br concentration in the perched aquifer water was approximately 1 mg/L, which contributed little to the Br concentration of the mixture.

The estimated average injection rate throughout the test at Well PV-4 was 70 gpm for 28 minutes of every hour. This injection rate was determined by the performance of the transfer pump which delivered effluent from the treatment system to Well PV-4. The daily injection volumes are shown in Figure 2-2. For modeling purposes, this injection rate was averaged to 32.7 gpm for 60 minutes of every hour. Averaging of the flow rate was done to represent the injection as a constant rate. Over the duration of the test, the effect of the averaged injection rate on the groundwater of

the perched aquifer was the same as injection at the higher rate for the fraction of each hour. For the entire duration of the tracer test, perched aquifer water was pumped from three of the wells, EW-1, EW-2, and EW-3, and routed to the treatment system. The pumping rate for each of the three wells was an approximate rate of 10 gpm for 60 minutes each hour.

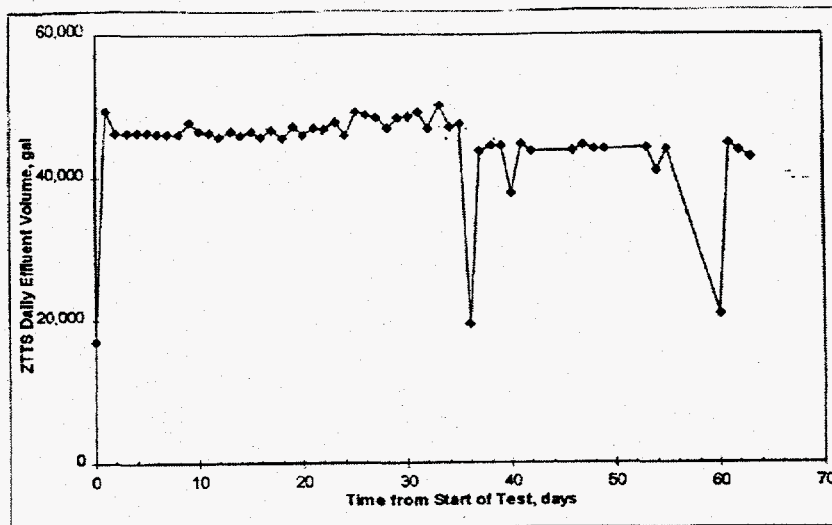


Figure 2-2: Daily Injection Volumes

Two power outages of significant time occurred during the tracer test. No injection or withdrawal in the aquifer took place during the power outages. The first power outage occurred on Day 36 of the tracer test. Due to an error with the data logger in Well PV-4, water elevations were not being recorded at this time and the exact length of this outage could not be determined. For modeling purposes, the outage was estimated to last one day. Examination of the water elevation data recorded by the data logger for Well PV-4 provided a good estimate of the length of the second power outage, which was 2.07 days, occurring between Day 57 and Day 60 of the test. The modeling accounts for these two periods when the pumps were not operating.

Toward the end of the test after water without any tracer had been injected for several days, there were some small concentrations of bromide (less than 20 mg/L) measured in the injected water resulting from the use of re-circulated water which had passed through the treatment system. Because bromide is not removed in the treatment system, it was detected in the effluent of the treatment system following breakthrough of the compound in the pumping wells. This water was then used as influent to the injection well, PV-4. Due both to the late time in the tracer test when this occurred and to the low bromide concentrations, the additional injected bromide had no effect

on the bromide breakthrough curves produced from measured concentrations at Wells EW-1, EW-2, and EW-3. Daily bromide concentrations in the injected water are shown in Figure 2-3.

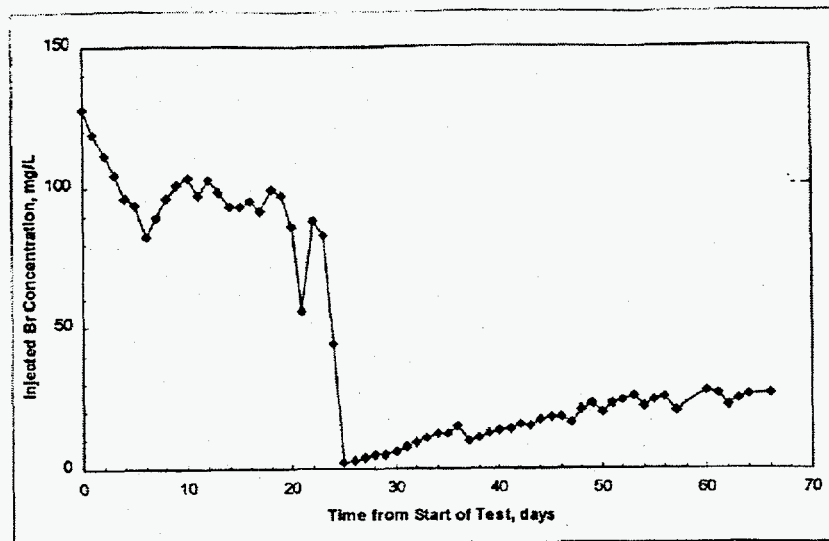


Figure 2-3: Daily Bromide Concentrations

### 2.3 TRACER TEST MONITORING

Monitoring during the tracer test consisted primarily of bromide, RDX, and water level measurements. Bromide and RDX concentrations were measured in the effluent from the three pumping wells, EW-1, EW-2, and EW-3, and in the effluent from the treatment system. Approximately one quart was collected from each location in separate glass sampling jars. A plastic lid with Teflon liner was used to seal each sampling jar, and each sampling jar was labeled immediately with the date, time, and the name of the sample location. The samples were stored for no more than 14 days at approximately 21° C. The samples were not exposed to direct sunlight during the storage period. Before use, the glass sampling jars were cleaned using a mechanical dishwasher, then heat dried. Every seventh day, a duplicate set of samples was collected for laboratory analyses at the ESL. Daily bromide samples were analyzed at the field site using an ion selective electrode (ASTM D 1246). The detection range of 0.5 to 1000 mg/L was applicable to the tracer concentration expected in the samples collected; therefore, dilutions were not required. The standards used to calibrate the equipment and validate the test procedure were 10, 30, 50, 75, and 100 mg/L.

An Orion model 920A with a bromide selective electrode was used in conjunction with a reference electrode to measure the concentration of bromide present in the samples. The Orion was

calibrated at the beginning of each set of 12 tests. A standard and a blank were inserted into the series for measurement after every four tests. Prior to calibration or measurement, two mL of 5.0 M NaCl solution was added to each 100-mL sample or standard tested. This step was done to equalize the ionic strength of the solutions.

Duplicate water samples were collected once each week of the test and sent to TTU's ESL for confirmation of bromide concentrations with ion chromatography using EPA method 300.00. Figures 2-4, 2-5, and 2-6 show the daily and weekly bromide concentrations in milligrams per liter (mg/L) measured from the water extracted at EW-1, EW-2, and EW-3 during the tracer test, respectively.

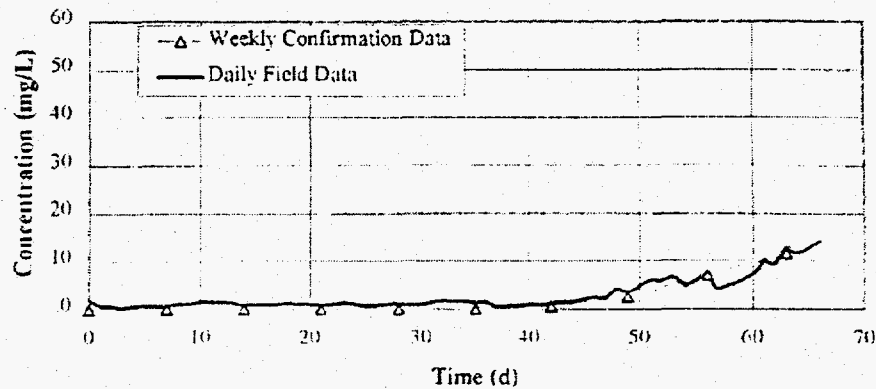


Figure 2-4: Weekly Bromide Concentrations

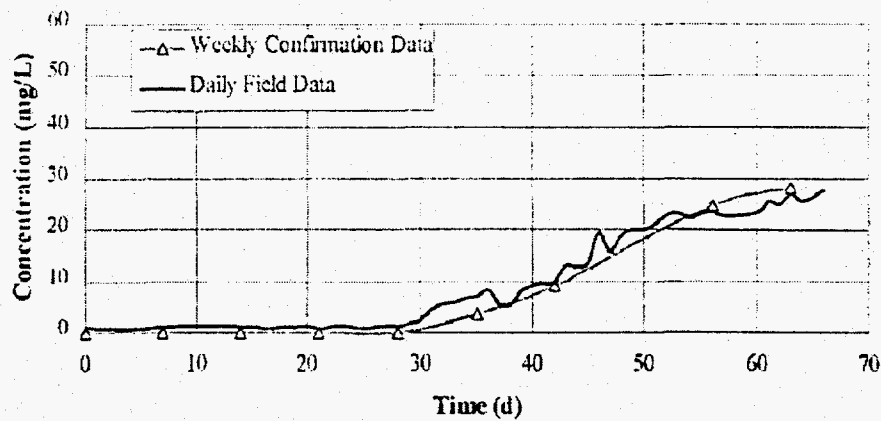


Figure 2-5: Weekly Bromide Concentrations

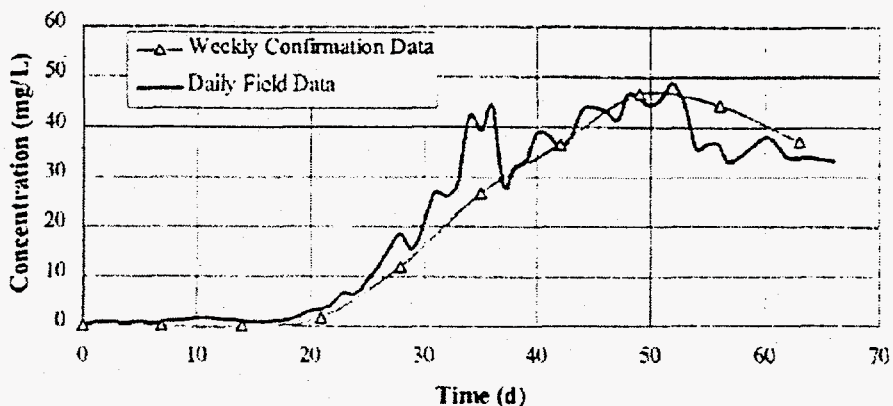


Figure 2-6: Weekly/Daily Bromide Concentrations

The breakthrough curves for each of the wells correspond to the expected results of bromide measurements. The expected outcome was for breakthrough to occur and tracer concentration to increase to a peak; beyond the peak, the tracer should have decreased until background concentration was reached. These three figures show breakthrough of the bromide tracer began at approximately Day 42 at Well EW-2, Day 30 at EW-2, and Day 20 at EW-3. For Well EW-3, the bromide breakthrough curve peaked around Day 50. The tracer test did not run long enough for peaks to be surpassed in breakthrough curves from EW-1 and EW-2.

The daily field data and weekly confirmation data for EW-1, EW-2, and EW-3 agreed reasonably well. There were a couple of times during the test, as shown in Figure 2-6 for Well EW-3, when concentrations between the daily and weekly samples differed by up to 14 mg/L. However, the differences between the two breakthrough curves were typically less than 5mg/L for all three of the wells.

Daily water samples were collected and analyzed at the field site using DTECH field kits (EM Science/Strategic Diagnostics, Inc., Gibbstown, NJ) which measures free RDX in water. The EPA approved the RDX method in 1994 as SW-846-4051. The DTECH tests consist of combining RDX-specific antibodies, covalently linked to small latex particles, an RDX analog that is covalently linked to alkaline phosphate, and free RDX in the water sample. The latex particles are collected on a filter device, then washed; an enzyme substrate is then added to the particles. Color is produced from this reaction. A hand-held reflectometer called a Dtechtor measures the color of the sample tested in comparison with a standard. A ratio between the two identifies the concentration of RDX in the sample.

Duplicate water samples were collected once each week and sent to the ESL for confirmation of RDX analysis using high performance liquid chromatography (HPLC) according to

EPA method SW-846-8330. Figures 2-7, 2-8, and 2-9 show the RDX concentrations in micrograms per liter measured in both daily and weekly samples from Wells EW-1, EW-2, and EW-3.

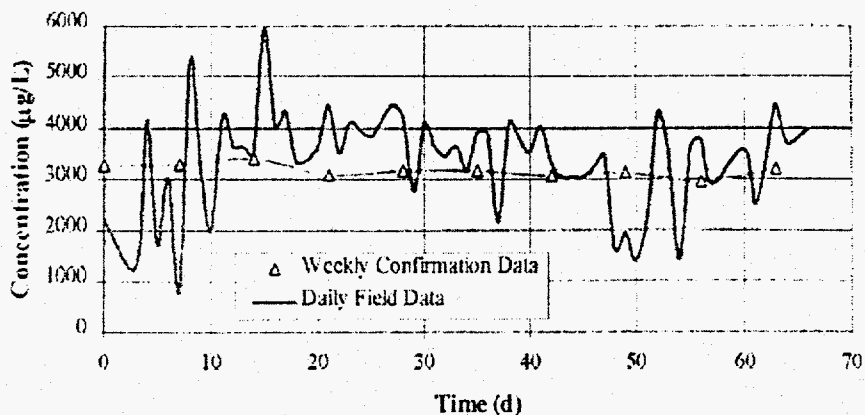


Figure 2-7: RDX Concentrations

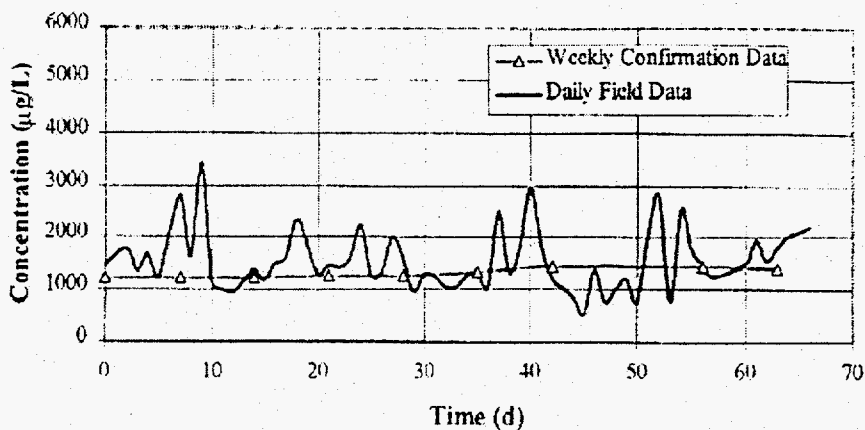


Figure 2-8: RDX Concentrations

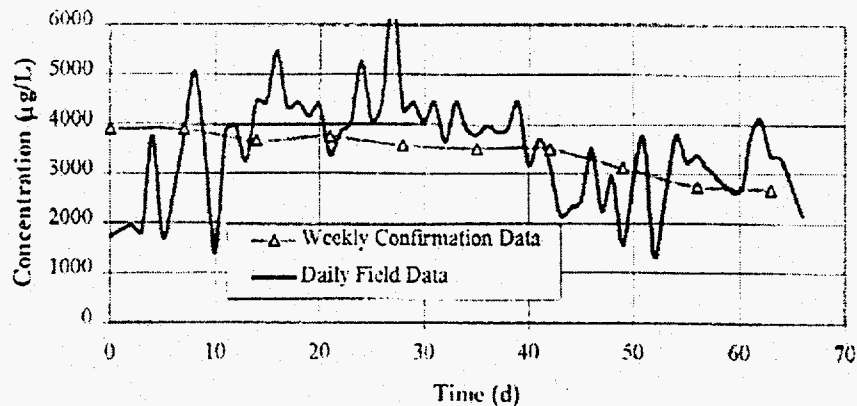
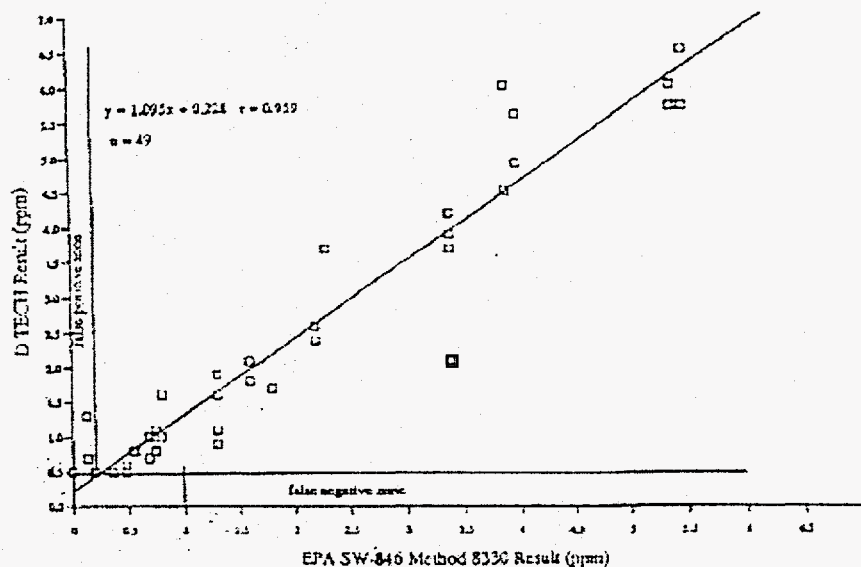


Figure 2-9: RDX Concentrations

The concentrations of the three RDX curves shown remained relatively constant until the breakthrough of the water that was injected in PV-4 occurred. At that time, the RDX concentrations in the samples should have decreased. The trend also depended upon the initial RDX contours in

the perched aquifer at the beginning of the tracer test. Results from the weekly confirmation samples sent to ESL for RDX analysis produced the expected trend in the clean water breakthrough curves. For samples collected from EW-1 and EW-2, the RDX concentration in the weekly samples remained fairly constant throughout the duration of the tracer test. This indicated that breakthrough of the injected water had not occurred by the time the test ended. The concentrations measured in weekly samples from Well EW-3 decreased in magnitude from approximately 4000 g/L at the start of the test to 2700 g/L at the end of the test. This decrease was the result of the breakthrough of injected water containing no RDX at EW-3.

The curves produced from RDX concentrations measured daily in the field with DTECH kits did not exhibit the expected trend. The concentrations of RDX measured in all three of the wells tend to vary substantially over the course of the test. Figure 2-10 shows results from a study whose data was provided by the DTECH manufacturer where 49 water samples were analyzed with the DTECH method and then sent to a lab for analysis using EPA Method 8330 (Teaney and Hudak, 1994). There was some variability in concentrations measured using the two methods. However, the DTECH kits gave reasonable results compared to those from HPLC analysis.



**Figure 2-10: Teaney and Hudak (1994) Comparison of DTECH RDX Test Results vs. EPA SW-846 8330 Results**

The same analysis was conducted here with the RDX concentrations measured from samples collected during the tracer test in the perched aquifer at the Pantex site. A total of 29 weekly confirmation samples were analyzed for RDX using EPA Method 8330 with HPLC at the ESL from Wells EW-1, EW-2, and EW-3. These results were compared to the daily samples analyzed with

the DTECH kits from the same well and day. Each of these points is plotted on Figure 2-11 and a best-fit line is inserted using linear regression. The correlation coefficient for this line was calculated to be 0.612 indicating a significant variation between the results of the two methods of analysis. This is a much lower value than the 0.959 provided by the manufacturer for a separate project.

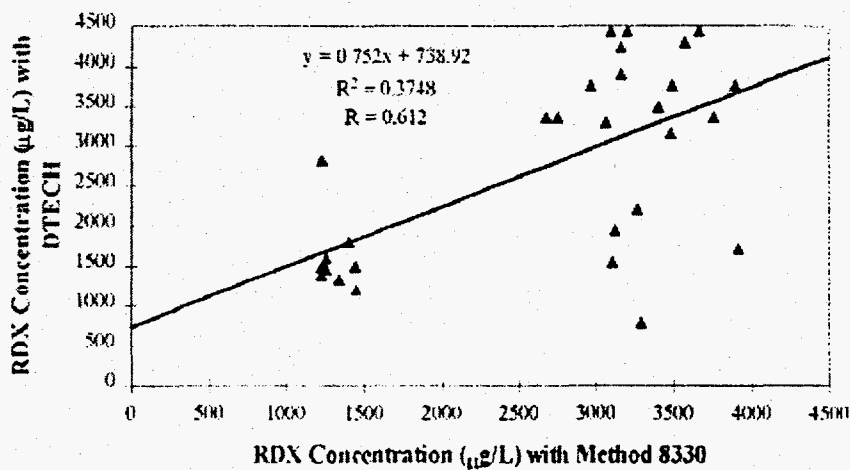


Figure 2-11: Comparison of DTECH RDX Results to Method 8330

Due to the variation between the two methods, only the data from the weekly confirmation samples were used to model the transport of the RDX in the groundwater of the perched aquifer. Water levels were monitored during the tracer test in the four passive vent wells, PV-1, PV-2, PV-3, and PV-4. Pressure transducers in each well connected to data loggers recorded changes in the water elevations. Figure 2-12 shows the elevations calculated from recorded data for wells PV-1, PV-2, and PV-3 over the duration of the test. This figure shows a gradual increase in the water elevations in these three wells during the test. This resulted from the injection of water at PV-4. Data from the transducers show that the water elevation increased by approximately one foot in Well PV-1 and by approximately two feet in both PV-2 and PV-3.

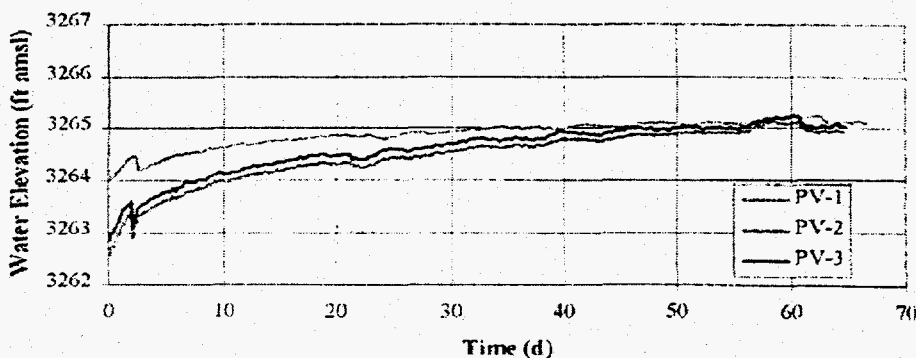


Figure 2-12: PV-1, PV-2, and PV-3 Water Elevations During the Tracer Test

Water was injected approximately 28 minutes out of every hour during the tracer test, resulting in a pattern of increasing and decreasing water elevations in Well PV-4. For groundwater modeling purposes, a one-hour moving average analysis of the water elevation data from Well PV-4 was conducted. The result of the moving average analysis is shown in Figure 2-13.

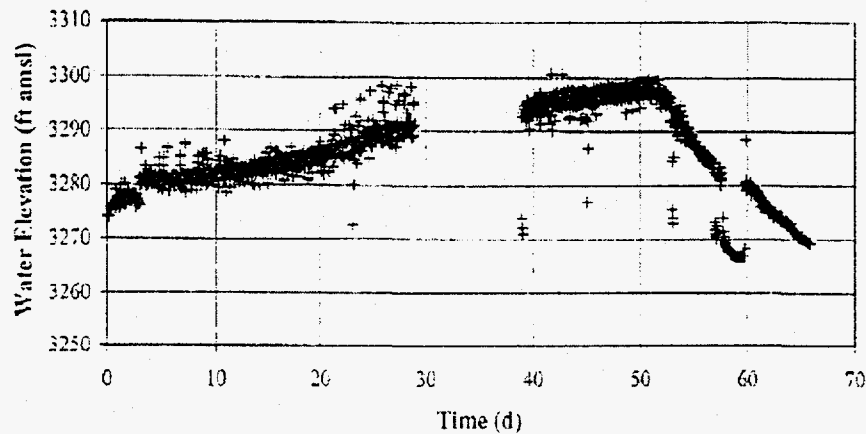


Figure 2-13: One Hour Moving Average of PV-4 Water Elevation

Most points produced in the moving average lie along a path which shows that the water level increased up to an elevation of approximately 3298 feet above mean sea level at Day 52 of the tracer test. The water elevation then decreased in PV-4 during the remainder of the test. The gap shown in the data from approximately Day 29 to Day 39 corresponds to the period when the data logger was not operating in PV-4. The drop in water elevation shown between Days 57 and 60 corresponds to the second power outage that occurred during the test.

Figure 2-14 summarizes the pumping rates for the wells in the treatment system and indicates the monitoring data that was collected during the tracer test of the perched aquifer. This information was used in the groundwater flow and RDX transport modeling.

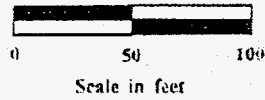
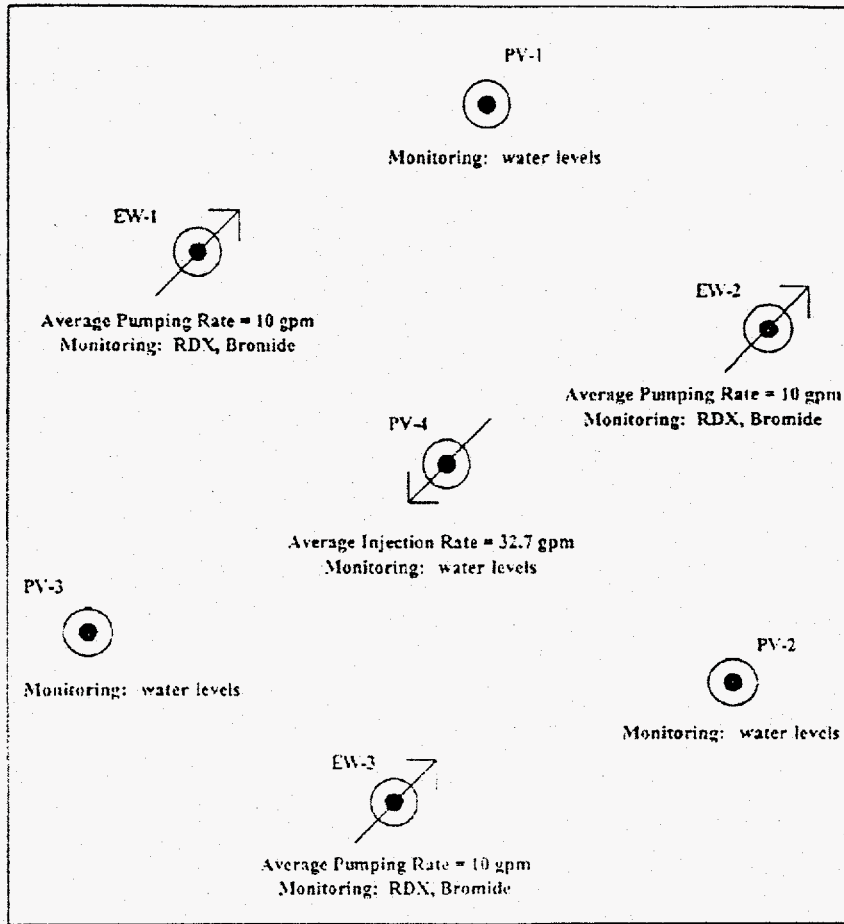
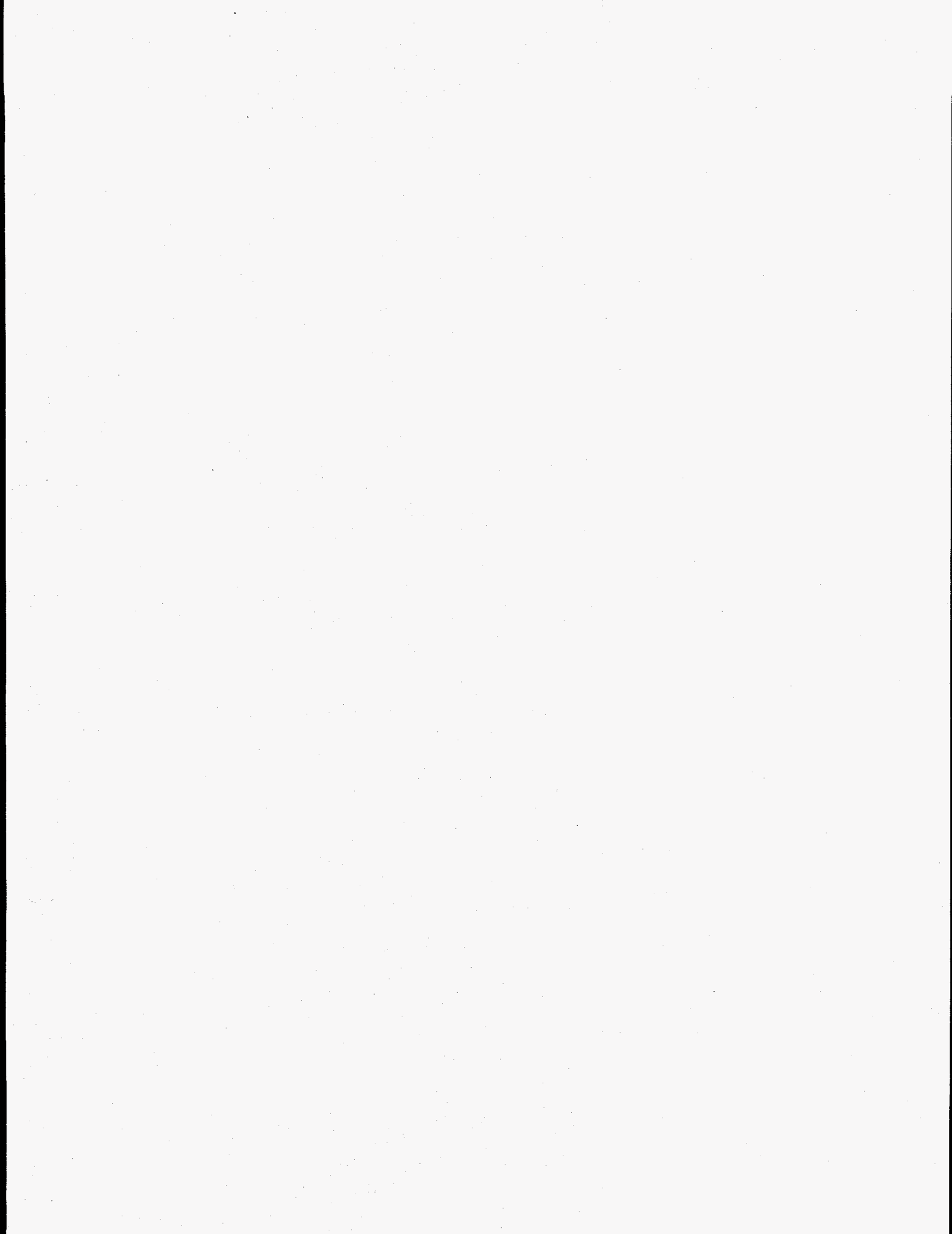


Figure 2-14: Pumping Rates and Monitoring During Tracer Test



### 3. THE GROUNDWATER MODELS

In the treatment area, the flow characteristics of the perched aquifer were modeled using the United States Geological Survey (USGS) Modular Three-Dimensional Groundwater Flow Model (MODFLOW) (McDonald and Harbaugh, 1988). Groundwater flow and head data computed in MODFLOW were then used to model the chemical transport in the Modular Three-Dimensional Transport Model (MT3D) (Zheng, 1990). Modelcad<sup>386™</sup> is the preprocessor used in this project to create the input files for both MODFLOW and MT3D. The following sections provide a brief description of each of the models, the methodologies upon which they are based, and the means of linking them. Additional information on MODFLOW and MT3D beyond that presented in this section is found in McDonald and Harbaugh, (1988d) and Zheng (1990).

#### 3.1 MODFLOW

MODFLOW is a three-dimensional (3-D), finite difference, groundwater flow model. Flow characteristics are determined using an iterative procedure to find a solution to the following partial-differential equation.

$$\frac{\partial}{\partial x} \left( K_{xx} \frac{\partial h}{\partial x} \right) + \frac{\partial}{\partial y} \left( K_{yy} \frac{\partial h}{\partial y} \right) + \frac{\partial}{\partial z} \left( K_{zz} \frac{\partial h}{\partial z} \right) - W = S_s \frac{\partial h}{\partial t} \quad (\text{Equation 3.1})$$

where

- x, y, z = Cartesian coordinates whose axes are aligned with major axes of hydraulic conductivity (L)
- K = hydraulic conductivity (L/T)
- S<sub>s</sub> = specific storage (1/L)
- W = source/sink term represented as volumetric flux per volume of porous media (1/T)
- h = hydraulic potential (L)

Equation 3.1 describes the 3-D transient movement of groundwater through a heterogeneous porous media. It is assumed that the fluid has a constant density.

The terms on the left-hand side of the equation represent the flow that occurs into and out of a cell. When  $W$  is positive, it represents a sink. The right hand side of the equation represents the rate change in storage that occurs in a cell.

Because of the complexity of most systems, Equation 3.1 cannot usually be solved directly. Instead, a numerical solution, such as the finite difference method used in MODFLOW must be used. The finite difference method for solving groundwater flow problems is based on the difference form of Equation 3.1, which is shown as Equation 3.2.

$$\begin{aligned}
 & K_{i-1,j,k} \Delta c_j \Delta l_k \frac{(h_{i-1,j,k,t} - h_{i,j,k,t})}{\Delta r_{i-1/2}} + K_{i,j,k} \Delta c_j \Delta l_k \frac{(h_{i,j,k,t} - h_{i+1,j,k,t})}{\Delta r_{i-1/2}} + \\
 & K_{i,j-1,k} \Delta r_i \Delta l_k \frac{(h_{i,j-1,k,t} - h_{i,j,k,t})}{\Delta c_{j-1/2}} + K_{i,j,k} \Delta r_i \Delta l_k \frac{(h_{i,j,k,t} - h_{i,j+1,k,t})}{\Delta c_{j-1/2}} + \\
 & K_{i,j,k-1} \Delta r_i \Delta c_j \frac{(h_{i,j,k-1,t} - h_{i,j,k,t})}{\Delta l_{k-1/2}} + K_{i,j,k} \Delta r_i \Delta c_j \frac{(h_{i,j,k,t} - h_{i,j,k+1,t})}{\Delta l_{k-1/2}} + \\
 & q_{i,j,k,t} = S_{s,i,j,k} \Delta r_i \Delta c_j \Delta l_k \left( \frac{h_{i,j,k,t} - h_{i,j,k,t-1}}{\Delta t} \right)
 \end{aligned}
 \tag{Equation 3.2}$$

where

- $K_{i,j,k}$  = hydraulic conductivity of cell  $i, j, k$  (L/T)
- $h_{i,j,k,t}$  = hydraulic potential in cell  $i, j, k$  (L)
- $q_{i,j,k,t}$  = source/sink term for cell  $i, j, k$  at time  $t$  (L<sup>3</sup>/T)
- $S_{s,i,j,k}$  = specific storage of cell  $i, j, k$  (1/L)
- $\Delta r_i$  = width of row  $i$  (L)
- $\Delta c_j$  = width of column  $j$  (L)
- $\Delta l_k$  = width of layer  $k$  (L)

The finite-difference method applies Equation 3.2 to every cell of a given grid, which represents the groundwater system. The grid consists of rows, columns, and layers as illustrated in Figure 3.1.

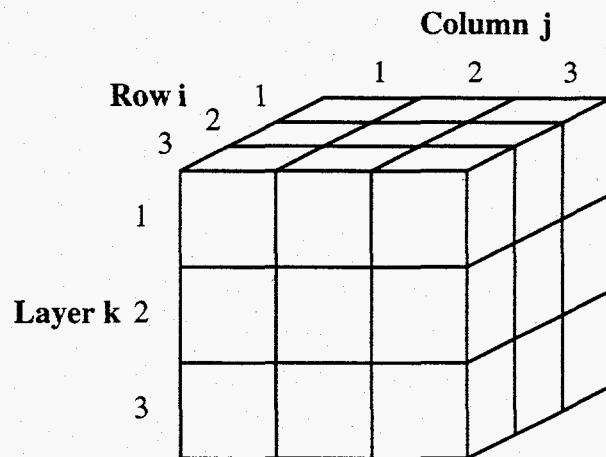


**Figure 3-1:** Row, Column, and Layer Configuration in a Finite-Difference Grid (Adapted from McDonald and Harbaugh, 1988)

MODFLOW uses a block-centered flow grid to compute the finite-difference solution. This means that the node of any individual cell is located in the center of blocks formed by parallel grid lines. Figure 3.2 illustrates the block-centered grid format. The node is the reference at the center of a given cell upon which the calculations are based.

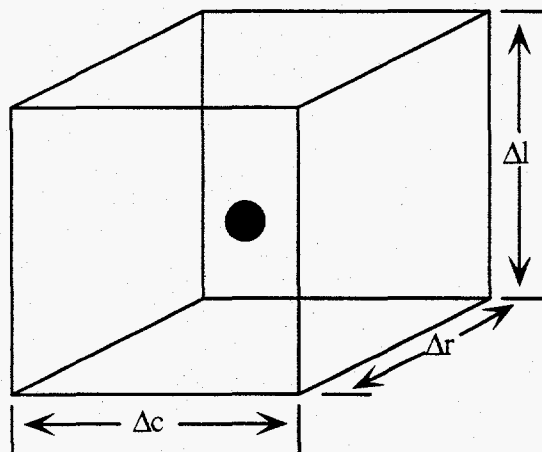


**Figure 3-2:** Block-Centered Cell Formation (Adapted from McDonald and Harbaugh, 1988)

Each cell in a finite-difference grid in MODFLOW may have adjacent cells to each of its six faces. Flow may occur in a given cell between itself and each of these six adjacent cells. Figure 3.3

illustrates how flow is represented in the model from one cell to another. It shows flow from cell  $i, j-1, k$  to cell  $i, j, k$ . The distance between the two nodes is represented as  $\Delta x_{j-1/2}$ .

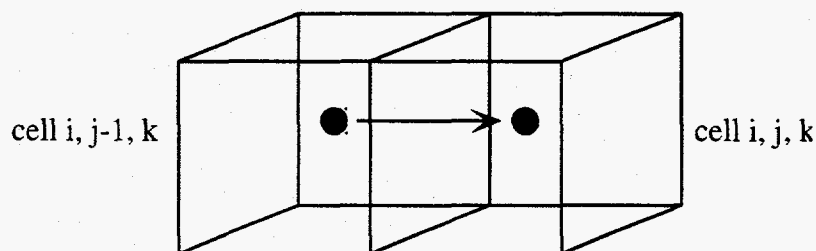


**Figure 3-3:** Flow through Cells in a Finite-Difference Grid (Adapted from McDonald and Harbaugh, 1988)

Appropriate boundary conditions must be assigned to the grid before solving the finite difference equation. Once boundary conditions are assigned, an iterative procedure is used in MODFLOW to find an appropriate solution for each cell of the grid. The iterative procedure consists of assigning an initial trial solution and calculating a new trial solution whose values are closer to the correct solution. This procedure is repeated until the solution meets an indicated accuracy criterion. This iterative solution procedure yields only an approximation of the actual result to the finite-difference equation that is generally satisfactory if it meets the desired accuracy criterion.

### 3.2 MT3D

MT3D utilizes the flow solution obtained from MODFLOW to determine the movement of contaminants in groundwater. The 3-D transport of a constituent in groundwater is described by the following partial-differential equation:

$$R \frac{\partial C}{\partial t} = -\frac{\partial}{\partial x_i} (v_i C) + \frac{\partial}{\partial x_i} \left( D_{ij} \frac{\partial C}{\partial x_j} \right) + \frac{q_s}{n} C_s - \lambda \left( C + \frac{\rho_s}{n} \bar{C} \right) \quad (\text{Equation 3.3})$$

where

- R = retardation factor (-)
- C = dissolved contaminant concentration in groundwater ( $M/L^3$ )
- t = time (T)
- $x_i$  = distance along respective Cartesian coordinate axis (L)

$D_{ij}$	=	dispersion coefficient ( $L^2/T$ )
$v_i$	=	seepage velocity ( $L/T$ )
$n$	=	porosity (-)
$q_s$	=	source/sink term represented as volumetric flux per volume of porous media ( $1/T$ )
$C_s$	=	concentration in sources/sinks ( $M/L^3$ )
$\lambda$	=	first-order reaction rate constant ( $1/T$ )
$\rho_s$	=	bulk density of the porous media ( $M/L^3$ )
$\bar{C}$	=	concentration sorbed to the porous media ( $M/M$ ).

On the right hand side of Equation 3.3, the first term represents the change in concentration that occurs as a result of advective transport, or transport with the flow of the groundwater. The second term represents the dispersive transport which is the mechanical phenomenon in which longitudinal, transverse, and vertical spreading of the solute particles occurs as a result of variations in groundwater flow velocity at the microscopic scale and by diffusion. The third term represents changes in the concentration that happen when sources and/or sinks are present. The  $q_s$  represent a source when its value is positive. Although  $q_s$  is related to  $W$  by  $q_s = -W$ , the notations for the two variables are maintained in this chapter as they are presented in McDonald and Harbaugh (1988) and Zheng (1990). The last term on the right hand side of Equation 3.3 is the decay term. This accounts for the disappearance of a constituent due to radioactive decay or biodegradation in both the dissolved phase and the sorbed phase.

### 3.2.1 Eulerian-Lagrangian Solution

Equation 3.3 can be expressed in both an Eulerian and a Lagrangian format. The MT3D model uses a mixed Eulerian-Lagrangian form of the equation to obtain a solution. To convert the equation to its Eulerian form, both sides are divided by the retardation factor,  $R$ , as follows:

$$\frac{\partial C}{\partial t} = -\frac{1}{R} \frac{\partial}{\partial x_i} (v_i C) + \frac{1}{R} \frac{\partial}{\partial x_i} \left( D_{ij} \frac{\partial C}{\partial x_j} \right) + \frac{q_s}{Rn} C_s - \frac{\lambda}{R} \left( C + \frac{\rho_s}{n} \bar{C} \right) \quad (\text{Equation 3.4})$$

Equation 3.4 solves for the change in concentration that occurs at a point. To convert to the Lagrangian form, the advection term must first be expanded with the chain rule as follows:

$$\frac{\partial}{\partial x_i}(v_i C) = v_i \frac{\partial C}{\partial x_i} + C \frac{\partial v_i}{\partial x_i} \quad (\text{Equation 3.5})$$

The Lagrangian form is where the substantial derivative, as shown in Equation 3.6, is the rate change in dissolved concentration which occurs along a pathline of a particle.

$$\frac{DC}{Dt} = \frac{\partial C}{\partial t} + \frac{v_i}{R} \frac{\partial C}{\partial x_i} \quad (\text{Equation 3.6})$$

$DC/Dt$  represents the concentration change for a fluid particle moving along a pathline at a velocity  $v_i/R$ , which can be approximated using its finite-difference form as shown in Equation 3.7.

$$\frac{DC}{Dt} = \frac{C_{t+1} - C_t}{\Delta t} \quad (\text{Equation 3.7})$$

The solution is obtained by substituting the finite-difference approximation of the dispersion, source/sink, and decay terms for  $DC/Dt$ . The result is that the advective term is represented as Lagrangian and the other terms are represented as Eulerian.

### 3.2.2 Hybrid Method of Characteristics Solution

The hybrid method of characteristics (HMOC) was utilized to solve the mixed Eulerian-Lagrangian transport equation. This method combines features of the method of characteristics (MOC) and the modified method of characteristics (MMOC). HMOC was developed in an attempt to invoke the best solution method depending upon the sharpness of the concentration front. This discussion will briefly outline the MOC and MMOC solutions to illustrate the importance of HMOC.

In the MOC procedure, a set of particles is distributed within a cell at the start of a time increment. Both a concentration and a position are assigned to each particle. These particles are tracked forward and at the end of the time increment, the concentrations of all of the particles in a

cell are averaged to find the concentration change due to advection. This value is used to find any changes that result from dispersion, source/sink, and decay. The concentration values of all particles in the cell are then replaced with new values to reflect the concentration changes resulting from all of the processes.

The MMOC procedure was developed to overcome a problem associated with the MOC procedure. The MOC solution requires significant amounts of computation time and computer memory. MMOC is similar to MOC with the exception of its solution procedure for the advective term. MMOC assigns only one particle with an associated concentration to a given cell located at the node for each new time,  $t+1$ . The particle is tracked backwards to find the concentration associated with its position at the previous time,  $t$ . Although the MMOC procedure typically requires less computational time and computer memory than the MOC procedure, there is, at times significant numerical dispersion that is undesirable. This is often the case where sharp concentration fronts are present.

The HMOC solution scheme is a combination of the MOC and MMOC procedures. HMOC allows the appropriate solution procedure to be implemented based on the sharpness of the concentration front. If the concentration front is sharp, the MOC procedure is used to solve for the advective term. If the concentration front is not sharp, the MMOC procedure is used to solve for the advective term. The HMOC solution attempts to minimize computational time and memory required and the numerical dispersion present in the solution.

### 3.3 LINKING MODFLOW AND MT3D

Equation 3.1 solved in MODFLOW and Equation 3.3 solved in MT3D are linked through the following relationship:

$$v_i = -\frac{K_{ii}}{n} \frac{\partial h}{\partial x_i} \quad (\text{Equation 3.8})$$

where

- $v_i$  = seepage velocity (L/T)
- $K_{ii}$  = hydraulic conductivity ( $K_{xx}$ ,  $K_{yy}$ , or  $K_{zz}$ ) (L/T)
- $n$  = porosity (-)
- $h$  = hydraulic potential (L)
- $x_i$  = distance along respective Cartesian coordinate axis (L)

Using an option in MODFLOW, output includes a file containing unformatted data consisting of hydraulic heads and other flow information. This information is required as input to MT3D and is linked to the transport equation using Equation 3.8.

## 4. GROUNDWATER MODELING OF THE PERCHED AQUIFER

Groundwater flow and RDX transport in the perched aquifer beneath the Zone 12 area of the Pantex Plant were simulated using the two groundwater models described in Chapter 3, MODFLOW and MT3D. This chapter presents the modeling process used for this case study and the results from the modeling efforts. The groundwater modeling process included representation of the perched aquifer as a finite-difference grid, obtaining initial estimates of the hydraulic parameters using water elevation data collected during the first few minutes of the tracer test, and calibration of the model using bromide concentration data collected in the test. After model calibration, a parameter sensitivity analysis was performed. Using the calibrated model, the linear sorption coefficient and the retardation of RDX were estimated for this site. Other results presented include an analysis of the removal of RDX from the perched aquifer during the tracer test and a discussion of the effectiveness of the re-circulation of groundwater during the test to enhance RDX extraction.

### 4.1 GRID REPRESENTATION OF THE PERCHED AQUIFER

A finite-difference grid was created to represent the perched aquifer beneath the Pantex Plant Zone 12-treatment system in the model. The three-dimensional grid was developed using Modelcad<sup>386™</sup>, which is preprocessing software that creates input files for use in the two groundwater models. The spatial discretization of the cells, the boundary conditions assigned to the borders and the top and bottom of the grid, and any sources and sinks present define the layout of the finite-difference grid for use in MODFLOW and MT3D. Each of these items is discussed.

#### 4.1.1 *Spatial Discretization*

The grid used in MODFLOW and MT3D to represent the perched aquifer consisted of a series of rows, columns, and layers. The area selected for the modeling effort was a 2000-foot by 2000-foot area with the Zone 12 treatment system located in the center. This is the area outlined in Figures 1-3 and 1-4. The finite-difference grid used to represent this area is divided into 74 rows, 74 columns, and 2 layers. The use of a two-layer model as opposed to a one-layer model was implemented during the calibration procedure. The decision to use the two-layer model is discussed subsequently in Section 4.3.

The larger cells, which are present toward the outer part of the grid, are assigned dimensions of 50 feet by 50 feet. The cell size decreases toward the center of the grid. The cells located near the center of the grid have dimensions of 10 feet by 10 feet. The smaller spacing included near the center of the grid provided a better resolution of the heads calculated with the groundwater flow model and the concentrations calculated with the transport model in the proximity of the treatment system. It was in the area closest to the treatment system where the analytical data was available from the tracer test for comparison to the model output.

#### ***4.1.2 Boundary Conditions***

Boundary conditions for the finite-difference grid are required inputs in the two groundwater models, MODFLOW and MT3D. For the part of the perched aquifer that was modeled, the upgradient and downgradient borders of the grid are represented as constant head boundaries. Based upon the groundwater contours, the upgradient border of the grid was assigned a constant head of 3269 feet above mean sea level (amsl). The downgradient border had a constant head of 3259 feet amsl. These upgradient and downgradient constant head boundaries resulted in a decrease in hydraulic head of ten feet over a linear distance of 2000 feet. This resulted in a hydraulic gradient, or the change in head per unit distance, of 0.005. The boundaries were a sufficient distance from the pumping system so they did not affect flow or transport at the center of the grid.

The two outer boundaries of the grid that were parallel to the direction of groundwater flow were represented as no-flow boundaries in the model grid. They were also a sufficient distance from the area where the treatment system was located to not affect the flow or contaminant transport near the center of the grid.

The bottom boundary of the perched aquifer was defined in the model grid by the top elevation contours of the FGZ in this area as shown in Figure 1-3. Because of the low permeability of the soils of the FGZ, it was represented as a confining layer beneath the perched aquifer in the model. The top of the perched aquifer was defined as unconfined in both the MODFLOW and MT3D models.

#### ***4.1.3 Sources and Sinks***

There were a total of four pumping wells used in the tracer test. These were PV-4, EW-1, EW-2, and EW-3. PV-4 was the injection well; it served as a source in the model. The other three wells, EW-1, EW-2, and EW-3 were where water is withdrawn from the perched aquifer and were

represented as sinks in the finite-difference grid. In the model, each of these four wells was represented spatially as a single cell within the grid. The volume of water pumped into or out of a given well was distributed throughout the cell which represents it. Figure 4-1 is an illustration of one layer of the grid used to represent the modeling area of the perched aquifer. It illustrates the spacing of the rows and columns and includes a designation of the assigned boundary conditions and the locations of the four pumping wells. Well PV-4 is the injection well located in the center of the three pumping wells. EW-1 is the well located closest to the top of the grid, EW-2 is the farthest to the right, and EW-3 is the remaining one located farthest to the left.

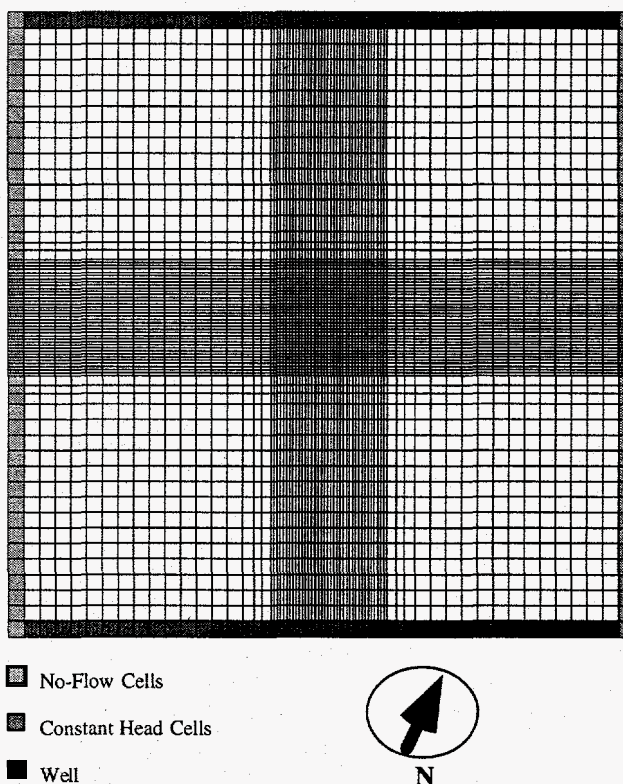


**Figure 4-1:** Grid Representation of the Perched Aquifer

#### 4.2 INITIAL INJECTION AT PV-4 DURING THE TRACER TEST

The water level in injection well, PV-4, was monitored closely during the initial 74 minutes of the tracer test in the perched aquifer at the Zone 12 treatment system. Measurements were recorded by a data logger connected to a transducer in the well at very small increments of time. This data was used to find an initial estimate of the primary hydraulic parameters of the perched aquifer. The first injection period for the KBr solution lasted 46 minutes at an approximate rate of 70 gpm. Injection then ceased for eight minutes and the water level in PV-4 decreased. The water elevation in PV-4 was monitored for an additional 20 minutes during the second increment of

injection of the solution. Figure 4-2 is a plot showing these trends in the water elevation measured in PV-4 during the first 74 minutes of the tracer test.

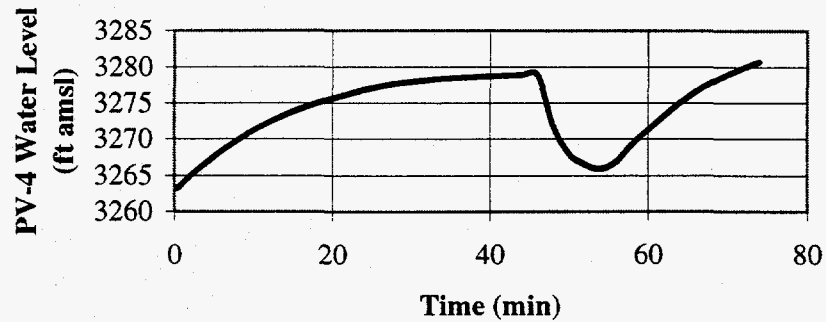


Figure 4-2: Water Elevation in PV-4 during Start of Tracer Test

Two analyses were conducted using the water elevations in Well PV-4 from the first 74 minutes of the test. First, MODFLOW was used to model the groundwater flow using this information; then a Theis analysis was conducted to estimate the transmissivity of the perched aquifer. Estimates of the hydraulic conductivity and the specific yield were found and used as starting values in the transport modeling. Hydraulic conductivity of groundwater is defined as the volumetric flux of the fluid through a given area per unit hydraulic gradient through the porous media. The specific yield is a term describing the storage or capacitance of unconfined aquifers. It refers to the volume of water released per unit area of unconfined aquifer per unit change in hydraulic head.

#### 4.2.1 MODFLOW Model of Initial Injection at PV-4

MODFLOW was used to model the first 74 minutes of the tracer test. The purpose of this modeling exercise was to conduct a transient simulation of these first minutes of the tracer test to obtain an estimate of flow parameters to use in the transport model. These estimates can also be used as a basis of comparison to the parameters determined through the transport modeling. Using the grid described in Section 4.1, multiple runs of MODFLOW were conducted in attempt of matching the water elevations from the cell in the model representing PV-4 to those measured in the field. The first 74 minutes were divided into three stress periods for MODFLOW based on varying pumping conditions. Their lengths and pumping conditions are shown in Table 4-1. For this exercise, only the source representing Well PV-4 was used.

**Table 4-1:** Temporal Discretization for Modeling of Initial Injection at PV-4

Stress Period	Start Time (min)	End time (min)	Pumping Condition
1	0	46	Injection at PV-4 at 70 gpm
2	46	54	No injection at PV-4
3	54	74	Injection at PV-4 at 70 gpm

One value of hydraulic conductivity and one value of specific yield were assigned to the grid because elevation data from only one well, PV-4, was being used. In the MODFLOW simulation of this injection, these two parameters were the only two that significantly affect the water elevation in PV-4. Therefore, an iterative procedure for matching the water elevations predicted with the model to those measured in the field was used. The values of hydraulic conductivity and the specific yield were altered in the model until the output yielded an acceptable approximation of the curve formed from the field data.

The first portion of the curve shown in Figure 4-2 where the slope is positive represents the first 46 minutes of the tracer test when solution was injected in PV-4. This part of the curve was approximated well with the model set at a hydraulic conductivity of 10 ft/d and the specific yield at 0.04. Unfortunately, with these values for the parameters, the second and third stress periods which represent the times when the injection stopped and was then restarted do not approximate the field data well. If the parameters were altered to obtain a better fit during the second and third stress periods, then the conductivity of 10 ft/d and specific yield of 0.04 and the field elevation data are shown in Figure 4-3.

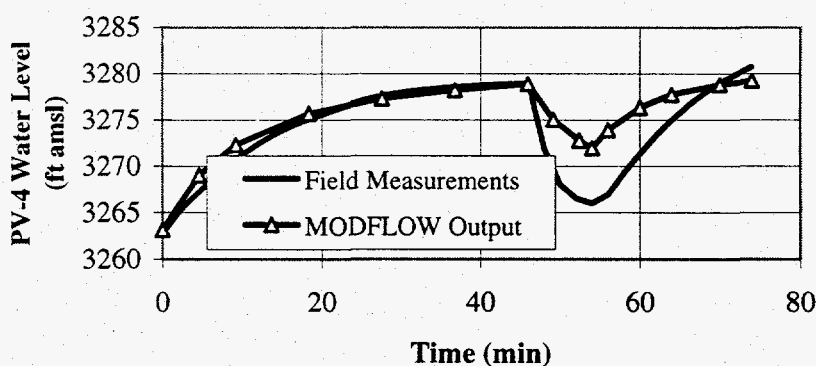


**Figure 4-3:** Water Elevations during Initial Injection Period at PV-4

A sensitivity analysis was conducted for variations of the hydraulic conductivity and the specific yield to examine the effects on the model output. Figure 4-4 shows the model sensitivity to hydraulic conductivity. The head in the cell in the model representing PV-4 was extremely sensitive to small changes in this parameter. Typically, hydraulic conductivity is discussed in terms

of orders of magnitude with a typical range of 0.28 to 2800 ft/d ( $10^{-7}$  to  $10^{-2}$  m/s) (Daniel, 1993). In this model, increasing or decreasing the value for hydraulic conductivity even slightly resulted in a significant change in the head value for this cell. Increasing the hydraulic conductivity from 10 ft/d to 12 ft/d caused the entire water elevation curve to drop by about one to two feet. Decreasing the hydraulic conductivity value from 10 ft/d to 8 ft/d in the model caused an increase in the predicted water elevation by about one to two feet over the entire curve.

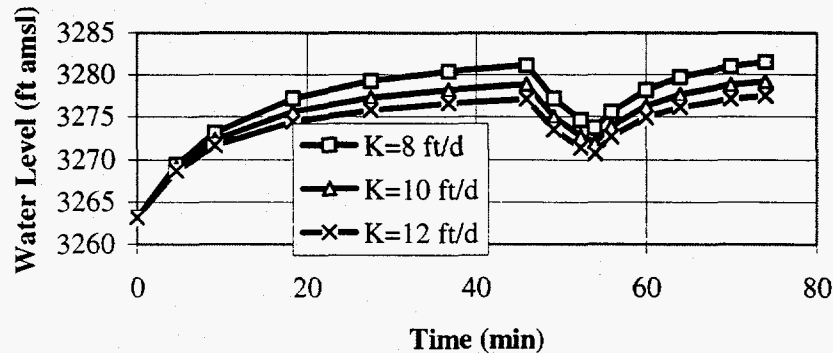


Figure 4-4: Sensitivity to Hydraulic Conductivity in Initial Injection Model at PV-4

The sensitivity of the flow model to changes in the specific yield is shown in Figure 4-5. The value of 0.04 for the specific yield that was estimated with the model was somewhat lower than typical values for this parameter. The specific yield values typically ranged from 0.1 to 0.3 for sandy material (Driscoll, 1986). However, small changes in the specific yield also had a significant impact on the simulated water elevations for Well PV-4. Increasing the specific yield value to 0.06 caused the water elevations calculated by the model to decrease by approximately one to two feet along the parts of the curve with increasing slopes indicating the time when water was injected. These periods correspond to the first and third stress periods in the model. Decreasing the specific yield value had the opposite effect; it caused the water elevations predicted with the model to increase by approximately one to two feet in the parts of the curve with an increasing slope.

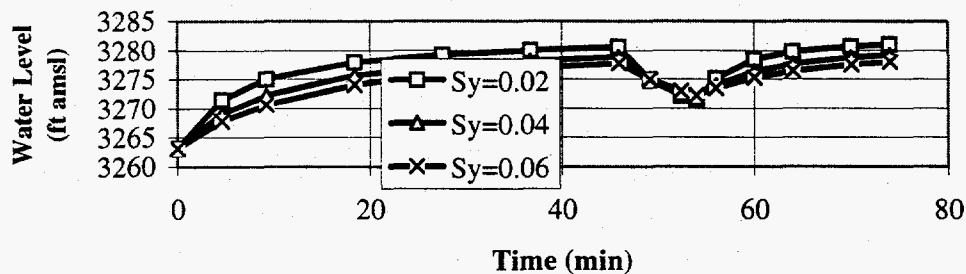


Figure 4-5: Sensitivity to Specific Yield in Initial Injection Model at PV-4

In examining Figures 4-4 and 4-5, they seem to indicate that a better fit might have been achieved if the hydraulic conductivity had been increased and the specific yield had been decreased. However, this was not the case. Further decreases in the specific yield values caused the slope in the initial part of the curve (approximately the first 5 to 10 days) to increase. Increasing the hydraulic conductivity has little effect on changing this result. Also, when the model was run with increased values of hydraulic conductivity and decreased values of specific yield, it did not predict a drop in the water level as great as that observed in the field. As a result, the part of the model output curve between 46 and 54 minutes did not match observed water elevations. Therefore, the model output curve did not agree with actual data when values of the specific yield less than 0.04 and higher values of hydraulic conductivity were used in the modeling.

A good simulation of the first 46 minutes of the solution injection at Well PV-4 was obtained with the MODFLOW representation using values of 10 ft/d for the hydraulic conductivity and 0.04 for the specific yield. The second and third stress periods of the model did not yield data that matched the field data well with these values of the parameters. Although a good simulation of the entire curve was not achieved, it can be surmised that, due to the extreme sensitivity to small changes in the hydraulic conductivity and specific yield, the actual values were likely close. Therefore, these were sufficient estimates to use for beginning the model simulation of the entire tracer test.

#### **4.2.2 Theis Analysis**

The Theis analysis is performed to relate drawdown in a confined aquifer to time,  $t$ , and radial distance from a well,  $r$ . Jacob's method is one approximation of the Theis equation used for small values of  $r/t$  that was utilized here to analyze the flow in the perched aquifer.

Due to the injection of the solution, the increase in the water level in PV-4 can be considered a negative drawdown in the well. Because the perched aquifer was unconfined, the corrected drawdown was calculated for use in the analysis. The corrected drawdown,  $s'$ , was calculated from Equation 4-1.

$$s' = s - \frac{s^2}{2b} \quad \text{(Equation 4-1)}$$

where

$s'$  = corrected drawdown (L)

$s$  = drawdown in the well (L)

$b$  = saturated thickness of the aquifer (L)

The corrected drawdown accounted for changes in the saturated thicknesses that occurred in an unconfined aquifer.

Using the Jacob method the transmissivity of the perched aquifer was calculated from the semi-log plot of the corrected drawdown versus time, which is shown in Figure 4-6. Transmissivity is the hydraulic conductivity multiplied by the saturated thickness of the aquifer.

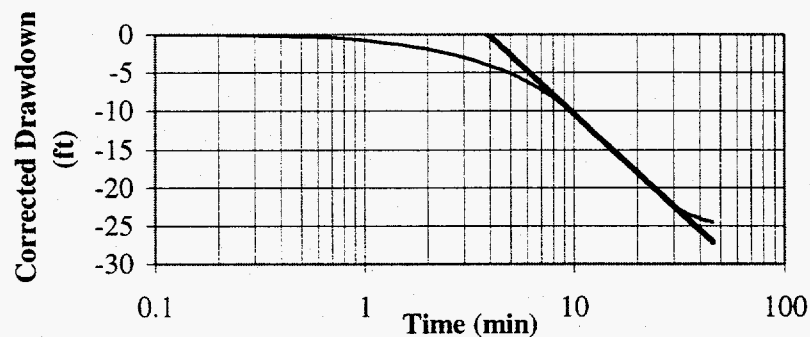


Figure 4-6: Corrected Drawdown in PV-4 during Initial Injection Period

The assumptions of the Jacob method were not met for early times, and the predicted linear curve departed from the observed data. Only the part of the curve corresponding to later times was used to calculate the transmissivity.

Equation 4-2 was used to calculate the transmissivity of the perched aquifer from the straight-line portion of the curve.

$$T = \frac{Q}{4\pi} \frac{\ln \frac{t_2}{t_1}}{s'_2 - s'_1} \quad (\text{Equation 4-2})$$

where

$T$  = aquifer transmissivity ( $L^2/T$ )

$Q$  = volumetric flow rate ( $L^3/T$ )

$t_1$  = time  $i$  (T)

$s'_i$  = corrected drawdown corresponding with time  $i$  (L)

The solution injection rate,  $Q$ , is 13475 ft<sup>3</sup>/d. From Equation 4-2, the resulting transmissivity was 96 ft<sup>2</sup>/d. Using the calculated transmissivity, the hydraulic conductivity in the aquifer,  $K$ , was calculated from Equation 4-3 and the storage coefficient,  $S$ , was calculated using Equation 4-4.

$$K = \frac{T}{b} \quad (\text{Equation 4-3})$$

where

$K$  = hydraulic conductivity (L/T)

$$S = \frac{2.25 T t_0}{r^2} \quad (\text{Equation 4-4})$$

where

$S$  = aquifer storage coefficient (-)

$t_0$  = time corresponding to  $s' = 0$  along the best fit line (T)

$r$  = radius of influence of the well (L)

For  $b = 14.2$  ft. and  $r = 1$  ft., the resulting value for  $K$  and  $S$  was 6.7 ft/d and 0.6, respectively. The storage parameter,  $S$ , was the volume of water released per volume of porous media as a result of the decompression of water. This value typically ranged from  $10^{-4}$  to  $10^{-3}$ , therefore, the value of 0.6 was much too high. The source of error in the calculation of this parameter was related to the injection during the first two to three minutes of the test.

Although the results from the storage parameter estimation fell outside the expected range, the estimation of the hydraulic conductivity was similar to that estimated using MODFLOW to model the initial injection period. Also, this parameter was determined using the slope of the best fit line in Figure 4.6; therefore, there was not any error associated with injection at early times. A value of 10 ft/d was estimated with MODFLOW and 6.7 ft/d was found through the Jacob analysis of the corrected drawdown curve. These values of hydraulic conductivity were very similar and were well within the typical ranges.

### 4.3 MODEL CALIBRATION

The purpose of calibrating the MODFLOW and MT3D models was to estimate the hydraulic and contaminant transport parameters in the perched aquifer based on measurements made in the

field. Data collected during the tracer test was used as a comparison with output produced by the models.

#### 4.3.1 Temporal Discretization

The model was divided into stress periods corresponding to varying pumping conditions during the tracer test. Each stress period was further divided into time steps (ranging from one to five in this model). Concentration data was recorded for each time step in the model. This model was divided into six stress periods according to the differing pumping conditions. Table 4-2 shows the lengths of the six stress periods and the differences in the pumping conditions between them.

**Table 4-2:** Temporal Discretization of the Perched Aquifer Model

Stress Period	Start Time	End Time	Stress Period Length (d)	Pumping Rates (gpm)				Condition
				EW-1	EW-2	EW-3	PV-4	
1	7/15/96 15:00	8/8/96 18:00	24.125	-10	-10	-10	32.7	KBr solution injection
2	8/8/96 18:00	8/20/96 0:00	11.25	-10	-10	-10	32.7	Clean water injection
3	8/20/96 0:00	8/21/96 0:00	1	0	0	0	0	Power outage
4	8/21/96 0:00	9/11/96 8:00	21.335	-10	-10	-10	32.7	Clean water injection
5	9/11/96 8:00	9/13/96 9:00	2.04	0	0	0	0	Power outage
6	9/13/96 9:00	9/19/96 13:00	6.17	-10	-10	-10	32.7	Clean water injection

**NOTE:** Pumping rate is "+" for injection and "-" for extraction.

The first stress period was the time that the bromide tracer was injected in solution at Well PV-4. The second, fourth, and sixth stress periods represent times when water without the bromide tracer was injected into the perched aquifer at PV-4. The two power outages, which interrupted the injection and withdrawal of water in the perched aquifer, were represented by the third and fifth stress periods. The transducer and data logger in Well PV-4 responsible for recording the water elevation changes allowed a close estimate of the actual length of the power outage represented by the fifth stress period, which was 2.07 days. However, the power outage represented as the third stress period occurred during the period when the data logger in PV-4 was not operating. Although

it is not known exactly how long this outage lasted, it was estimated as one day for inclusion in the model.

#### **4.3.2 Grid Zones**

The model grid was divided into different zones for the estimation of parameters. Each zone was assigned a different value of any given parameter. For this model, the grid was divided into 3 zones of hydraulic conductivity and porosity since bromide concentrations were monitored for 3 wells during the tracer test. Because these two parameters had the most significant effect on the transport in the aquifer, the grid was divided into zones whose values varied. Specific yield, dispersivity, vertical hydraulic conductivity, and the storage coefficient had a much less significant effect on the transport in the model. Therefore, values for these parameters were assumed to be constant throughout the grid.

#### **4.3.3 Use of a Two-Layer Model**

After many attempts at using a one-layer model, it was determined that an acceptable approximation of the bromide curve corresponding to the breakthrough at Well EW-3 during the tracer test could not be obtained. Curves matching the breakthrough exhibited in the EW-1 and EW-2 were successfully achieved using MT3D with the one-layer model. The curve that was typically produced which represented the breakthrough at EW-3 followed two patterns: in the first situation, the hydraulic conductivity reached a value high enough that the breakthrough time and the part of the curve where the concentration in the EW-3 effluent increased were approximated well within the model. However, this curve would peak and then indicate a decrease in concentration at an earlier time than that observed in the field. In the second situation, the hydraulic conductivity for this portion of the grid was decreased in an attempt to delay the peak of the output curve from MT3D and delay the time when the output showed concentration decreasing. This caused the initial breakthrough time in the model to lag behind the time observed in the bromide data from the field for EW-3. Altering other model parameters, porosity, specific yield, and dispersivity had little effect on this problem. Figure 4-7 shows an example of a typical curve produced for Well EW-3 with the one-layer model. The peak occurred approximately 10 days earlier than the time observed in the field data. Also, the bromide concentration predicted with the model was significantly lower at the end of the test than what was observed in the field data.

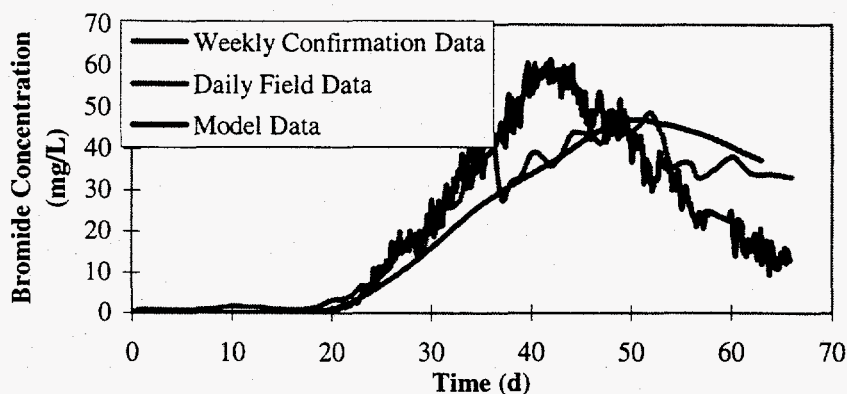


Figure 4-7: Model Predicted Breakthrough Curve at EW-3 from One-Layer Model

The two-layer model provided an alternative representation. There was physical evidence of the existence of stratification in the perched aquifer. When there were multiple layers present in an aquifer, each with its own hydraulic conductivity, there were two separate fronts of tracer that reached a well during a tracer test.

The first evident to support to the use of a two-layer model to represent the perched aquifer was the cross-section of lithology developed from boring logs of the same wells shown in Figure 1-5. This is shown in Figure 4-8. The figure indicates the presence of a sand and gravel layer present above the main sand layer. The bottom of this sand and gravel layer was located approximately five feet above the top of the FGZ. The second evidence was the shape of the bromide breakthrough curve for Well EW-3. Visual inspection showed that there were two steps to the bromide breakthrough curve for the field data. This indicated the presence of two layers with different values of hydraulic conductivity. Support for this observation was suggested by Mercado, 1967. In testing at the Haifa Bay Experimental Field in 1964-65, a step pattern was observed in breakthrough curves produced from samples collected at observation wells in a tracer test. The aquifer where the test was conducted has four strata, each with an individual thickness and hydraulic conductivity previously determined. The tracer test that was performed used one injection well and one extraction well pumping at approximately equal rates. Figure 4-9 is a figure from Mercado (1967) showing the locations of the injection well, P.R.6, and the extraction well, P.R.5, along with several observation wells. Also shown is the presence of the four strata present in the aquifer. The estimated positions of the front of the injected water are shown on Figure 4-10 for different times during the field experiment. These positions are theoretical based on an analytical model. Figure 4-11 includes a series of four graphs, which are the breakthrough curves produced at four observation wells during the tracer test. Both the idealized curves for a non-stratified aquifer and the actual

curves based on field measurements are shown for each observation well. The steps of each breakthrough curve obtained from field data correspond to the number of strata present in the aquifer. This response is similar to that seen in the EW-3 breakthrough curve where there are two steps indicating the presence of stratification with two layers in this area of the perched aquifer.

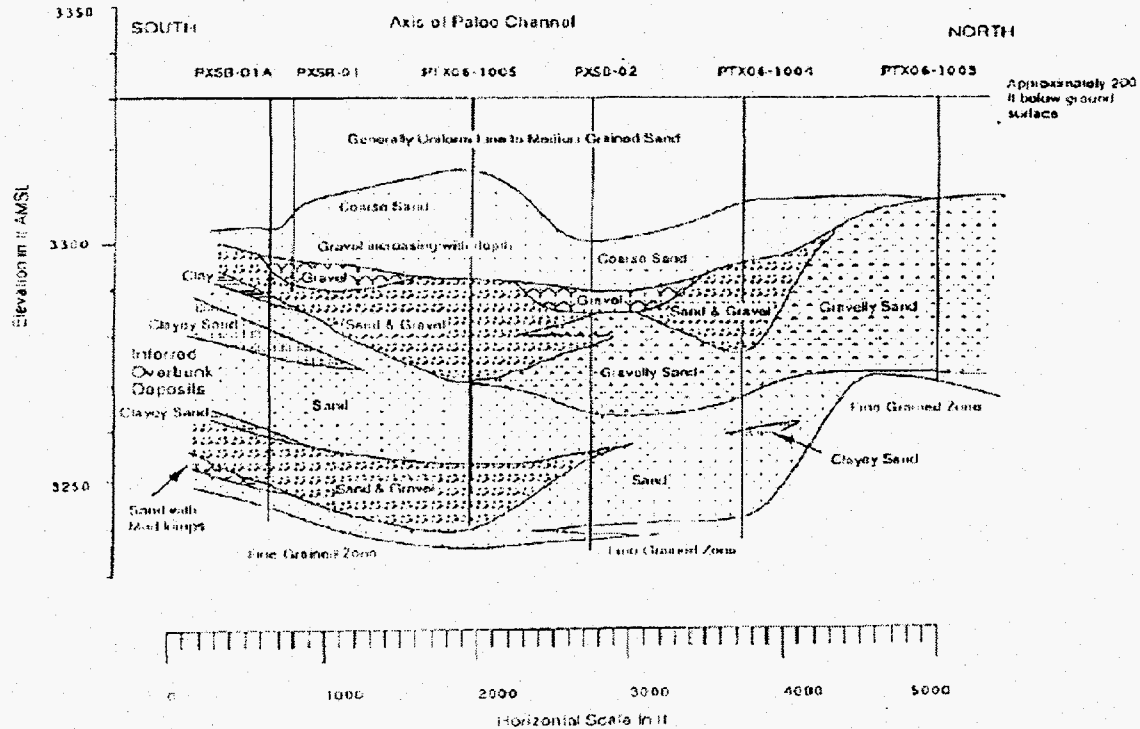


Figure 4-8: Lithology of Perched Aquifer Cross-Section (Argonne, 1995)

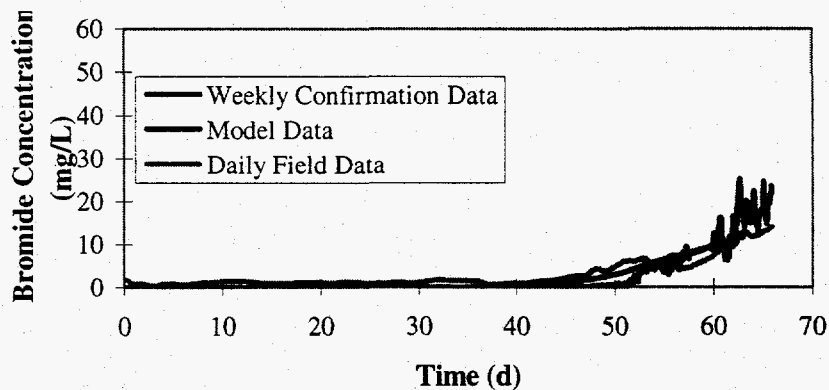


Figure 4-9: Comparison of Model Breakthrough to Field Breakthrough for EW-1

Based on evidence from the cross-section and the presence of steps in the breakthrough curves, the use of a two-layer model was implemented. The results, which follow, were based on this two-layer grid design. The bottom elevation of the top layer of the grid, layer 1, is five feet

above the top of the FGZ. The hydraulic conductivity in Zone 3, which contains Well EW-3, is assumed to have different values for the two layers. Because the same trend was not observed in breakthrough curves for EW-1 and EW-2, the hydraulic conductivity for Zones 1 and 2 are assigned the same value for both layers indicating no observed effect due to stratification. Also, all of the parameters in the model, which were adjusted in the calibration, were assumed to have the same magnitude for layers 1 and 2.

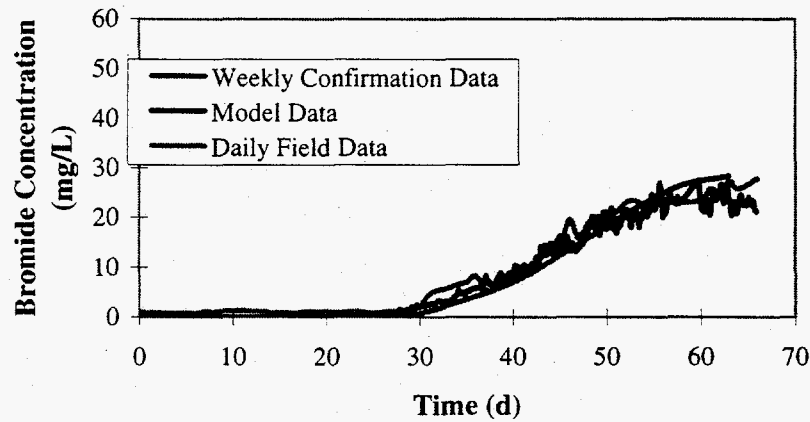


Figure 4-10: Comparison of Model Breakthrough to Field Breakthrough for EW-2

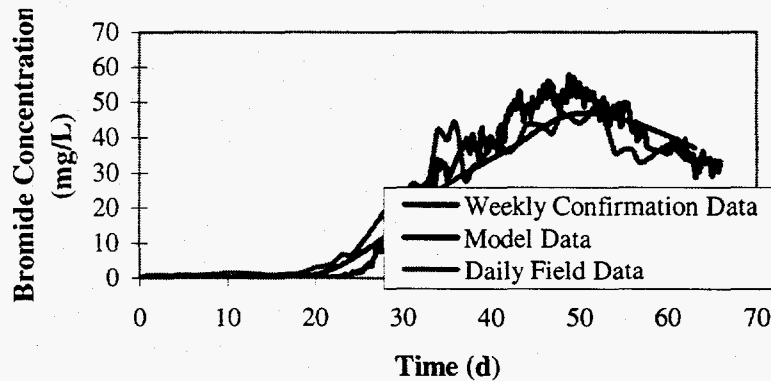


Figure 4-11: Comparison of Model Breakthrough to Field Breakthrough for EW-3

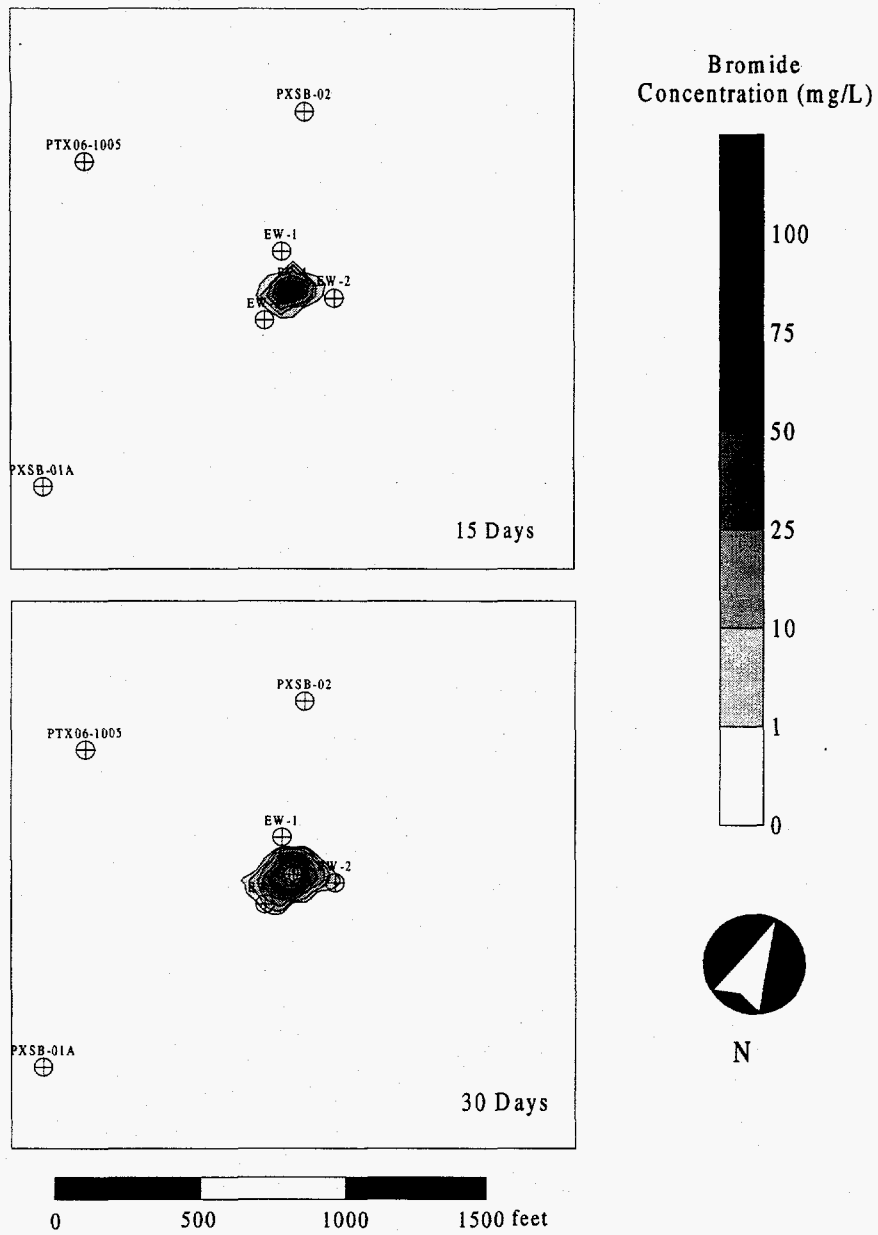
#### 4.3.4 Fitting the Breakthrough Curves

Fitting data produced by the transport model to field data is an iterative procedure involving changing one of a series of parameters, running the model, plotting the output, and conducting a statistical analysis. Then, either the value of the same parameter or a different parameter could be

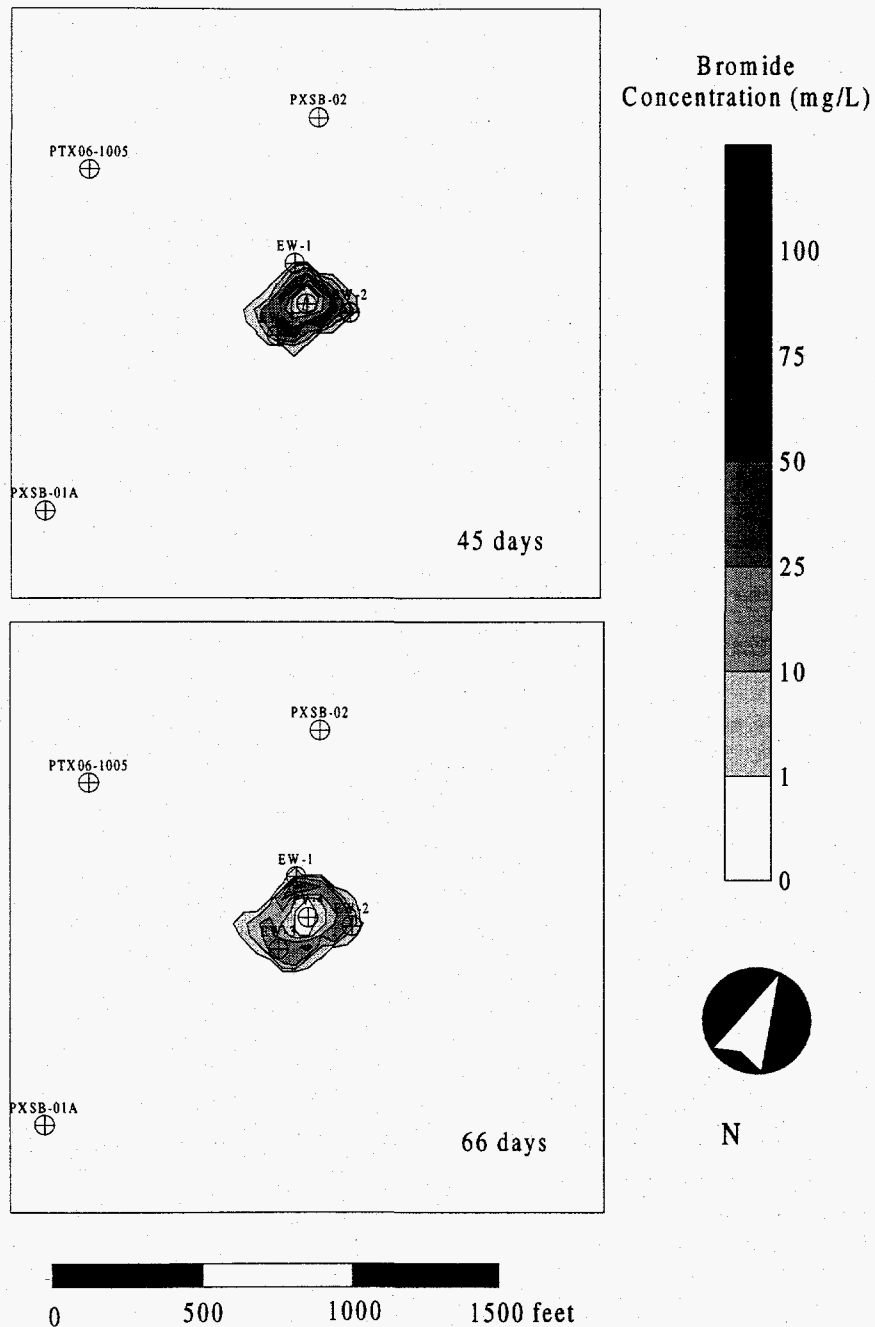
changed, and the procedure repeated. Once the parameters, which yield the best fit of the model output to the field analytical data, are determined, the calibration of the model is complete. The statistical analysis was performed because it was difficult to identify the best fit through visual inspection alone. The statistical method used to compare the data sets is a root mean square analysis. The parameters selected as those providing the best fit to field data produced the smallest error in the root mean square analysis.

The breakthrough curves selected as the final model based on the statistical results are presented in Figures 4-9, 4-10, and 4-11 for Wells EW-1, EW-2, and EW-3, respectively. There was some oscillation apparent in the data produced in MT3D. The reason there was significant oscillation in the model output for EW-1 in the last six days of the run is unknown. However, an overall good fit was obtained for the bromide data from all three of the wells.

The tracer test lasted 66 days. Figures 4-12 through 4-15 show contours of the bromide concentration in the modeling area at four intervals during the tracer test. These contours were produced using Golden Software's Surfer program with data included in the model output. They represent average bromide concentrations over both layers of the model.



Figures 4-12 and 4-13: Bromide Contours for 15 and 30 Days of the Tracer Test



Figures 4-14 and 4-15: Bromide Contours for 45 and 66 Days of the Tracer Test

#### 4.3.5 Hydraulic Conductivity

The most important parameter affecting the breakthrough curves produced as output of the transport model was the hydraulic conductivity. Guven, et al., 1992 concluded from a study of two-well tracer tests that three-dimensional variations in the hydraulic conductivity have a significant effect on the transport of a constituent. This was supported with evidence presented by Mas-Pla, et

al., 1992. This group of researchers was unable to obtain an appropriate model prediction of breakthrough in a well in a simulation of a tracer test. They were using a two-dimensional flow and transport model. This result could not account for variations in hydraulic conductivity due to the layering in the aquifer.

In the three-dimensional simulation of the perched aquifer from the Pantex site, slightly changing the values of the hydraulic conductivity had a significant effect on the shape of the output curves. The final values of hydraulic conductivity selected in the model calibration are shown in Figures 4-16 and 4-17. Figure 4-16 shows the values for the top layer in the perched aquifer; the values range from 7 ft/d to 25 ft/d. The Zone 3 value of 25 ft/d corresponds to the area where there was evidence that the soil consisted of a sand and gravel mixture. Therefore, it was reasonable to believe a slightly higher hydraulic conductivity existed in this zone.

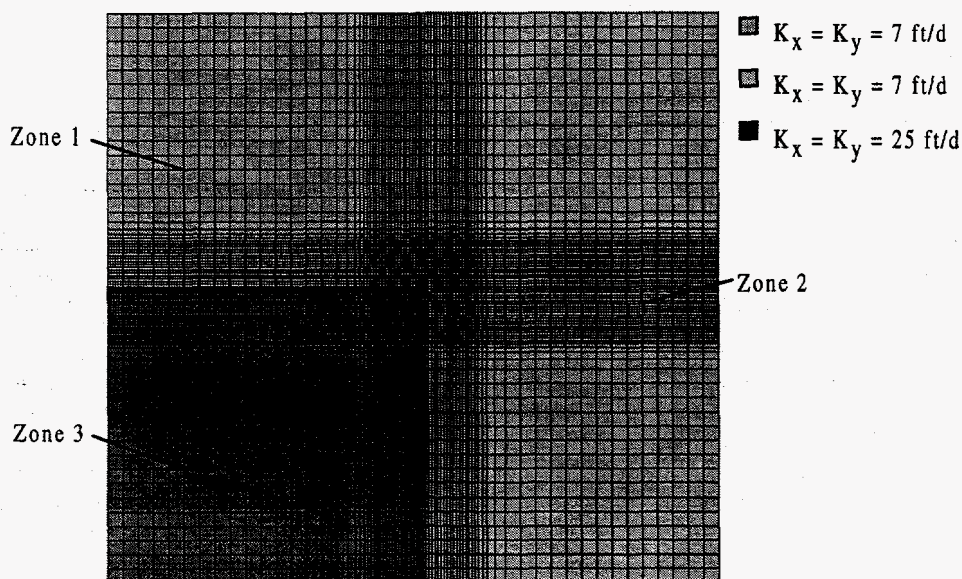
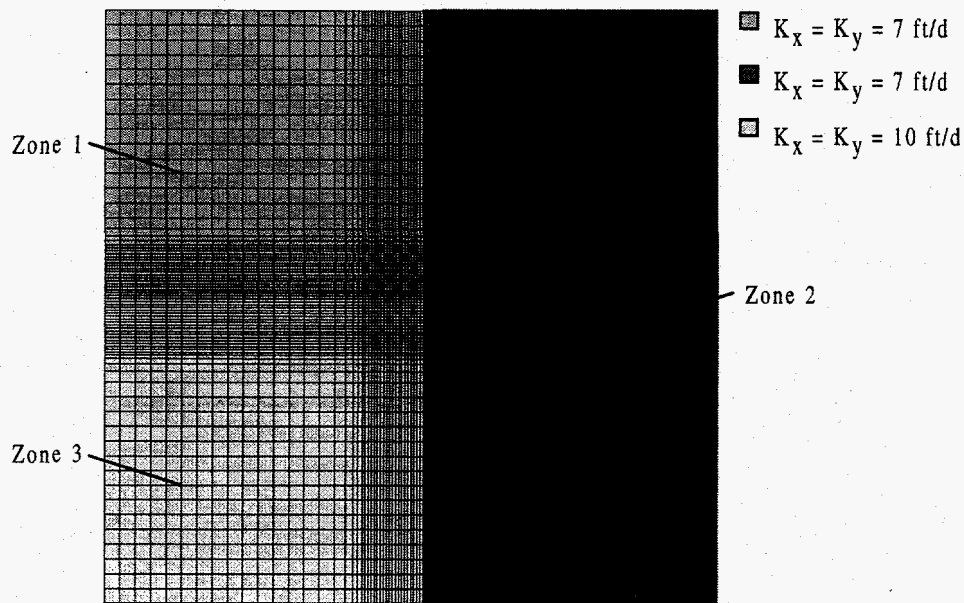


Figure 4-16: Hydraulic Conductivity Zones for Layer 1



**Figure 4-17:** Hydraulic Conductivity Zones for Layer 2

Figure 4-17 shows the hydraulic conductivity values that were obtained through calibrating the model for the bottom layer. These values range from 7 ft/d to 10 ft/d. The fact that the range in values of hydraulic conductivity was small indicates few heterogeneities affect flow in the bottom part of the perched aquifer.

#### **4.3.6 Porosity**

The second most important parameter in the model in terms of its influence on the shape of the output breakthrough curves is the porosity. Values for the porosity of sand typically range from 0.25-0.4 and values for sand and gravel mixes range from 0.1-0.35 (Driscoll, 1986). The same porosity zones were designated for both layers of the transport model. Figure 4-18 shows the final porosity zones for both layers. The values range from 0.30 to 0.35, which was within the range of typical values for this parameter.

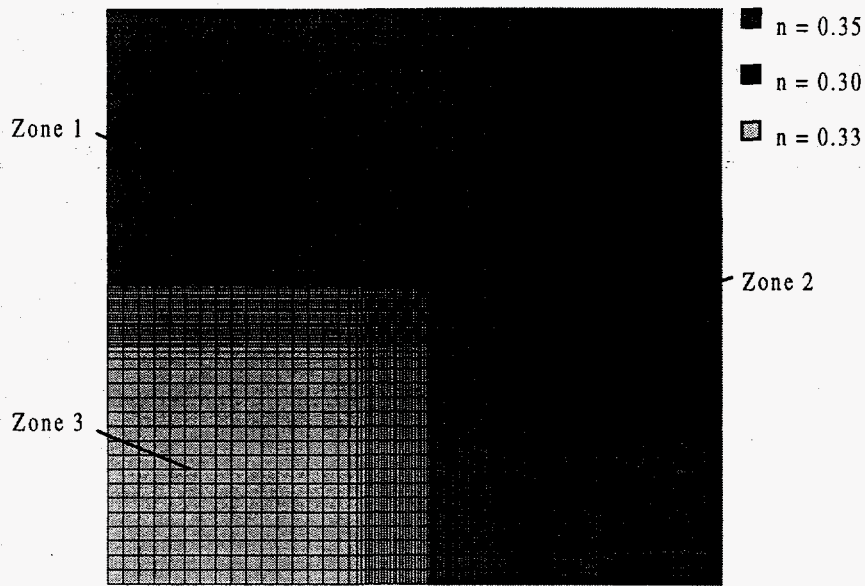


Figure 4-18: Porosity Zones for Layers 1 and 2

#### 4.3.7 Specific Yield

Changing the value of the specific yield in the model had very little effect on the output breakthrough curves produced using MT3D. Primarily, the specific yield influenced the rate the water elevation rose in the observation well cells of the model that represented wells PV-1, PV-2, and PV-3. These wells were the locations where the water elevations were monitored during the tracer test.

Figures 4-19, 4-20, and 4-21 show water elevations predicted with MODFLOW compared to measured field values using 0.2 for the specific yield which was within the range of typical values.

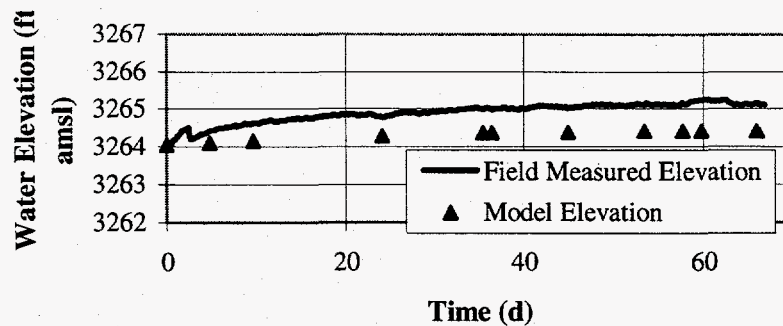


Figure 4-19: PV-1 Field and Model Groundwater Elevations

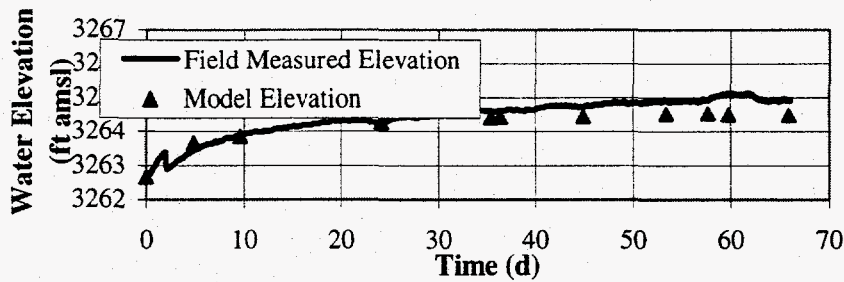


Figure 4-20: PV-2 Field and Model Groundwater Elevations

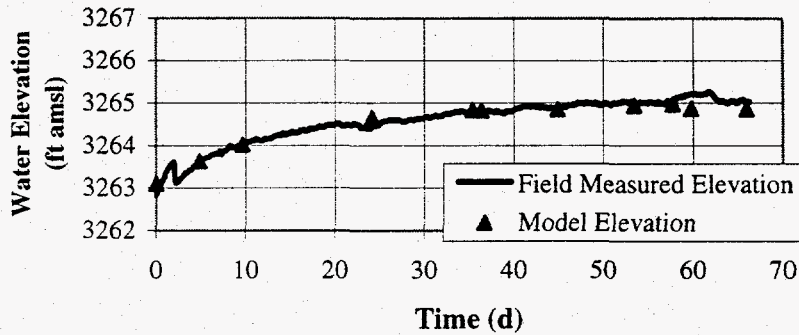


Figure 4-21: PV-3 Field and Model Groundwater Elevations

Because the comparison of the water elevations was not the primary factor considered in the calibration of the transport model, the match between the field data and the model data was not exact. The model predicted the water elevation rose approximately 0.5 feet in the cell corresponding to PV-1 when it actually increased slightly more than one foot. For PV-2, the water elevation in the model rose about two feet compared to the actual rise of about 2.5 feet. The water elevation of the cell in the model representing PV-3 was very close to the recorded data from the field. The comparisons of the water elevations for Wells PV-1 and PV-2 were not as close as they could have been had other parameters been changed. The primary parameter that affected these elevations was the hydraulic conductivity. If this is decreased to cause the increase in the water elevations in the model, there would have been a lag in the breakthrough curves produced by the model indicating that the tracer migrated was slower than its concentrations in field measurements show.

The method of selecting a value of 0.2 for the specific yield for this model involved running the MODFLOW at varying values of this parameter. The water elevations for the observation wells were then plotted. The change that occurred was the rate that the water level increased. At early

times during the tracer test, the model predicted the elevations in the observation wells closely with a value of 0.2.

#### 4.3.8 Dispersivity

Dispersion of a contaminant in a groundwater system is primarily caused by variations in the flow velocities from the mean. In the finite-difference model, dispersivity represents variations from the mean caused by heterogeneities smaller than the grid block scale. The dispersion in a system is scale-dependent; it increases with increasing distance from the source. Because this parameter is scale-dependent, its value is typically difficult to quantify. Also, for cases where stratification is present in an aquifer, and the values of hydraulic conductivity vary in the different layers, a large value of longitudinal dispersivity may mistakenly be used in a model to achieve an appropriate fit of breakthrough data to compensate for effects actually due to the layering (Huyakorn, 1986). For these reasons, a number of models have been developed to approximate dispersion at a given distance from the source.

Pickens and Grisak, 1981, developed expressions for field-scale longitudinal dispersivity based on single-well and two-well tracer tests that were conducted. Depending on the type of stratification (normal, lognormal, or arbitrary), the proposed values for longitudinal dispersivity range from 0.041-0.256 times the distance between the injection and the receptor well.

A second model was developed empirically based on field observations by the U.S. EPA during their development of their Resource Conservation and Recovery Act land disposal restrictions for hazardous wastes. This method is presented in the Federal Register, Volume 51, No. 9. Expressions used for estimating longitudinal and transverse dispersivity are as follows:

$$a_L = 0.1X_r \quad \text{(Equation 4-5)}$$

$$a_t = \frac{1}{3}a_L \quad \text{(Equation 4-6)}$$

where

$a_L$  = longitudinal dispersivity (L)

$X_r$  = distance to the receptor (L)

$a_t$  = transverse dispersivity (L)

A third model for estimating dispersivity is discussed in Charbeneau 1995, and is presented in background documents for the EPA Composite Landfill Model (EPCML). The method suggests that longitudinal dispersivity be distributed randomly in three classes each with a certain probability of occurrence. The estimation is based on a receptor well located 500 feet from the origin. Each of the classes and their probabilities are shown in Table 4-3.

**Table 4-3: EPACML Method of Estimating Longitudinal Dispersivity**

Class	1	2	3
Longitudinal Dispersivity (m)	0.1-1	1-10	10-100
Probability	0.1	0.6	0.3

Equation 4-7 is provided to estimate the dispersivity receptor distances not equal to 500 feet. Equation 4-8 is used to estimate the transverse dispersivity.

$$a_L(x) = a_{L(500\text{ ft})} \sqrt{\frac{X_r}{500}} \quad (\text{Equation 4-7})$$

$$a_T = \frac{1}{8} a_L \quad (\text{Equation 4-8})$$

Table 4-4 presents the estimates of dispersivity values with each of these three methods.

**Table 4-4: Calculated Dispersivity with Analytical Models**

Method	$a_L$	$a_T$
Pickens and Grisak	6.2-38 ft.	
EPA land disposal regulations	15 ft.	5 ft.
EPACML	6.5-65 ft.	0.8-8 ft.

Gelhar, et al, 1992, examined measurements of dispersivity values determined for 59 field sites. Based on results from these 59 sites, they concluded that for a given scale, the longitudinal dispersivity typically ranges over two to three orders of magnitude. For a scale on the order of  $10^2$ , their data showed that longitudinal dispersivity measurements range from  $10^0$  to  $10^2$ . Transverse dispersivities were estimated for 23 of the sites. These data show that for a scale of  $10^2$ , values of the transverse dispersivity range from  $10^2$  to  $10^1$ .

For the model of the perched aquifer from the Pantex site, the longitudinal dispersivity estimated with the model calibration is 10 feet and the transverse dispersivity is 1 foot. The

longitudinal dispersivity value is within the ranges found for the Pickens and Grisak analytical model and the EPACML model. It is also consistent with the data presented in Gelhar, et al.

#### ***4.3.9 Vertical Hydraulic Conductivity***

The vertical hydraulic conductivity had little effect on the transport of the bromide modeled with MODFLOW and MT3D. However, a value did have to be assigned for the model. A value of 0.1 ft/d was used in the transport modeling. The significance of this value is examined in Section 4-4 with the sensitivity analysis.

#### ***4.3.10 Storage Coefficient***

Because a two-layer model was used to simulate the perched aquifer, the storage coefficient had to be designated for the bottom layer. The storage coefficient was associated with the volume of water released resulting from its decompression in the porous media. This parameter is typically associated with a confined aquifer.

The value of the storage coefficient used for the bottom layer of the grid had little effect on the transport of the contaminant. A value of 0.0001 was used for the storage coefficient in the model simulations.

### **4.4 SENSITIVITY ANALYSIS**

A sensitivity analysis was conducted to determine how the model was affected by variations in those parameters, which affected the transport of the conservative constituent through the perched aquifer. The method used in the analysis was altering the value of one parameter at a time, running the model, and evaluating the significance of changes in the model output. The parameters used in the model, which were evaluated in the sensitivity analysis, were hydraulic conductivity, porosity, specific yield, dispersivity, vertical hydraulic conductivity, and the storage coefficient.

#### ***4.4.1 Sensitivity to Hydraulic Conductivity***

The calibrated MT3D model of transport of the conservative bromide tracer in the perched aquifer consisted of two layers. Each layer had three zones of hydraulic conductivity as was shown in Figures 4-16 and 4-17. The hydraulic conductivity values of the calibrated model were the same for Zones 1 and 2 in both the top and bottom layer, but were different for Zone 3.

Therefore, the examination of changes of four individual hydraulic conductivity values was necessary to evaluate the sensitivity of the model to this parameter. These were the hydraulic conductivity of Zone 1 (layers 1 and 2), Zone 2 (layers 1 and 2), Zone 3 (layer 1), and Zone 3 (layer 2). Twelve figures, four for each of the three pumping wells, EW-1, EW-2, and EW-3, were prepared and are included in Appendix A to examine the model's sensitivity to varying values of hydraulic conductivity. Table 4-5 shows which figures correspond to their respective zones, layers, and observation wells.

**Table 4-5: Figures Corresponding to Zone, Layer, and Well for Hydraulic Conductivity Sensitivity Analysis**

Zone	Layer(s)	Well	Figure
1	1 and 2	EW-1	A-1
		EW-2	A-2
		EW-3	A-3
2	1 and 2	EW-1	A-4
		EW-2	A-5
		EW-3	A-6
3	1	EW-1	A-7
		EW-2	A-8
		EW-3	A-9
3	2	EW-1	A-10
		EW-2	A-11
		EW-3	A-12

The hydraulic conductivity in sand and gravel aquifers can vary over several orders of magnitude. However, to show the extreme sensitivity of the model to this parameter, this analysis was conducted by varying the hydraulic conductivity value.

When this hydraulic conductivity in Zone 1 was increased from 7 ft/d to 17 ft/d, the initial breakthrough time of the tracer predicted at EW-1 in the model was 10 days earlier. Also, the maximum breakthrough concentration of the tracer predicted at this well is significantly higher. There was little effect in the responses predicted with the model at the other two wells, EW-2 and EW-3.

Changing the hydraulic conductivity value in Zone 2 by the same amount resulted in an increase in the breakthrough concentration of tracer predicted at Well EW-2 and predicted a shortened time until breakthrough by about 5 days. The concentration at EW-1 was not affected much; the breakthrough predicted at EW-3 decreased.

The value for hydraulic conductivity varies for the top and bottom layers in Zone 3. When the value of hydraulic conductivity was increased in the top layer of Zone 3 from 25 ft/d to 35 ft/d, the initial breakthrough time predicted with the model for Well EW-3 was approximately three days earlier. Also, the maximum concentration of the breakthrough curve was increased by

approximately 8 mg/L and the peak occurred at an earlier time. There was only a slight effect predicted in the breakthrough curves for Wells EW-1 and EW-2.

When the hydraulic conductivity value for the bottom layer in Zone 3 was increased from 10 ft/d to 20 ft/d, there was no effect to the initial breakthrough time predicted with the model at EW-3. However, the maximum breakthrough concentration increased by approximately 10 mg/L. There was no significant effect seen in the breakthrough concentrations for Wells EW-1 and EW-2.

#### 4.4.2 Sensitivity to Porosity

Porosity is the parameter that has the second most significant effect on the model output. The values of porosity assigned to the zones for both layers were the same for all zones in the model. Therefore, this part of the sensitivity analysis was conducted by changing the values for each zone.

The model was run with both an increase and a decrease in the porosity in each of the zones of the calibrated model. Table 4-6 indicates which figures in Appendix A correspond to each zone for the sensitivity to changes in the porosity.

**Table 4-6:** Figures Corresponding to Zone, Layer, and Well for Porosity Sensitivity Analysis

Zone	Layer(s)	Well	Figure
1	1 and 2	EW-1	A-13
		EW-2	A-14
		EW-3	A-15
2	1 and 2	EW-1	A-16
		EW-2	A-17
		EW-3	A-18
3	1 and 2	EW-1	A-19
		EW-2	A-20
		EW-3	A-21

When 0.03 from 0.35 to 0.38 increased the porosity in Zone 1, there was a decrease in the maximum breakthrough concentration predicted with the model by the ending day of the tracer test by approximately 5 mg/L. Also, the initial breakthrough of the tracer was predicted to occur approximately three days later. Decreasing the porosity in Zone 1 had the opposite effect on the breakthrough curve. Changes due to an increase in porosity occurred because there was more void space available to hold water. There was little change in the breakthrough curves produced for Wells EW-1 and EW-2.

The same analysis was conducted for the porosity in Zone 2. The value was increased from 0.30 to 0.33 and the model was run. There was no significant change in the EW-1 and EW-3 breakthrough curves. For the EW-2 breakthrough curve, the maximum breakthrough concentration predicted with the model was about 5 mg/L less. When the porosity in Zone 2 was decreased from 0.30 to 0.27, the maximum breakthrough concentration was increased by about 5 mg/L.

When the porosity for Zone 3 was decreased from 0.33 to 0.30, the breakthrough curve predicted with the model shifted slightly to the left, corresponding to an earlier initial breakthrough by about two days. The maximum concentration predicted for the breakthrough of the tracer was approximately 5 mg/L greater. When the porosity value was increased from 0.33 to 0.36, the breakthrough curve predicted with the model shifted slightly to the right. There was no significant effect apparent in the breakthrough curves for Wells EW-1 and EW-2.

#### ***4.4.3 Sensitivity to Specific Yield***

The specific yield was assumed as a single value throughout the grid for the flow and transport model. A typical range for specific yield values in an aquifer is 0.1 to 0.3. The value estimated for the perched aquifer is 0.2 which is in the middle of this range. To examine the sensitivity of the model to this parameter, the model was run with specific yield values at the extremes of the typical range. The model output for Wells EW-1, EW-2, and EW-3 are shown in Figures A-22, A-23, and A-24, respectively. These figures show that changes in the value for specific yield only have a slight effect on the model output at the observation wells. This was the expected result because the specific yield was associated with the water that was released when the pumping began; the long-term effects were the result of the hydraulic conductivity.

#### ***4.4.4 Sensitivity to Dispersivity***

The sensitivity of the model to changes in the values of dispersivity was evaluated by multiplying and dividing the values of longitudinal and transverse dispersivity used in the model by a factor of two. The ratio of the transverse to the longitudinal dispersivity was maintained at 0.1. One figure was produced for each of the three pumping wells: Figures A-25, A-26, and A-27, for Wells EW-1, EW-2, and EW-3, respectively.

Results from this analysis show the breakthrough curves predicted with the model for Wells EW-1 and EW-3 were not significantly affected by these changes. However, there was an effect to the breakthrough curve predicted with the model for Well EW-2. When the longitudinal

dispersivity was increased from 10 feet to 20 feet and the transverse dispersivity was increased from one foot to two feet, the initial breakthrough predicted with the model occurred about seven days earlier. This effect can likely be attributed to the fact that EW-2 was not located either in an upgradient or downgradient position from the injection well as EW-1 and EW-3 were. Instead, the head in the perched aquifer at EW-2 was approximately the same as the injection well, PV-4. As a result, the increase in the value of the transverse dispersivity may have caused the tracer to spread in the direction of EW-2 faster than when the value was lower.

#### **4.4.5 Sensitivity to Vertical Hydraulic Conductivity**

A value of 0.1 ft/d was used in the groundwater transport model for the vertical hydraulic conductivity. Increases and decreases in the value of this parameter had limited effect on the breakthrough curves predicted with the transport model. The sensitivity of the model to this parameter was evaluated by running the model with a vertical hydraulic conductivity value one order of magnitude higher and one order of magnitude lower than 0.1 ft/d. The figures that correspond to the results of this analysis for pumping Wells EW-1, EW-2, and EW-3 are Figures A-28, A-29, and A-30.

There was little noticeable change in the breakthrough curves produced for Wells EW-1 and EW-2 when the vertical hydraulic conductivity value was varied. There was a slight effect noticeable in the breakthrough curves for Well EW-3. When the vertical hydraulic conductivity was increased to 1.0 ft/d, the maximum breakthrough concentration predicted for Well EW-3 is approximately 3 mg/L less and the peak breakthrough occurred about one day earlier than when the value was 0.1 ft/d. When the value was 0.01 ft/d, the maximum breakthrough concentration for EW-3 was approximately 3 mg/L greater and the peak breakthrough occurred about one day later.

#### **4.4.6 Sensitivity to Storage Coefficient**

The sensitivity of the transport model of the perched aquifer to the storage coefficient was evaluated by increasing the value of 0.0001, which was used in the model by one order of magnitude and decreasing the value by one order of magnitude. Increasing or decreasing the storage coefficient by one order of magnitude had no significant effect on the breakthrough curves predicted with the model for EW-1, EW-2, and EW-3. The figures corresponding to these three wells are A-31, A-32, and A-33, respectively.

#### **4.4.7 Additional Model Parameters**

There are a number of internal parameters within the MT3D model relating to the solution to the advective portion of the transport problem. A sensitivity analysis was conducted to determine the effects of changes in these parameters. The results from this analysis indicated that as long as the values were maintained for all of these parameters suggested in Zheng 1990, there was little effect on the model output. A list of these parameters is provided in Appendix B along with the values that were maintained throughout the modeling of the perched aquifer. Further explanation of each of these parameters can be found in the MT3D manual (Zheng, 1990).

#### **4.5 RDX RETARDATION**

The retardation of a given compound is sometimes not incorporated into predictions in transport rates in groundwater. This can lead to serious errors when evaluating the time necessary for the adequate remediation of the compound. Because groundwater remediation can potentially take a long time and have a high cost, it is important to incorporate the retardation of the constituent of concern traveling in groundwater into calculations on which decisions are based. This helps to ensure that the appropriate estimates of time and cost are made for remediation projects.

Retardation of a constituent in groundwater occurs when it adsorbs to the porous media. This affects the rate of migration of the constituent in the groundwater. Many factors influence this process including the amount of organic material present in the soil or suspended in the groundwater, the chemistry of the constituent, the groundwater, and the soil, and the competition for sorption sites from other chemicals. Higher rates of sorption of a constituent to the porous media correspond to slower rates of migration. A compound that adsorbs to aquifer material will move through groundwater at a slower rate than a non-adsorbing compound, or conservative compound, such as the bromide tracer, which was used in this project.

The process undergone by an adsorbing compound moving through groundwater can be divided into two phases. The first phase of the adsorption process occurs when the breakthrough of the constituent first occurs at a given point. Some of the constituent will adsorb to the aquifer material reducing the concentration in the groundwater and slowing the migration of the plume. The sorption of the constituent is assumed to be reversible (Rogers, 1992). As a result, once the portion of the contaminant plume with the peak concentration has passed a given point, some of the adsorbed compound will begin to desorb and dissolve again into the groundwater (Borden and

Bedient, 1987). This is sometimes a very slow process and as a result, some contaminant plumes may persist in groundwater for a very long time.

Retardation is defined by Equation 4-9.

$$R = \frac{V_n}{V_a} = 1 + k_d \frac{\rho_s}{n} \quad (\text{Equation 4-9})$$

where

R = retardation

$V_n$  = groundwater velocity of non-adsorbing compound (L/T)

$V_a$  = groundwater velocity of adsorbing compound (L/T)

$k_d$  = linear sorption coefficient ( $L^3/M$ )

$\rho_s$  = bulk density of the porous media ( $M/L^3$ )

n = porosity

The linear sorption coefficient,  $k_d$ , is assumed to be valid for situations where the concentrations of a constituent in a solution are low relative to its solubility. This is typically the case with dissolved contaminants in groundwater. As a result, the linear sorption is used to estimate the RDX retardation in this model.

#### **4.5.1 Procedure for Estimation of RDX Retardation**

RDX retardation in the Zone 12 area of the Pantex facility was estimated using the calibrated groundwater model, the initial RDX contours for the modeling area, and the RDX concentrations measured from Wells EW-1, EW-2, and EW-3 during the tracer test. During the tracer test, RDX concentrations were expected to decrease in effluent from the wells as the clean water breakthrough occurred resulting from the water injected through Well PV-4.

In order to evaluate RDX retardation, each cell in the model grid was given an initial concentration defined by the initial RDX contours of the area. Next, the transport model was operated under the same pumping conditions used in the tracer test, with water that did not contain RDX injected at passive vent Well PV-4. In each successive run of the model, the  $k_d$  value was altered until an appropriate fit to curves created from analytical results of the test was achieved. As

noted in Chapter 2, only the analytical data from weekly RDX samples evaluated with HPLC was used for comparison in the model. The final value of  $k_d$  estimated from running the model is 0.050 liters per kilogram (L/kg). A root mean square analysis was conducted to determine which  $k_d$  value led to output that closest fit the analytical data. Figures 4-22, 4-23, and 4-24 show the model output of the RDX concentrations for  $k_d$  of 0.050 L/kg compared to the analytical data.

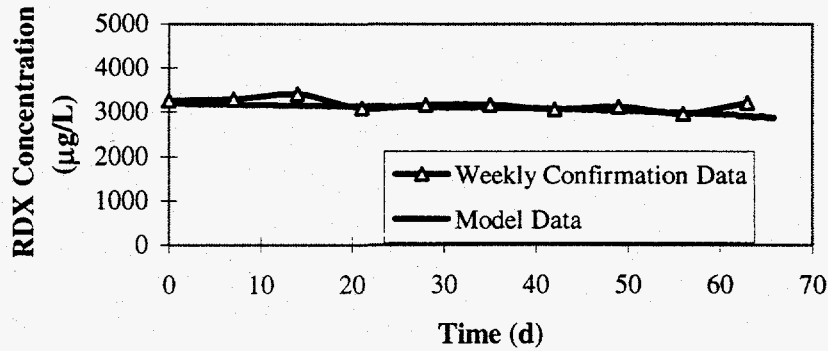


Figure 4-22: Comparison of Model Output to RDX Analytical Data for EW-1

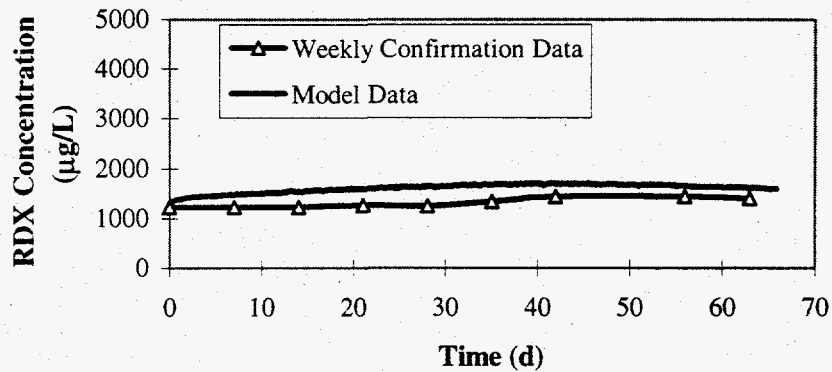


Figure 4-23: Comparison of Model Output to RDX Analytical Data for EW-2

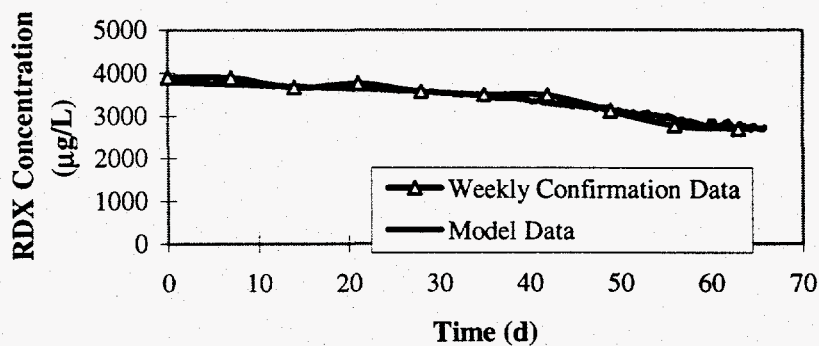


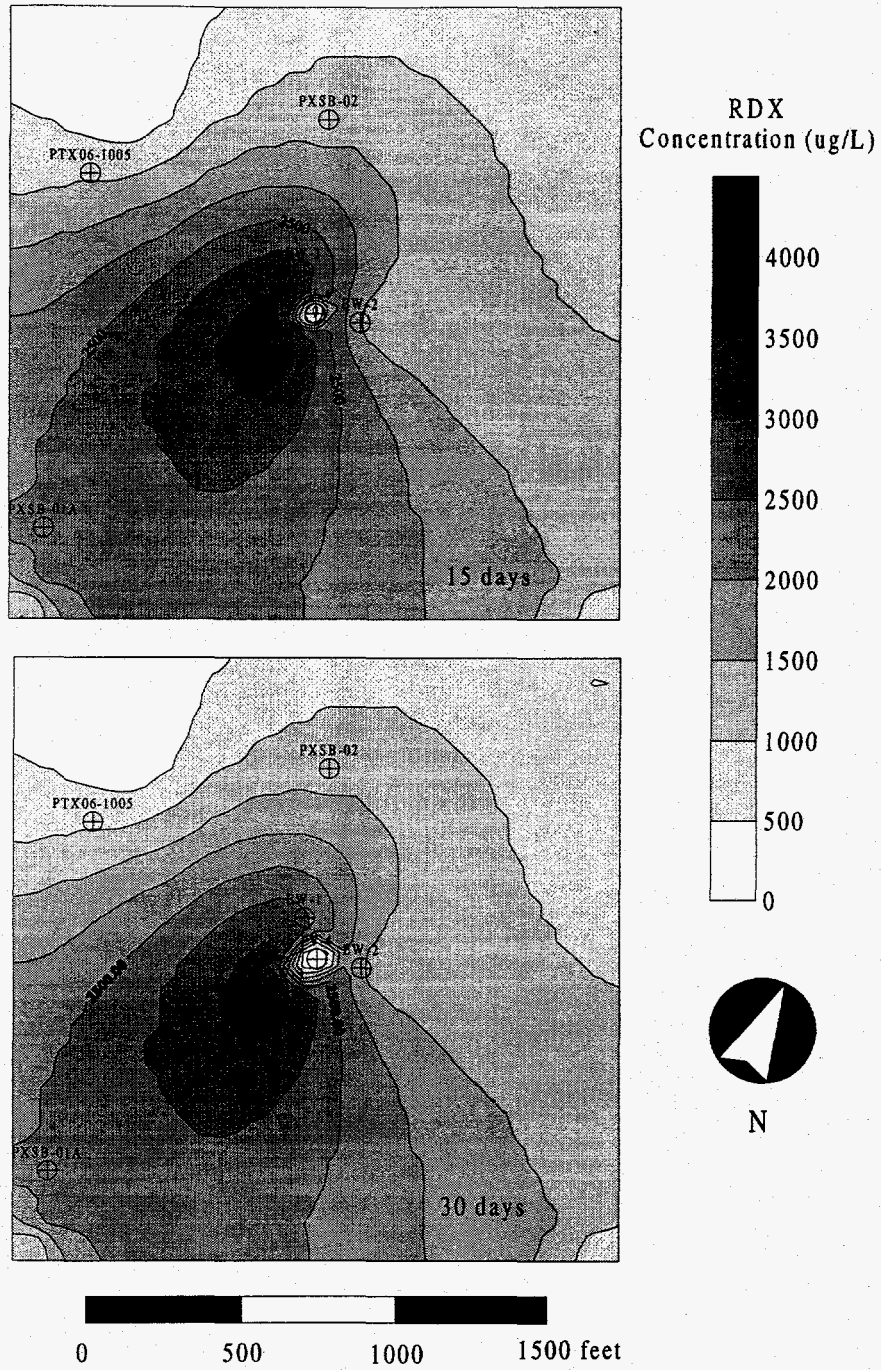
Figure 4-24: Comparison of Model Output to RDX Analytical Data for EW-3

Calculation of the retardation of the RDX in the groundwater depends on the  $k_d$  value, the bulk density of the soil, and the porosity. The  $k_d$  value was estimated as 0.050 L/kg. The bulk density of the soil was assumed to be 2530 kilograms per cubic meter ( $\text{kg/m}^3$ ). The porosity values estimated through the calibration of the model ranged from 0.30 to 0.35. With this range in porosity, the calculated retardation ranged from 1.36 to 1.42. Therefore, the retardation of RDX in the perched aquifer at the Pantex Plant was estimated as 1.4.

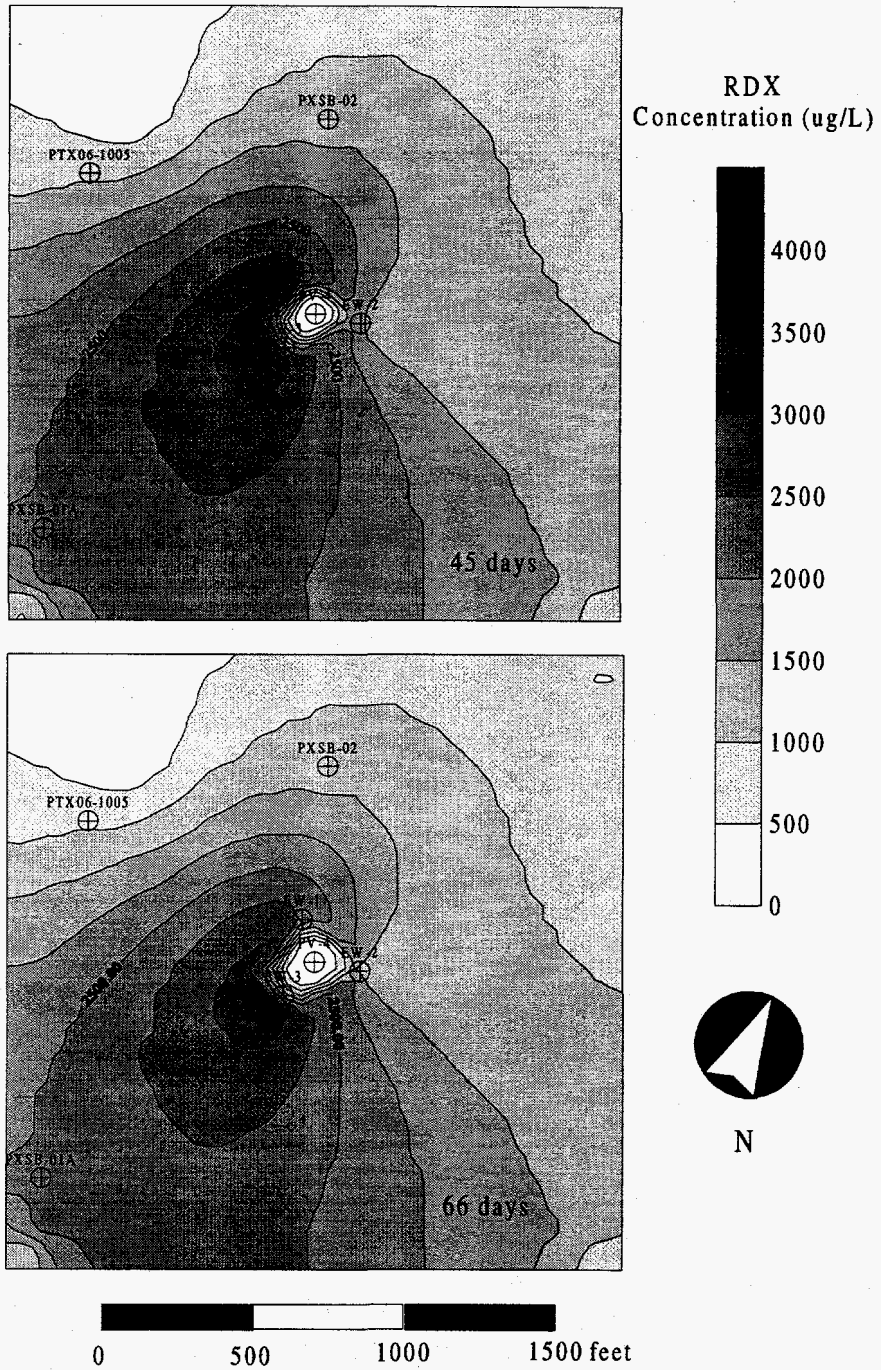
#### ***4.5.2 Removal of RDX from Perched Aquifer during the Tracer Test***

During the duration of the tracer test, significant volumes of water were injected at Well PV-4 and extracted at Wells EW-1, EW-2, and EW-3. This resulted in changes in the RDX concentrations in the perched aquifer in the area of the treatment system over the duration of the tracer test. Four figures are included which show the RDX contours in the area of the perched aquifer, which was modeled at various times during the tracer test. Figures 4-25, 4-26, 4-27, and 4-28 show the RDX concentration contours predicted with the model corresponding to Days 15, 30, 45, and 66 of the tracer test.

Water containing no RDX was injected at PV-4 at the start of the tracer test. Beginning at this time, a zone surrounding Well PV-4 where the RDX concentration was 0 mg/L forms. The size of this zone continually increases at later times during the test. Also, there was no increase in RDX concentrations outside the ring formed by the three extraction wells surrounding PV-4. This indicated that these three wells, EW-1, EW-2, and EW-3, were providing appropriate hydraulic control within their respective boundary.



Figures 4-25 and 4-26: RDX Contours at 15 and 30 Days in the Tracer Test



Figures 4-27 and 4-28: RDX Contours at 45 and 66 Days in the Tracer Test

#### 4.6 EVALUATION OF RE-CIRCULATION

The use of the re-circulation of treated water in a groundwater pump-and-treat system generally has positive effects on remediation efforts. These potential benefits of groundwater re-circulation are discussed in Hoffman, 1993, and are listed as follows:

- Increase the gradient from the injection to the pumping well and increasing groundwater velocity in the vicinity of the injection well.
- Facilitate the desorption of constituents to speed the clean up rate.
- Avoid de-watering.
- Hydraulic control.

In the case of the tracer test in the perched aquifer in the Zone 12 area of the Pantex facility, the groundwater extracted from Wells EW-1 and EW-3 was transferred to the treatment system where the compounds including the RDX were removed using a carbon adsorption system. Effluent from the treatment system was re-injected into the perched aquifer through Well PV-4.

One effect of using groundwater re-circulation during the tracer test in the perched aquifer was an increased gradient between the injection well, PV-4, and each of the three extraction wells, EW-1, and EW-2, and EW-3. Although this increased gradient caused the zone of capture to be decreased for each of the three extraction wells, the benefits of the use of re-circulation during the tracer test still outweigh the negative effects.

During the tracer test, the time needed for the breakthrough of the bromide at EW-1, EW-2, and EW-3 was decreased with the use of re-circulation of the treated water from what the time needed would have been if re-circulation was not used. Also, because there are compounds present such as RDX which adsorb to the aquifer material, the treated water which is re-injected into the aquifer aids in enhancing the desorption of these chemicals so they can be extracted with the groundwater. These two benefits of the use of re-circulation have significant implications for future remediation efforts for the perched aquifer in the Zone 12 area of the Pantex Plant.

## 5. SUMMARY, CONCLUSIONS, AND RECOMMENDATIONS

This chapter summarizes the objectives, which were addressed in the groundwater modeling of the perched aquifer in the Zone 12 area of the Pantex Plant. A list of the conclusions from the groundwater flow and RDX transport modeling are listed as well along with recommendations relating to future work at the site.

### 5.1 SUMMARY

A field tracer test was successfully performed at the Zone 12 Treatability site at the Pantex Plant. The test could not have happened without the cooperation of the Battelle Pantex Environmental Restoration division, who made the original conceptual design of the Treatability site, and engineering-environmental Management, who installed and operated the system. The Treatability site included three extraction wells that produced groundwater contaminated with HE from the perched aquifer, with treatment of the produced water in granular activated carbon columns. The test was designed to utilize a central vent well for injection of a solution of bromide mixed with the treated effluent. A bromide solution was introduced at the central well for 24 days, followed by almost 42 days of treated effluent only. The first objective of the injection was to cause breakthrough of Br and HE-free water at the extraction wells. Bromide and RDX concentrations were monitored in the field through daily sampling and analysis with field analytical methods. Weekly samples were taken to the laboratory for regular verification with fixed instruments. The total duration of the test was limited by operational constraints beyond the control of the research team, including significant power outages that finally ended the test.

The second objective of the flow and transport modeling was to estimate the retardation of RDX in the perched aquifer. Using the calibrated model and the initial concentration contours of RDX in the Zone 12 area, the linear sorption coefficient was increased until the model output marched RDX concentration measurements from the field.

The third objective of the groundwater modeling was to evaluate the removal of RDX from the perched aquifer. RDX concentration contours were developed four times during the tracer test based upon the model output. These contours show that the concentration of RDX was decreasing in the area of the perched aquifer located in the middle of the three extraction wells, EW-1, EW-2, and EW-3.

The last objective of the groundwater modeling was to evaluate the use of re-circulating treated water to enhance the extraction of RDX from the perched aquifer. In the tracer test, groundwater was re-injected into the aquifer through Well PV-4 following treatment. One effect of the injection of this water was a decrease in the time needed until breakthrough of the bromide tracer at the observation wells. A second potential effect was that the re-injected water aided in the desorption of compounds sorbed to aquifer material so they could be extracted in the groundwater.

## 5.2 CONCLUSIONS

There are a number of conclusions which can be made based on the evidence presented using MODFLOW and MT3D to model the groundwater flow and RDX transport in the perched aquifer at the Pantex Plant. These conclusions are listed as follows:

- The design and installation of the injection system into the existing Treatability system was successful.
- Due to the short test duration, the tracer test demonstrated breakthrough of Br and HE-free effluent at only one of the three extraction wells.
- The DTECH field kits for RDX analysis did not provide adequate results to be used in the estimation of the RDX retardation using the groundwater models. There was significantly greater variability in the data collected from the Pantex site than the data provided by the manufacturer from another site when compared to the HPLC method of analysis. The DTECH kits might be useful strictly as a screening tool for this site but the analytical results are not recommended for use in a quantitative analysis.
- Based on the evidence presented from the tracer test and the modeling, there seems to be at least two stratigraphic layers present within regions of the perched aquifer. The groundwater of different layers has different values of hydraulic conductivity, and therefore, they influence the flow and transport of RDX in that portion of the perched aquifer beneath the Zone 12 area. For the system modeled in this work, the hydraulic conductivity of the bottom layer estimated using

the model ranges from 7ft/d to 10ft/d. The hydraulic conductivity is estimated as 25ft/d in the upper layer of the portion of the aquifer where there is evidence that the two layers exist.

- The parameter with the most substantial effect on the transport of constituents in the groundwater of the perched aquifer is the hydraulic conductivity. Porosity is the parameter, which has the second most significant effect on transport in the model. Even small variations in the values of their two parameters can significantly affect the transport of RDX through the groundwater.
- The porosity of the soils of the perched aquifer predicted with the models range from 0.30 to 0.35.
- The specific yield value predicted with the flow model is 0.2. This has little effect on the transport of RDX through the groundwater in the perched aquifer at the Zone 12 site.
- Changes in the values for the vertical hydraulic conductivity and the storage coefficient (layer 2 only) have an insignificant effect on the transport of the contaminant in the groundwater. Therefore, no conclusion can be made on the actual values of these two parameters in the perched aquifer.
- The linear sorption coefficient,  $k_d$ , for RDX in the perched aquifer in the Zone 12 area, is estimated at 0.050 L/kg using the groundwater flow and transport models. With this  $k_d$  value, the retardation coefficient of the RDX is calculated as 1.4. This indicated the rate of migration of the RDX plume through the perched aquifer.
- This type of pump and treat system provides an effective means of removing significant amounts of RDX from the perched aquifer at the Pantex site. The re-injection of the treated water can enhance the ability of such a system in the removal of RDX from the groundwater in the perched aquifer.

These conclusions aid in increasing the understanding of the flow and the RDX transport in the perched aquifer beneath the Zone 12 area. The information provided can be used in future efforts to remove some of the contaminants from the subsurface in this area.

The TTU team would like to gratefully acknowledge the cooperation of several people that made the tracer test possible. Dr. Darrell Brownlow and Mr. Scot Laun of e<sup>2</sup>M were instrumental in negotiating access to the ZTTS. Mr. Johnny Weems of the Environmental Restoration group of Battelle-Pantex granted permission for the test to occur. Mr. Dan Ferguson of the DOE Amarillo Area Office encouraged the test to be pursued. Ms. Michelle Brown of Battelle-Pantex was the Plant point of contact for access and offered her staff to assist with sample collection if necessary.

### **5.3 RECOMMENDATIONS**

Some recommendations are presented here for future study and work related to the contamination in the perched aquifer in the Zone 12 area of the Pantex Plant. These recommendations are based upon evidence discussed regarding the groundwater flow and RDX transport modeling in the perched aquifer.

- Evidence from the flow and transport modeling of the perched aquifer in the Zone 12 area indicates that pump and treat is an effective technology for the extraction of RDX in the groundwater. Therefore, this technology should be utilized for further removal of RDX from the groundwater in the perched aquifer at the Pantex site.
- Although compounds other than RDX which were detected in the perched aquifer (HMX, VOCs) were not the target of this investigation, the pump and treat system is likely effective in removing significant concentrations of these compounds. Further investigation is necessary to verify that this is true.
- Evidence from the transport modeling of RDX shows that the retardation of the RDX in the perched aquifer is approximately 1.4. This factor needs to be taken into consideration for all future remediation efforts for RDX at this site when estimating adequate time and cost needed.

- One of the most important results of the use of groundwater re-circulation in a pump and treat remediation scheme is that it enhances the desorption of compounds which are sorbed to the aquifer material. For this reason, it is important to incorporate the re-circulation of the treated water into future pump and treat efforts at the Pantex site when there is the potential that the target compounds may be sorbed to the soil particles. This will help decrease the time needed for remediation efforts.

## REFERENCES

1. Argonne National Laboratory Environmental Research Division. "Draft Final Report: Phase II Expedited Site Characterization for the DOE Pantex Zone 12 Groundwater Investigation," July 1995.
2. Black, Sara and Ken Rainwater. "The Perched Aquifer Tracer Test: Methodology and Observations." Texas Tech University Water Resources Center, Lubbock, Texas, January 1997.
3. Borden, Robert C. and Philip B. Bedient. "In Situ Measurement of Adsorption and Biotransformation at a Hazardous Waste Site." Water Resources Bulletin, August 1987, pp. 629-636.
4. Browlow, Darrell T., Ph.D., and Jim Rogers. "Treatability Study Test Plan for Groundwater Pump and Treat/Soil Vapor Extraction System," Pantex Zone 12 Treatability Study, July 1995
5. Charbeneau, Randall J. "Groundwater Hydraulics and Pollutant Transport." The University of Texas at Austin, 1995.
6. Daniel, David E., ed. "Geotechnical Practice for Waste Disposal." New York 1993.
7. Driscoll, Fletcher G. "Groundwater and Wells." St. Paul, Minnesota, 1986.
8. Gelhar, Lynn W., Claire Welty, and Kenneth R. Rehfeldt. "A Critical Review of Data on Field-Scale Dispersion in Aquifers." Water Resources Research, Vol. 28, No.7, July 1992, pp. 1955-1974.
9. "RCRA Land Disposal Restrictions." Federal Register. Vol. 51, No. 9, pp. 945-957.
10. Guven, O., R.J. Molz, J.G. Melville, S. El Didy and G.K. Boman. "Three-Dimensional Modeling of a Two-Well Tracer Test." Ground Water. November-December 1992, Vol. 30, No.6, pp. 945-957.
11. Hoffman, Fredric. "Ground-Water Remediation Using 'Smart Pump and Treat'." Ground Water. January-February 1993, Vol. 31, No. 1, pp. 98-106.
12. Huyakorn, Peter S., Peter F. Andersen, Fred J. Molz, Oktay Guven, and Joel G. Melville. "Simulations of Two-Well Tracer Tests in Stratified Aquifers at the Chalk River and the Mobile Sites." Water Resources Research, July 1986, Vol. 22, No. 7, pp. 1016-1030.
13. Kendrick, James Oliver III. "An Investigation of Vadose Zone Remediation at the Pantex Plant Site." M.S. Thesis, The University of Texas at Austin, 1996.

14. Mason & Hanger-Silas Mason Co., Inc. "As-Built Drawings for Groundwater Pump and Treat/Soil Vapor Extraction System." Pantex Zone 12 Treatability Study, November 1995.
15. Mas-Pla, Joseph, T., Jim Yeh, Hogn, R. McCarthy, and Williams, T.M.. "A Forced Gradient Tracer Experiment in a Coastal Sandy Aquifer, Georgetown Site, South Carolina." Ground Water. November-December 1992, pp. 958-964.
16. McDonald, Michael G. and Harbaugh, Arlen W. "A Modular Three-Dimensional Finite-Difference Ground-Water Flow Model." U.S. Geological Survey, 1984.
17. Mercado, A. "The Spreading Pattern of Injected Water in a Permeability Stratified Aquifer." Symposium on Haifa, Artificial Recharge and Management of Aquifer, IAHS ASIH, 1967, pp. 23-36.
18. "Pantex Facility, Amarillo, Texas." <http://www.pantex.com/ds/index.hmt> (February 6, 1997).
19. Pickens, John F. and Gerald E. Grisak. "Scale-Dependent Dispersion in a Stratified Granular Aquifer." Water Resources Research. August 1981, Vol. 17, No. 4, pp.1191-1211.
20. Rainwater, Ken. "Revised Tracer Test Work Plan." Memo to Mickey Brown, BMI/Pantex. June 3, 1996.
21. Rogers, L. "History Matching to Determine the Retardation of PCE in Ground Water." Ground Water. January-February 1992, Vol. 30, No. 1, pp. 50-60.
22. U.S. Department of Energy, Amarillo Area Office, Environmental Restoration Project. "Zone 12 Groundwater Treatability Study: Dual Phase Groundwater/Soil Vapor Extraction Project," 1995.
23. U.S. Department of Health and Human Services. "Toxicological Profile for HMX." June 1994.
24. U.S. Department of Health and Human Services. "Toxicological Profile for RDX." June 1995.
25. Zheng, C. "A Modular Three-Dimensional Transport Model for Simulation of Advection, Dispersion and Chemical Reactions of Contaminants in Groundwater Systems." October 1990.
26. Engineering-Environmental Management, Inc., 1996. "Pantex Zone 12 Treatability Study, Interim Data Report #4, Vol. I, Text," submitted to Mason & Hanger-Silas Mason Co., Inc., Pantex Plant, Amarillo, TX.
27. Teaney, G. and Hudak, R., 1994. "Development of an Enzyme Immunoassay Based Field Screening for the Detection of RDX in Soil and Water," presented at the 87th Annual Meeting, Air and Waste Management Association, Paper 94-RP143.05, Cincinnati, OH, June 19-24.

## APPENDIX A: SENSITIVITY ANALYSIS FIGURES

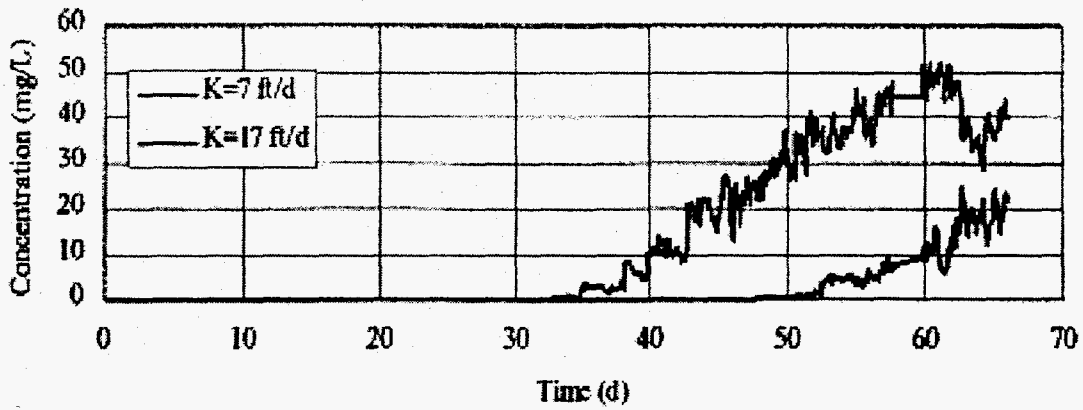


Figure A-1  
Sensitivity at EW-1 to Changes in Zone 1 Hydraulic Conductivity

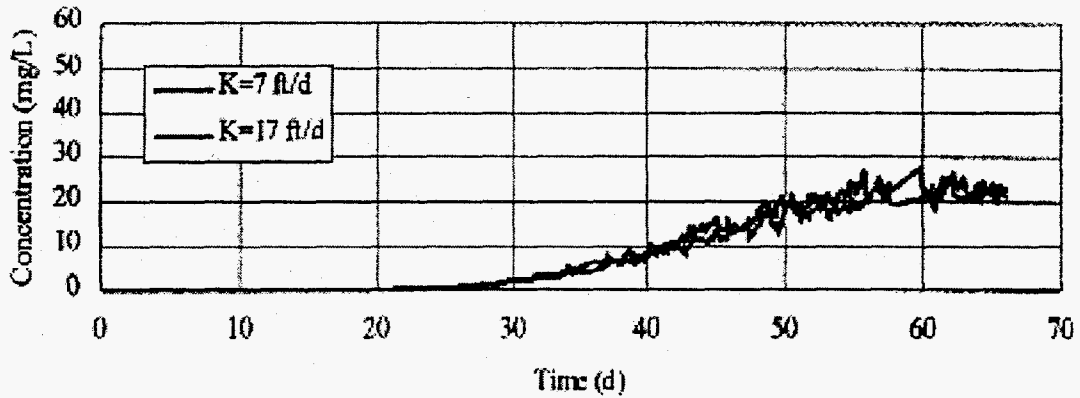


Figure A-2  
Sensitivity at EW-2 to Changes in Zone 1 Hydraulic Conductivity

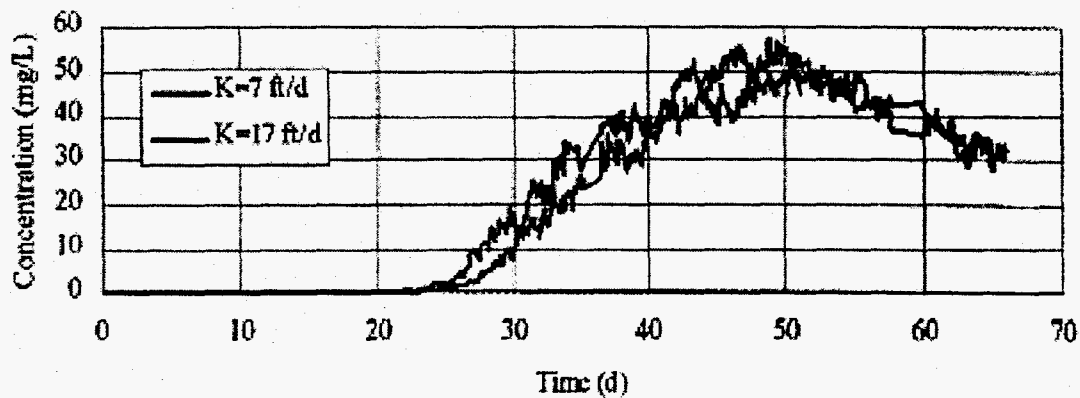


Figure A-3  
Sensitivity at EW-3 to Changes in Zone 1 Hydraulic Conductivity

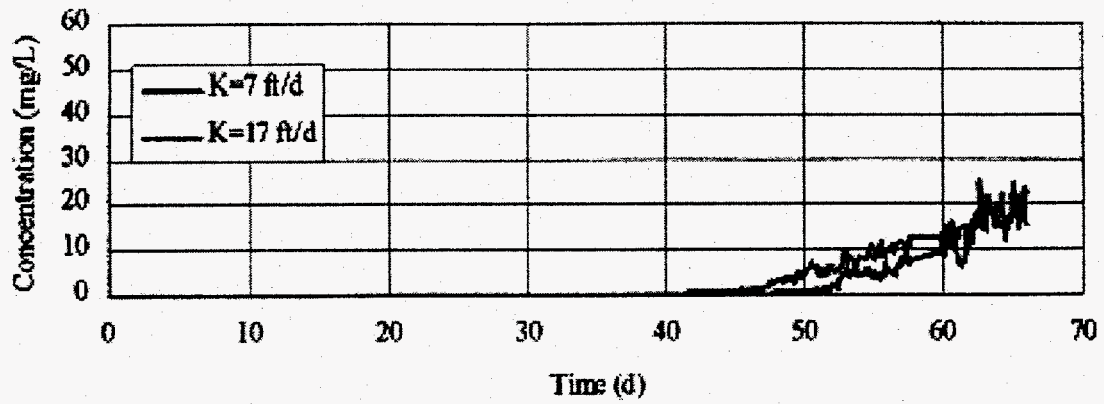


Figure A-4  
Sensitivity at EW-1 to Changes in Zone 2 Hydraulic Conductivity

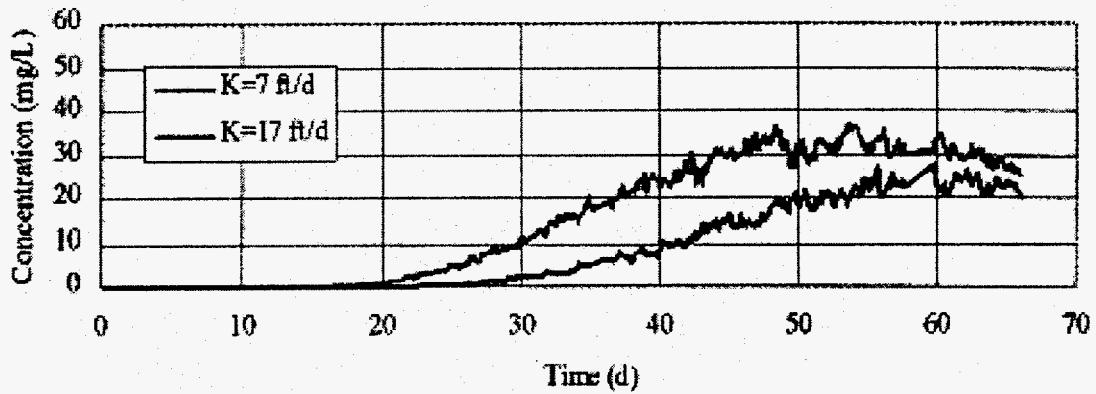


Figure A-5  
Sensitivity at EW-2 to Changes in Zone 2 Hydraulic Conductivity

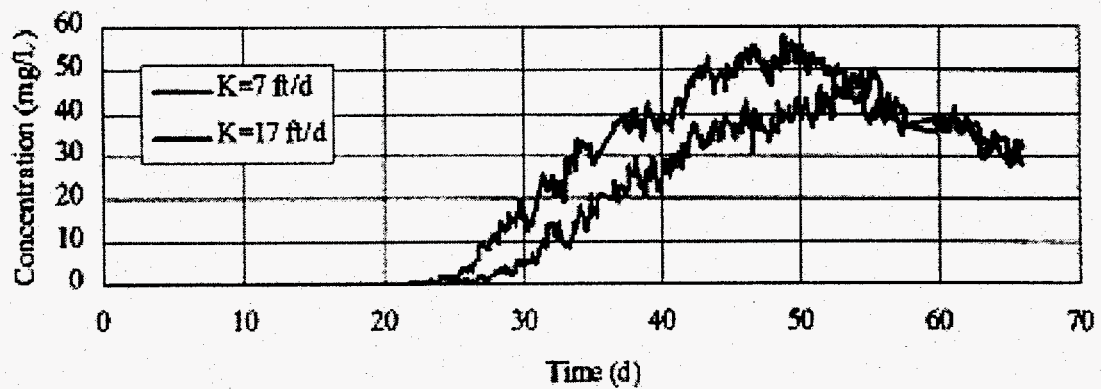


Figure A-6  
Sensitivity at EW-3 to Changes in Zone 2 Hydraulic Conductivity

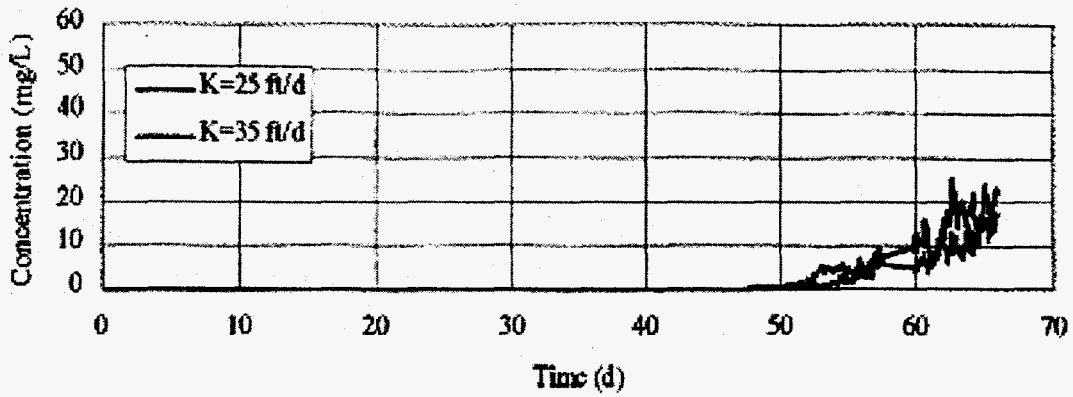


Figure A-7  
Sensitivity at EW-1 to Changes in Zone 3, Layer 1 Hydraulic Conductivity

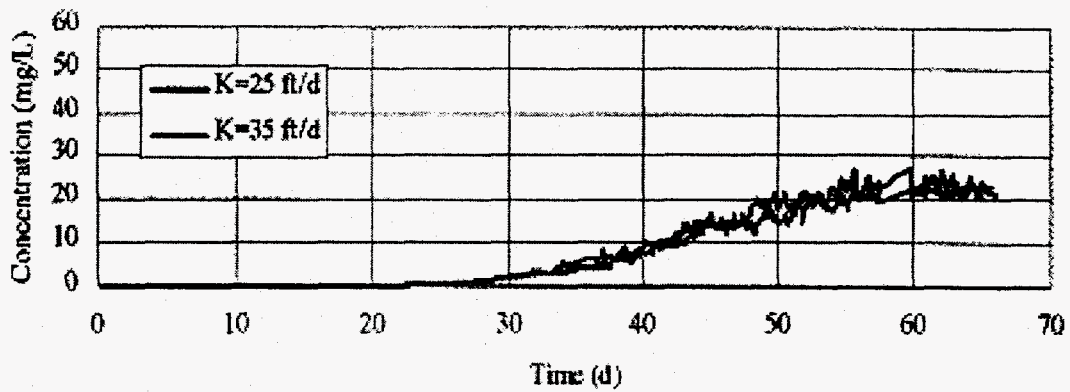


Figure A-8  
Sensitivity at EW-2 to Changes in Zone 3, Layer 1 Hydraulic Conductivity

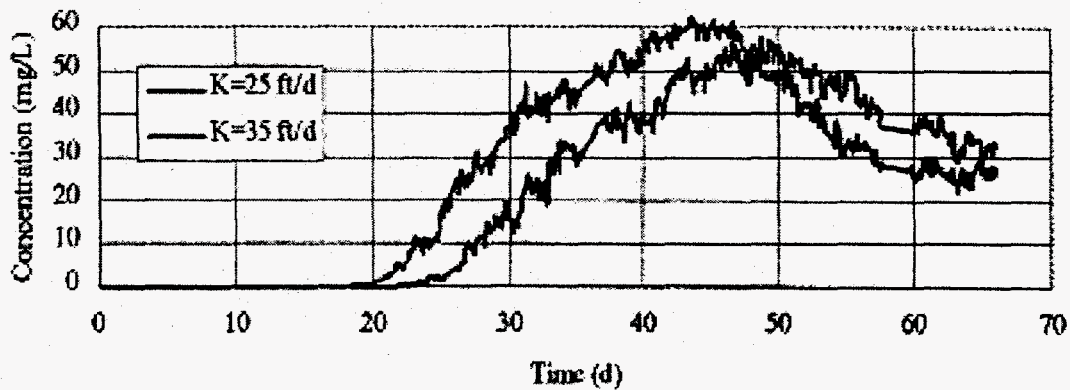


Figure A-9  
Sensitivity at EW-3 to Changes in Zone 3, Layer 1 Hydraulic Conductivity

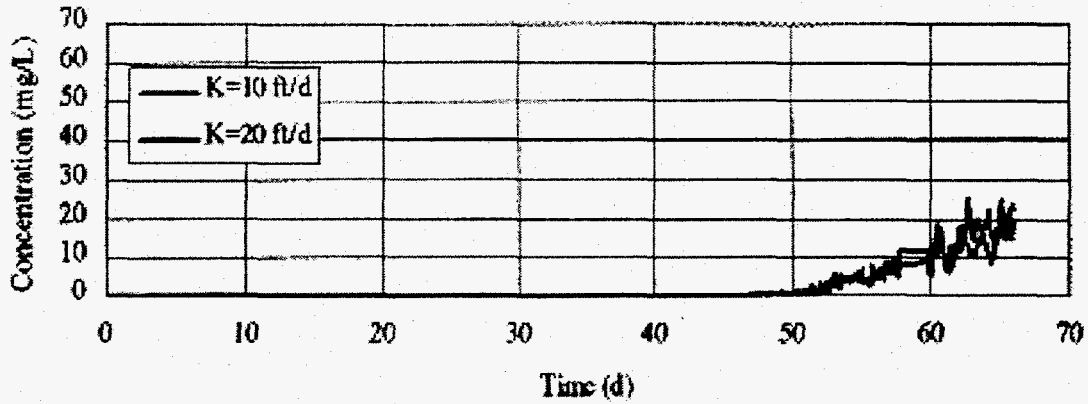


Figure A-10  
Sensitivity at EW-1 to Changes in Zone 3, Layer 2 Hydraulic Conductivity

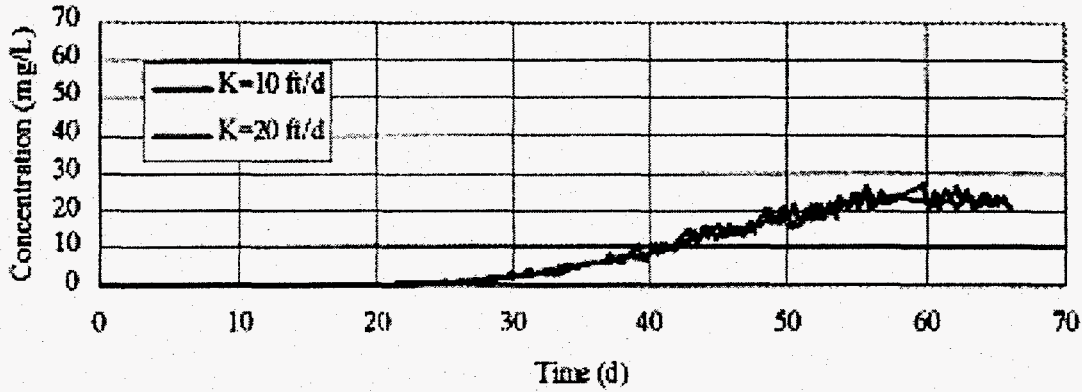


Figure A-11  
Sensitivity at EW-2 to Changes in Zone 3, Layer 2 Hydraulic Conductivity

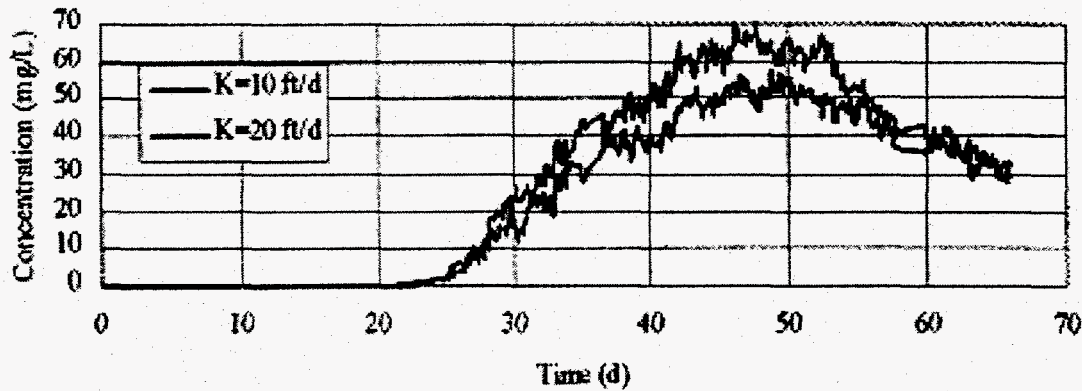


Figure A-12  
Sensitivity at EW-3 to Changes in Zone 3, Layer 2 Hydraulic Conductivity

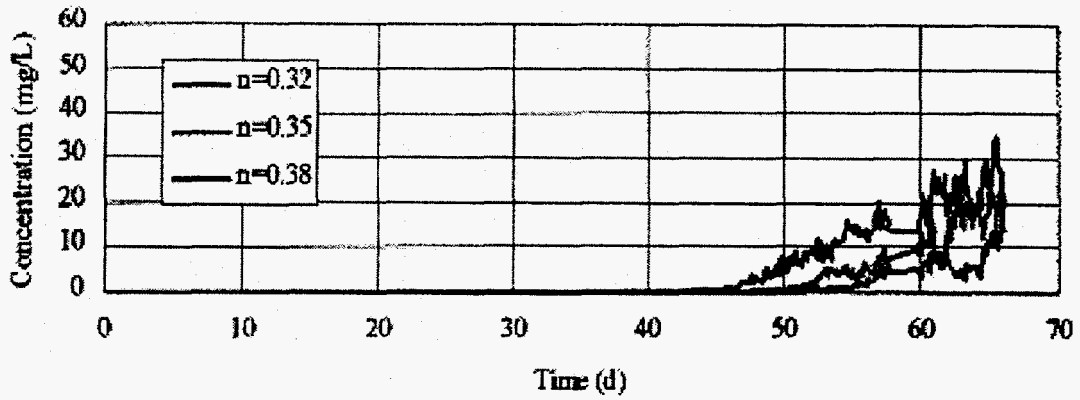


Figure A-13  
Sensitivity at EW-1 to Changes in Zone 1 Porosity

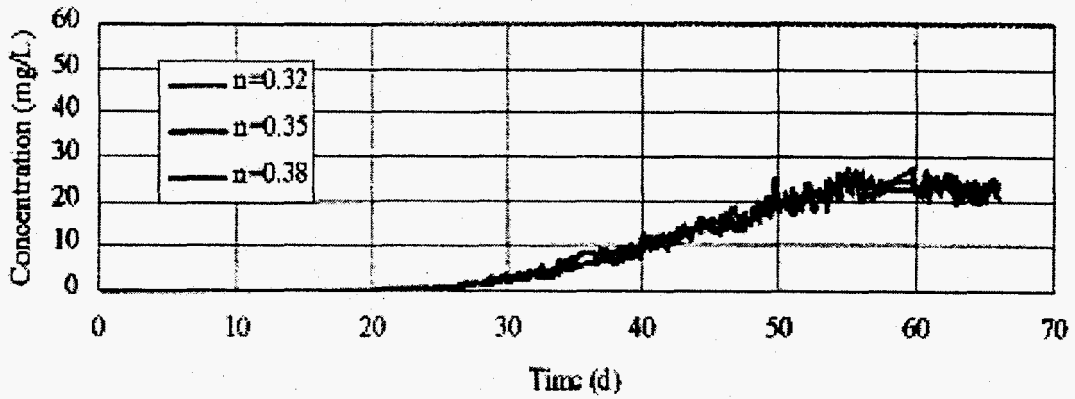


Figure A-14  
Sensitivity at EW-2 to Changes in Zone 1 Porosity

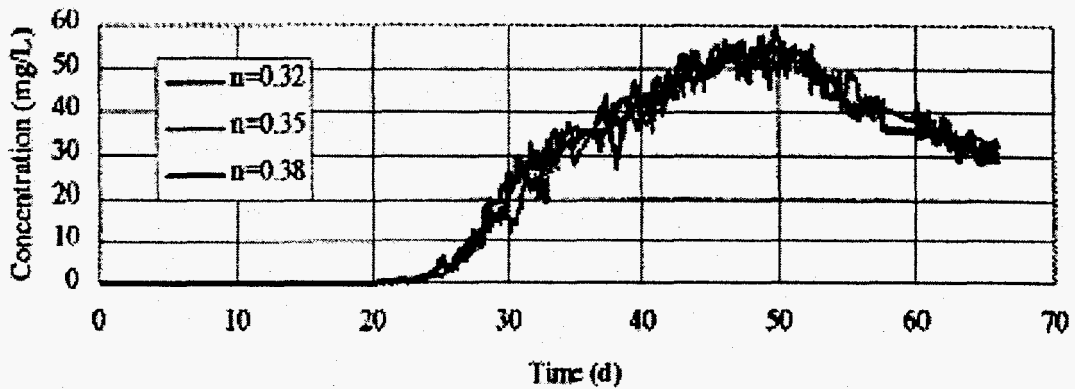


Figure A-15  
Sensitivity at EW-3 to Changes in Zone 1 Porosity

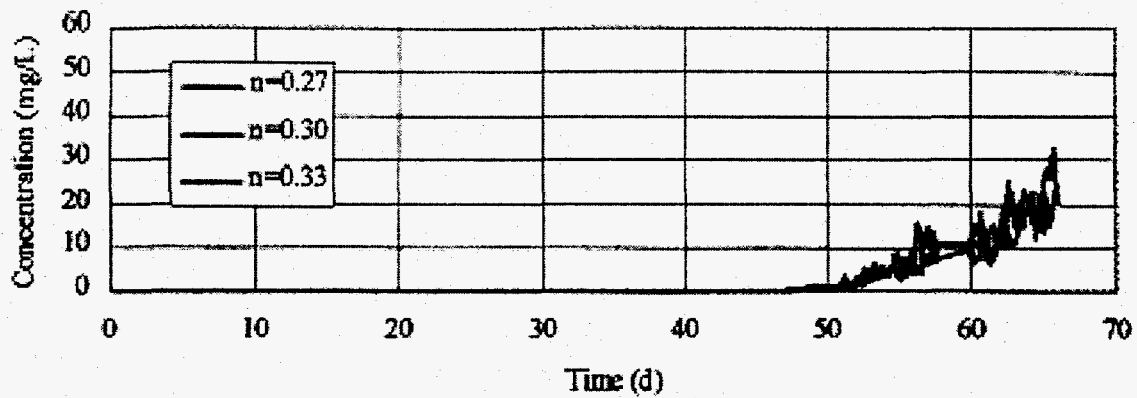


Figure A-16  
Sensitivity at EW-1 to Changes in Zone 2 Porosity

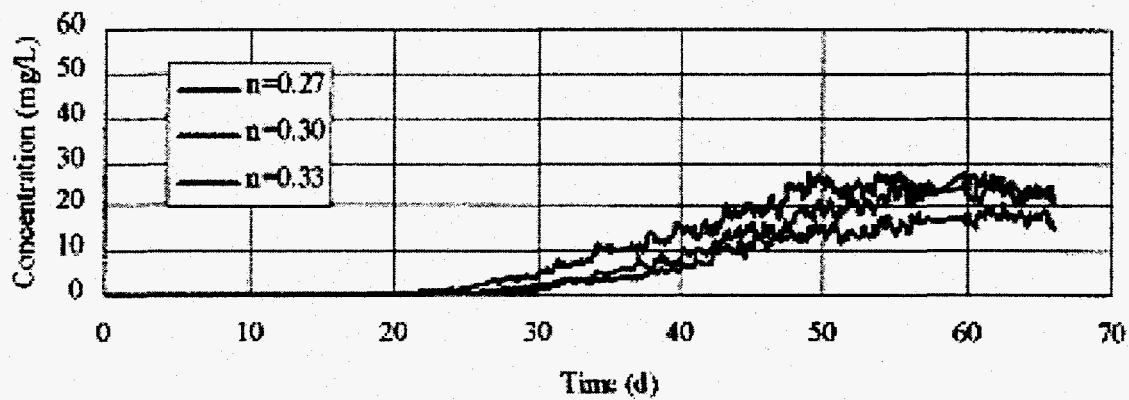


Figure A-17  
Sensitivity at EW-2 to Changes in Zone 2 Porosity

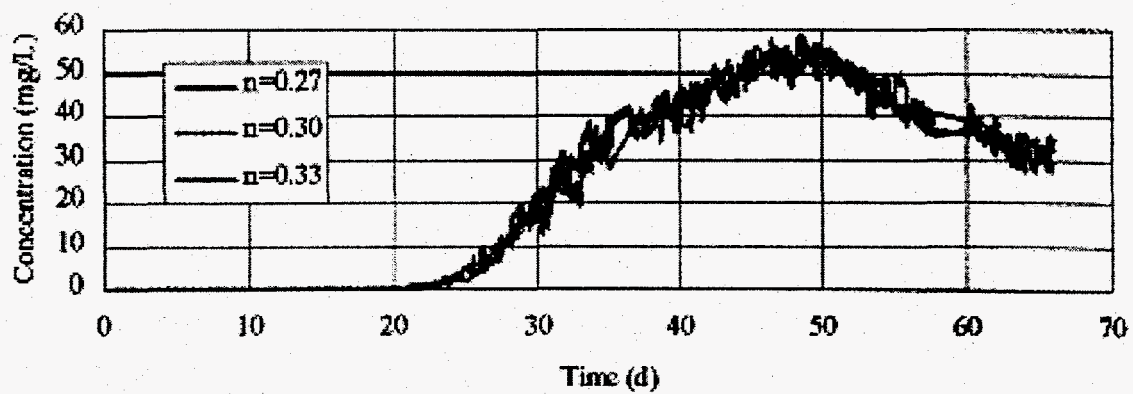


Figure A-18  
Sensitivity at EW-3 to Changes in Zone 2 Porosity

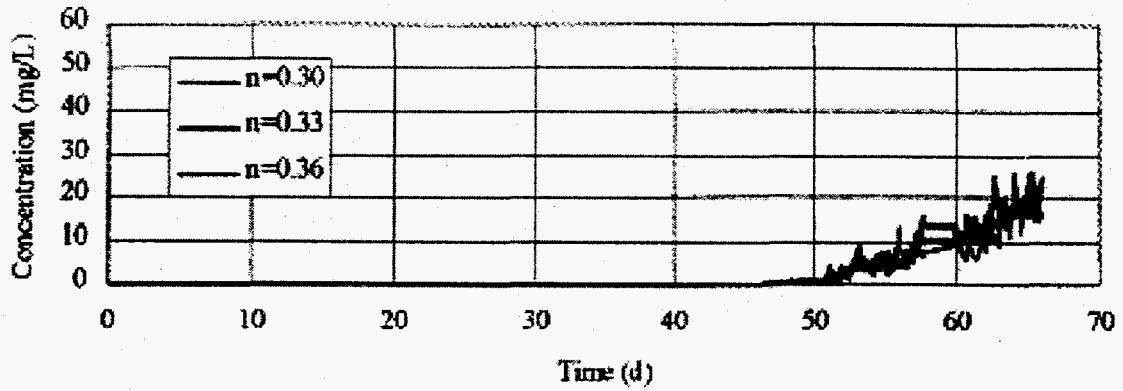


Figure A-19  
Sensitivity at EW-1 to Changes in Zone 3 Porosity

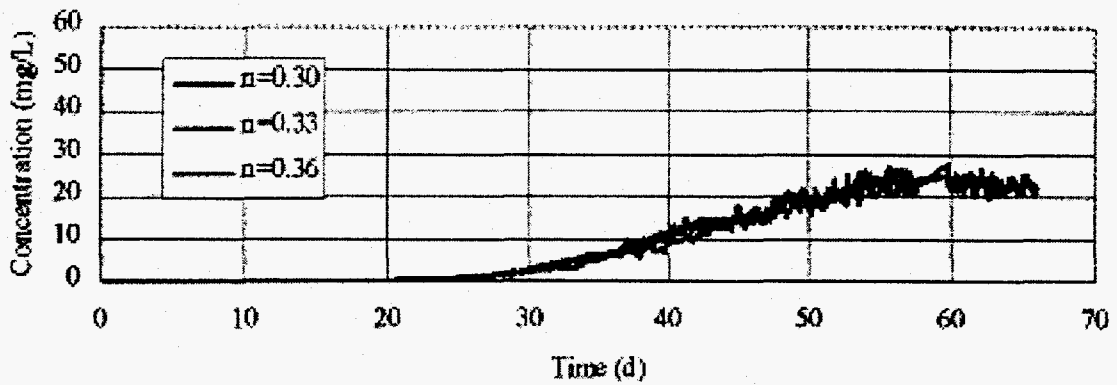


Figure A-20  
Sensitivity at EW-2 to Changes in Zone 3 Porosity

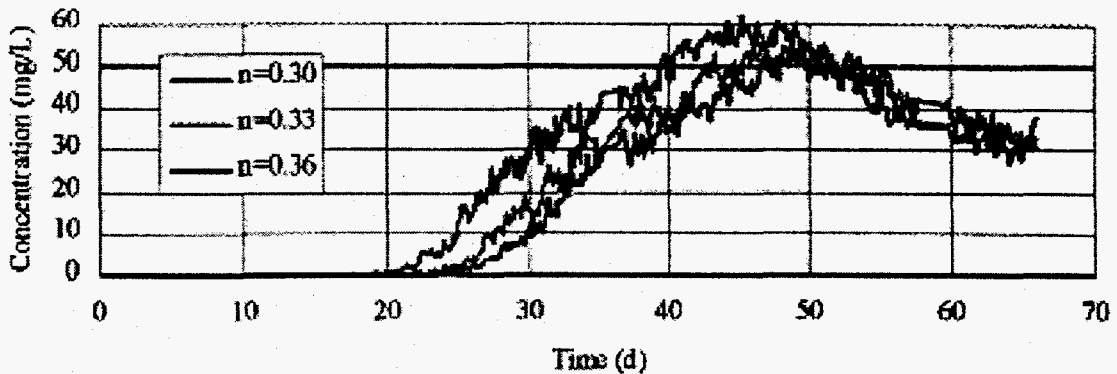


Figure A-21  
Sensitivity at EW-3 to Changes in Zone 3 Porosity

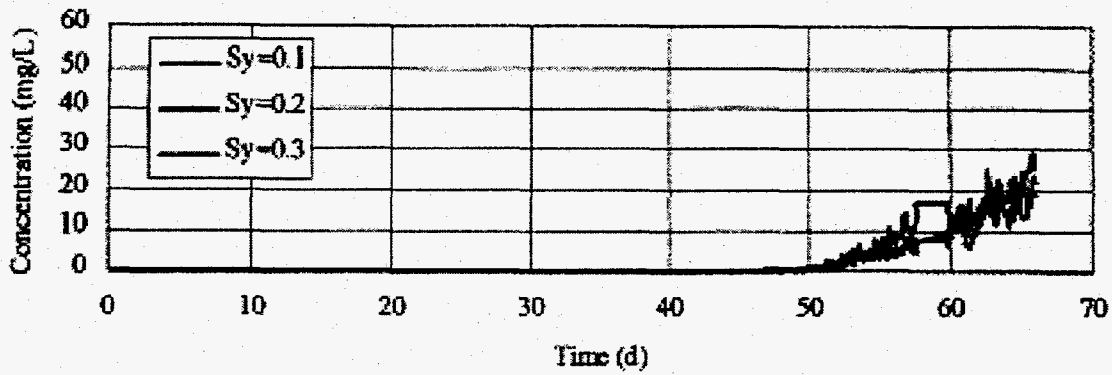


Figure A-22  
Sensitivity at EW-1 to Changes in Specific Yield

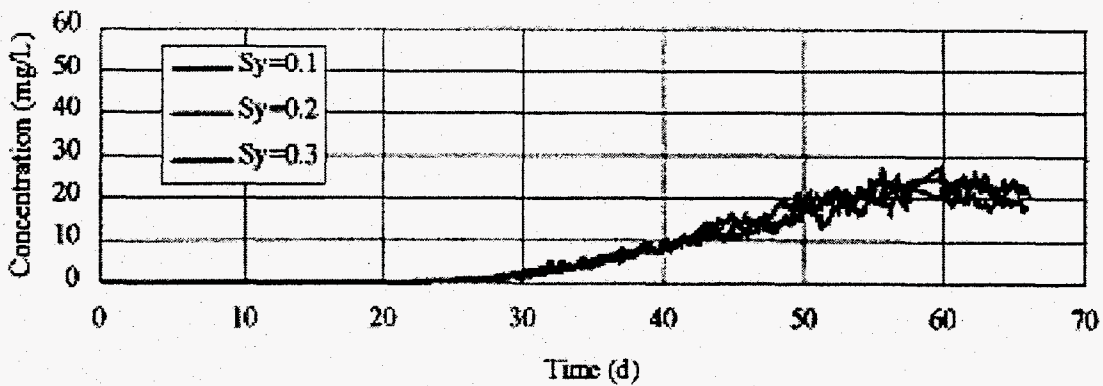


Figure A-23  
Sensitivity at EW-2 to Changes in Specific Yield

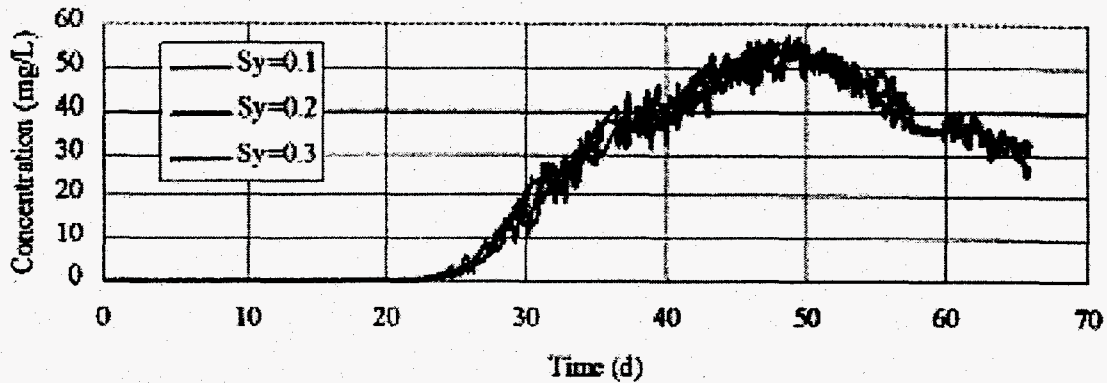


Figure A-24  
Sensitivity at EW-3 to Changes in Specific Yield

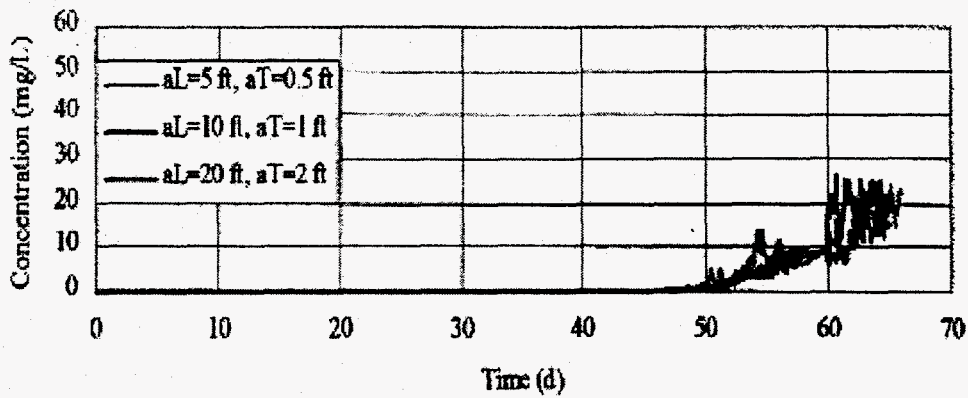


Figure A-25  
Sensitivity at EW-1 to Changes in Dispersivity

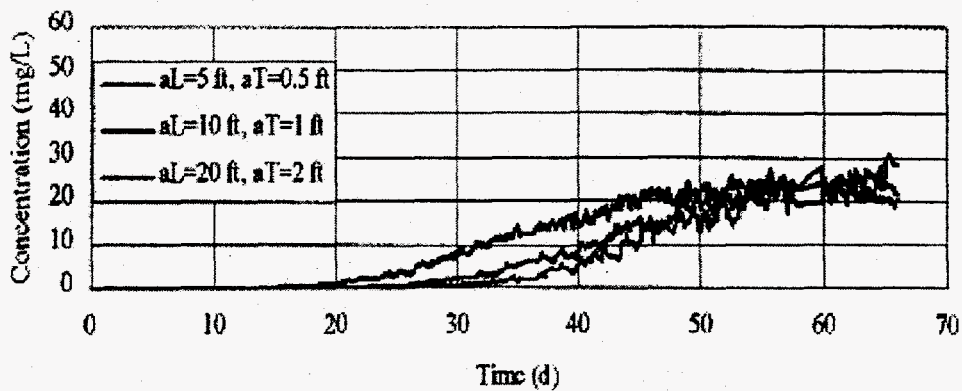


Figure A-26  
Sensitivity at EW-2 to Changes in Dispersivity

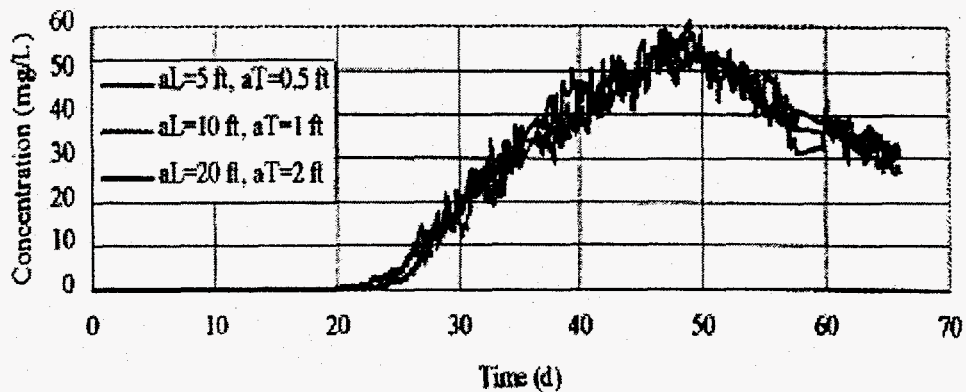


Figure A-27  
Sensitivity at EW-3 to Changes in Dispersivity

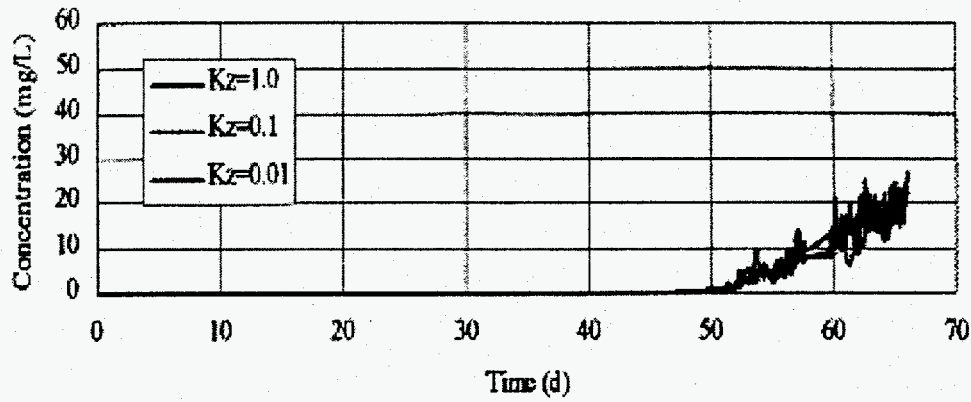


Figure A-28  
Sensitivity at EW-1 to Changes in Vertical Hydraulic Conductivity

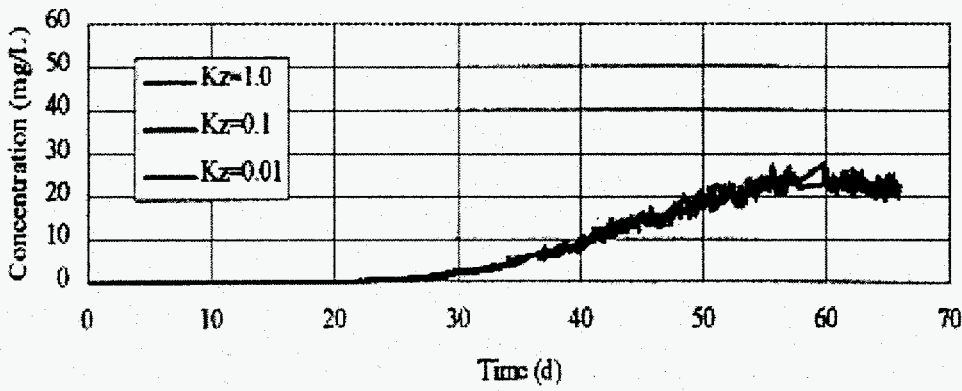


Figure A-29  
Sensitivity at EW-2 to Changes in Vertical Hydraulic Conductivity

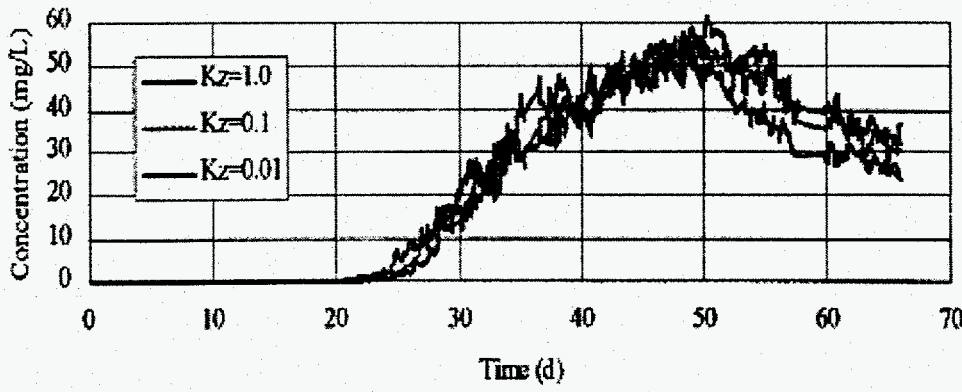


Figure A-30  
Sensitivity at EW-3 to Changes in Vertical Hydraulic Conductivity

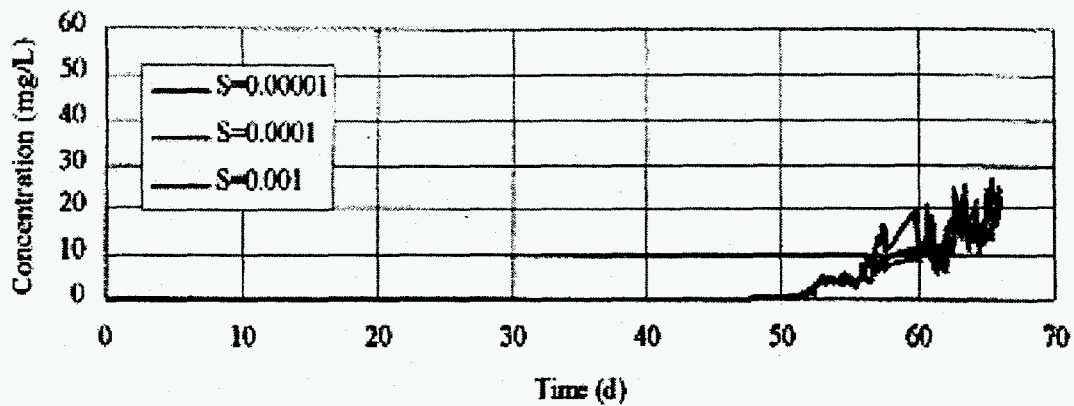


Figure A-31  
Sensitivity at EW-1 to Changes in Storage Parameter

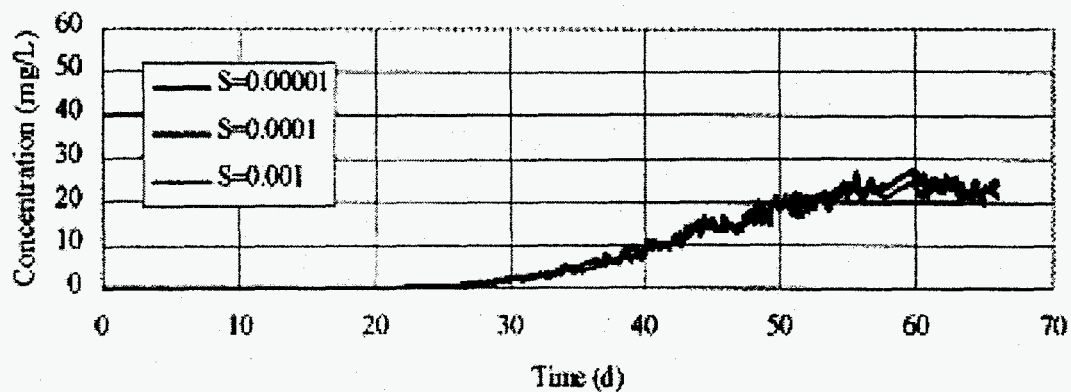


Figure A-32  
Sensitivity at EW-2 to Changes in Storage Parameter

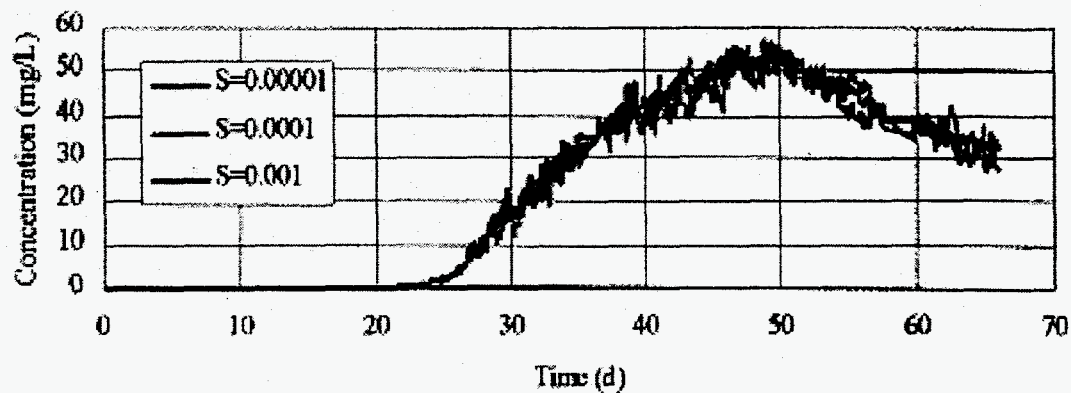


Figure A-33  
Sensitivity at EW-3 to Changes in Storage Parameter

**APPENDIX B: MT3D INTERNAL PARAMETERS RELATED  
TO ADVECTIVE TRANSPORT**

**Table A-1**

## MT3D Internal Parameters Related to Advective Transport

Parameter	Value
Courant number	1.0
Concentration Weighting Factor	0.5
Initial Placement of Particles	random
Initial particles per cell (low)	0
Initial particles per cell (high)	12
Minimum particles per cell	2
Maximum particles per cell	24
Multiplier for source cells	1.0
Concentration interpolation method	linear
Particle placement pattern in sinks	random
Number of particles in sinks	16
Critical concentration gradient	1.0